

Spring School on Numerical Relativity and Gravitational Wave Physics

Gravitational Waves from colliding Compact Star Binaries in the context of Strange/Exotic Matter

*ROOM 6620
ITP NEW BUILDING, BEIJING
15.-25. MAY, 2017*

MATTHIAS HANAUSKE

*FRANKFURT INSTITUTE FOR ADVANCED STUDIES
JOHANN WOLFGANG GOETHE UNIVERSITY
INSTITUTE OF THEORETICAL PHYSICS
DEPARTEMENT OF RELATIVISTIC ASTROPHYSICS
D-60438 FRANKFURT AM MAIN
GERMANY*

Chapter 1

Contents of the whole Lecture

- **Chapter 1**

- General Relativity of Black Holes and Compact Stars
- Elementary Particle Physics and the Interior of a Compact Star

- **Chapter 2**

- Numerical Relativity and Relativistic Hydrodynamics
- The Einstein Toolkit

- **Chapter 3**

- Binary Mergers of Compact Stars
- Gravitational Waves and Internal Properties of Hypermassive Neutron Stars

General Things

- Transparencies and additional Information:
 - <http://th.physik.uni-frankfurt.de/~hanauske/VARTC/ssnr2017/>
 - <http://th.physik.uni-frankfurt.de/~hanauske/VARTC/> (in German)
- Software and Computer-Codes:
 - Maple
 - C++, MPI and OpenMP
 - Einstein Toolkit
 - Python

[Intro 介绍](#)

[Chapter I 第一章](#)

[Chapter II 第二章](#)

[Chapter III 第三章](#)

[e-learning 电子学习](#)

Spring School on Numerical Relativity and Gravitational Wave Physics

15th-25th May 2017, Beijing
Room 6620, ITP New Building, Beijing



Invited Lecturers:

Niels Warburton (University College Dublin)
Andrea Taracchini (Max Planck Institute for Gravitational Physics)
David Hilditch (Theoretical Physics Institute, University of Jena)
David Weir (Helsinki Institute of Physics, University of Helsinki)
Koutarou Kyutoku (KEK, IPNS)
Matthias Hanauskę (Goethe University Frankfurt)

(Spring School on Numerical Relativity and Gravitational Wave Physics)

Vorlesungsreihe (6 Vorlesungen) über
Gravitationswellen von kollidierenden kompakten Sternen und die
Eigenschaften seltsamer Materie
(Gravitational waves from colliding compact star binaries in the context of
strange/exotic matter)
致密星碰撞引起的引力波和奇异物质的性质
Beijing, China, 15.-25. May 2017

Die im Jahre 2017 gehaltene Vorlesungsreihe führt einerseits in die Allgemeine Relativitätstheorie ein, andererseits fokussiert sie sich auf den speziellen Teilaspekt der relativistischen Astrophysik kollidierender hybrider Neutronensterne, in deren innerem Bereich es zur Bildung seltsamer und exotischer Materie kommen kann. Kollabiert ein instabiler Neutronenstern zu einem schwarzen Loch oder zu einem Quark Stern? Wie kann man anhand des ausgesandten Gravitationswellen-Signals zweier kollidierender kompakter Sterne die Eigenschaften der Nuklearen- und Quark-Materie entschlüsseln?

(The series of lectures held in 2017. Topics: theory of general relativity theory, relativistic astrophysics of colliding hybrid neutron stars, strange and exotic matter in the interior of compact stars. Questions: Does an unstable neutron star collapse to a black hole or quark star? How can we extract the strange properties of high density nuclear and quark matter by means of the emitted gravitational wave signal of two colliding compact stars?)

在2017年开设的课程,一方面介绍广义相对论理论,另一方面聚焦于相对论天体物理中的一个特殊部分:混合致密星碰撞,以及在其内部可能生成的奇异和异常物质。一个不稳定的中子星是会坍缩成黑洞还是夸克星?如何根据两个致密星碰撞发射的引力波信号来解码核物质和夸克物质的奇异特性?

Chapter I

Practical part of Chapter I

- Learn how to use Maple to solve several (not too complicated) problems in GR
 - Learn the basics of parallel programming in C/C++ MPI-OpenMP

$$R_{\mu\nu} - \frac{1}{2} g_{\mu\nu} R = -8\pi T_{\mu\nu}$$

$$\frac{d^2 x^\mu}{d\tau^2} + \Gamma_{\nu\rho}^\mu \frac{dx^\nu}{d\tau} \frac{dx^\rho}{d\tau} = 0$$

Non-Rotating Black Holes

Event horizon, photon-sphere, test particle falls into a black hole, geodesic motion of a massive test particle (or a massless photon) around a black hole, ISCO, ...

Properties of Neutron Stars

Density profile inside a neutron star, mass-radius relation, spacetime curvature inside and outside the neutron star, ...

Rotating Black Holes

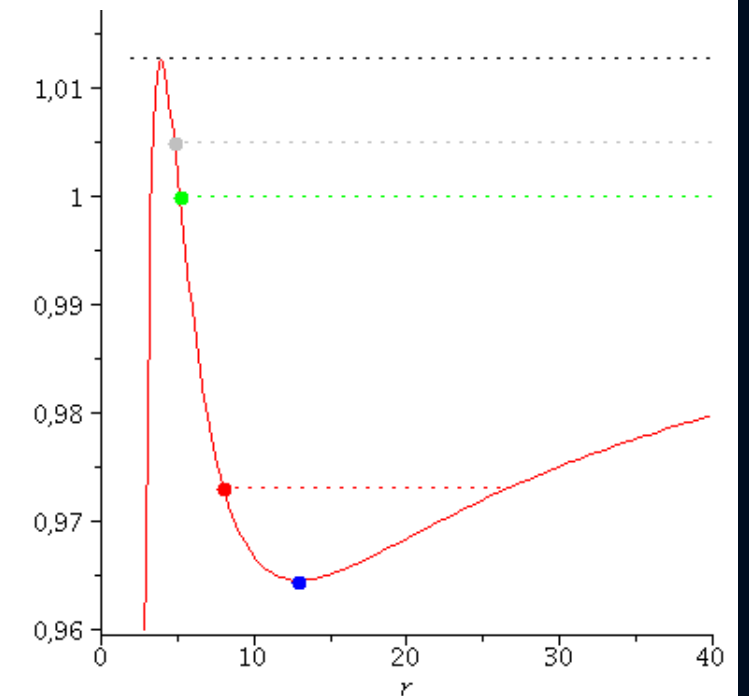
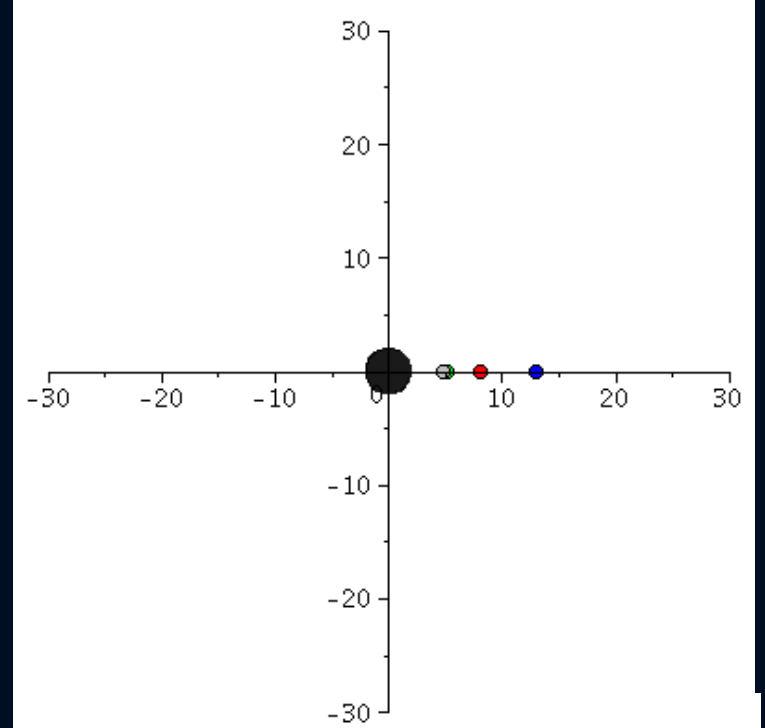
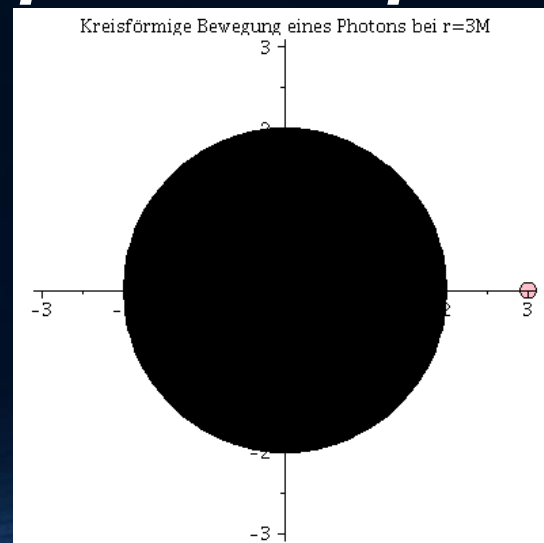
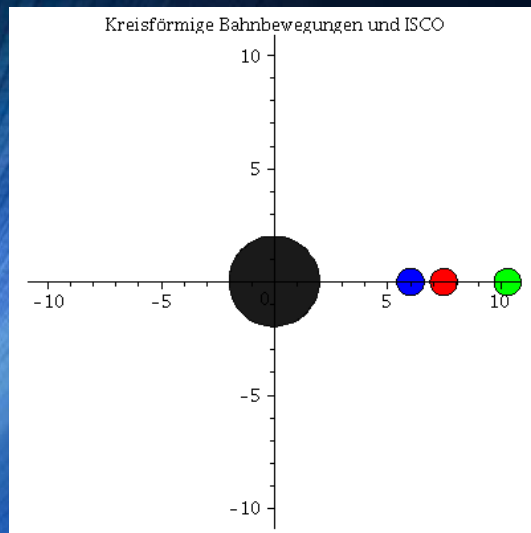
Horizons, ergosphere, the frame-dragging effect, ISCO's, ...

Geodesic motion around a black hole

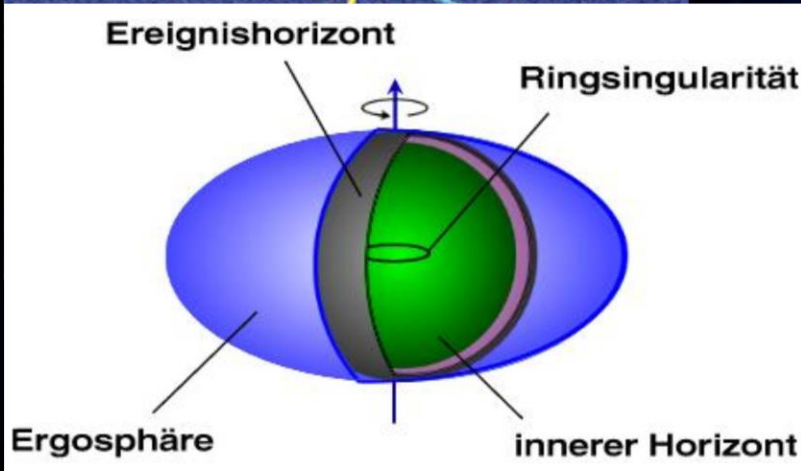
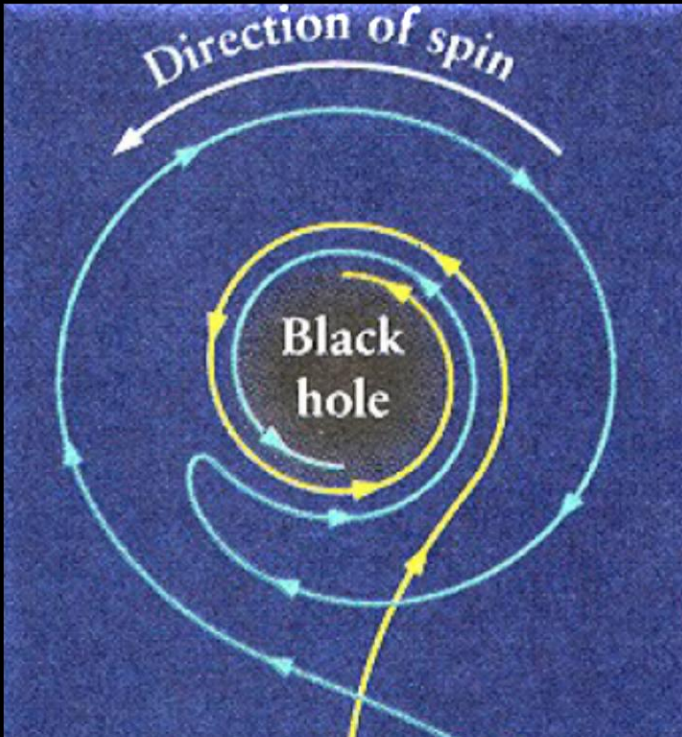
$$R_{\mu\nu} - \frac{1}{2} g_{\mu\nu} R = -8\pi T_{\mu\nu}$$

$$\frac{d^2 x^\mu}{d\tau^2} + \Gamma^\mu_{\nu\rho} \frac{dx^\nu}{d\tau} \frac{dx^\rho}{d\tau} = 0$$

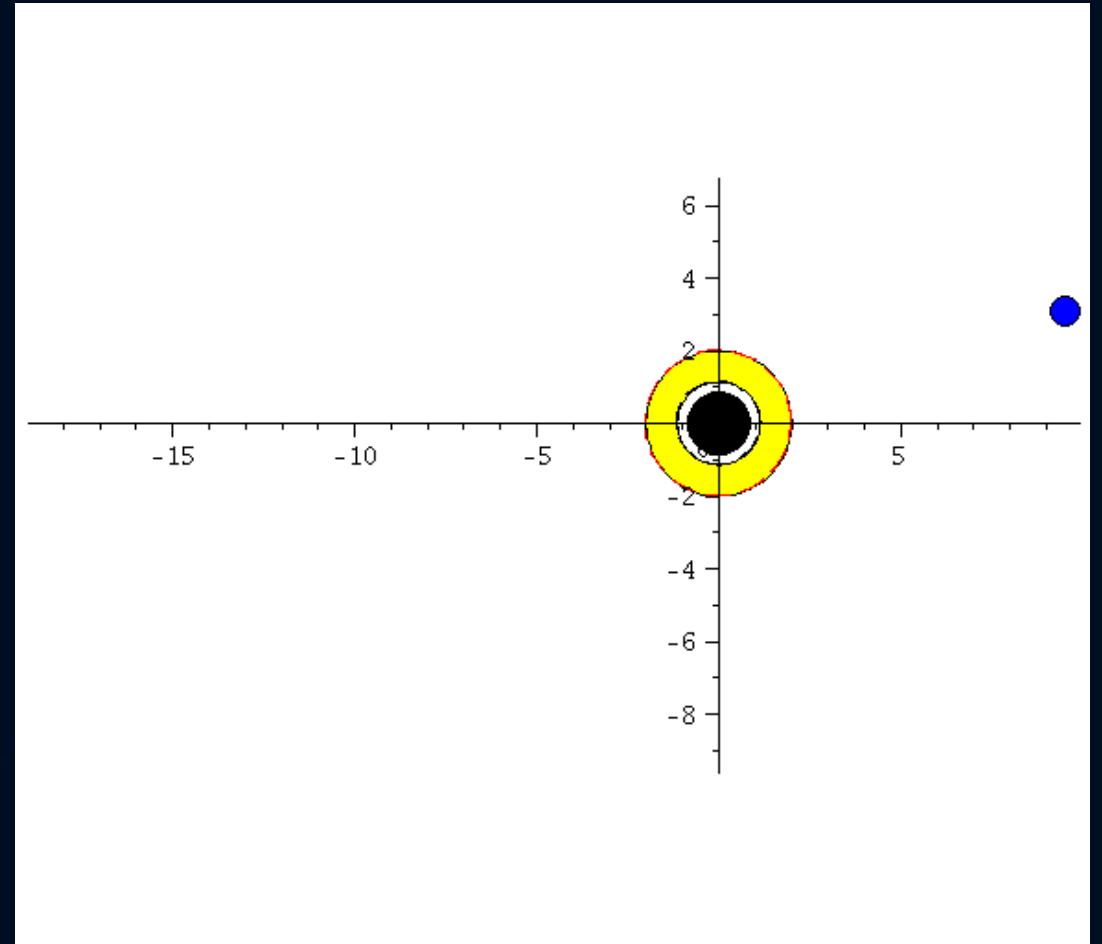
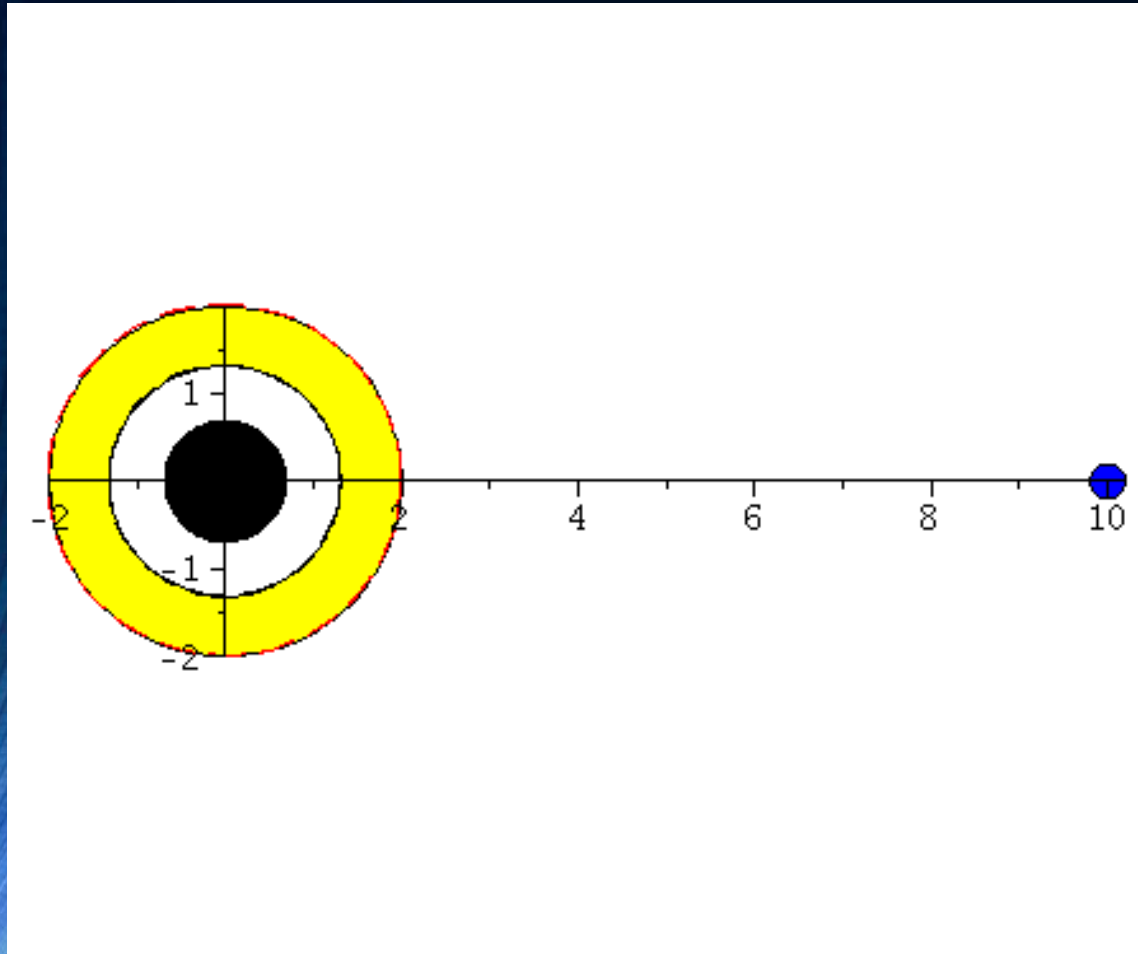
The *ISCO* and the *photon sphere*



Rotating Black Holes (Kerr black holes)



Frame dragging and gravitomagnetism

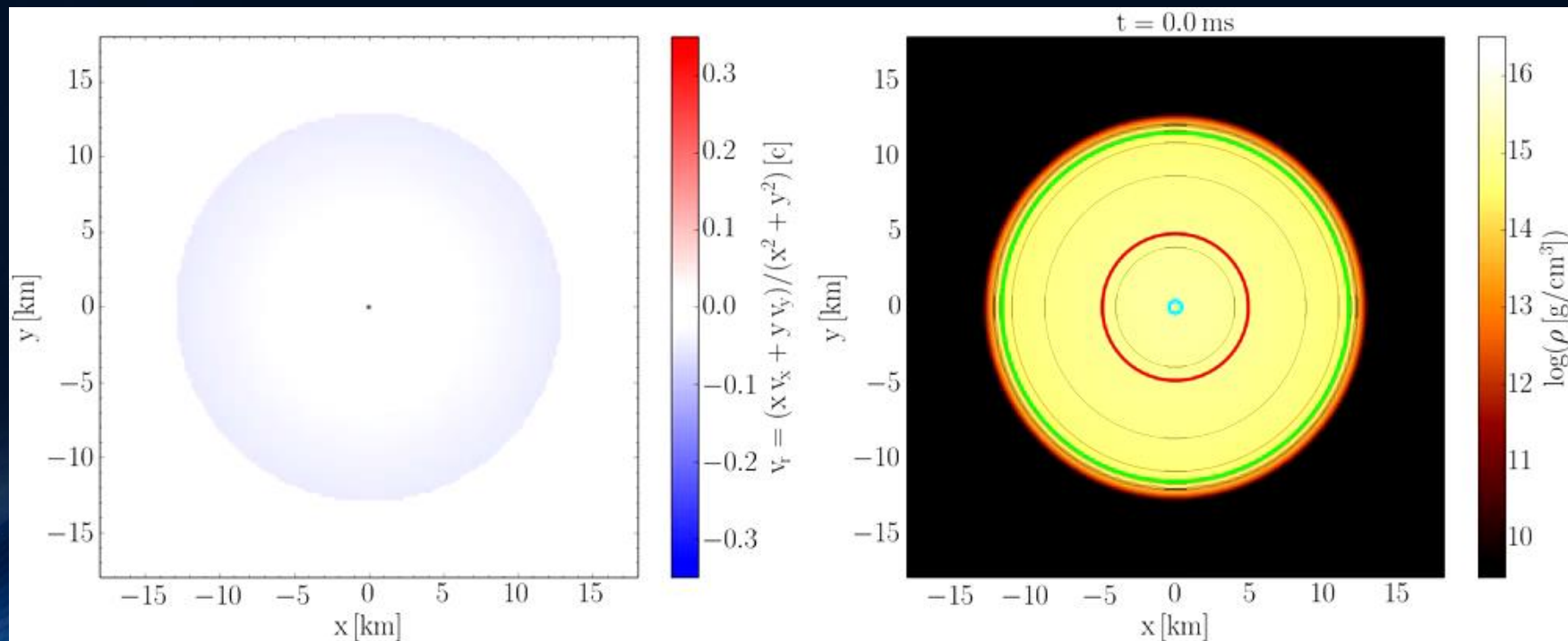


Chapter II



Practical part of Chapter II

- How to download and build (compile) the Einstein Toolkit
- How to run a test simulation (static_tov.par)
- Run and visualize (Mathematica or Python) one of the following problems
 - Migration of an unstable neutron star to a stable configuration
 - Collapse of an unstable neutron star to a black hole
 - Collapse of a neutron star to a quark star (twin star collapse)



Chapter III

Gravitational Waves from colliding Compact Star Binaries in the context of Strange/Exotic Matter

**Credits: Cosima Breu, David Radice
and Luciano Rezzolla**



Density

8.5 14



$\lg(\rho)$ [g/cm^3]

Temperature

0 50



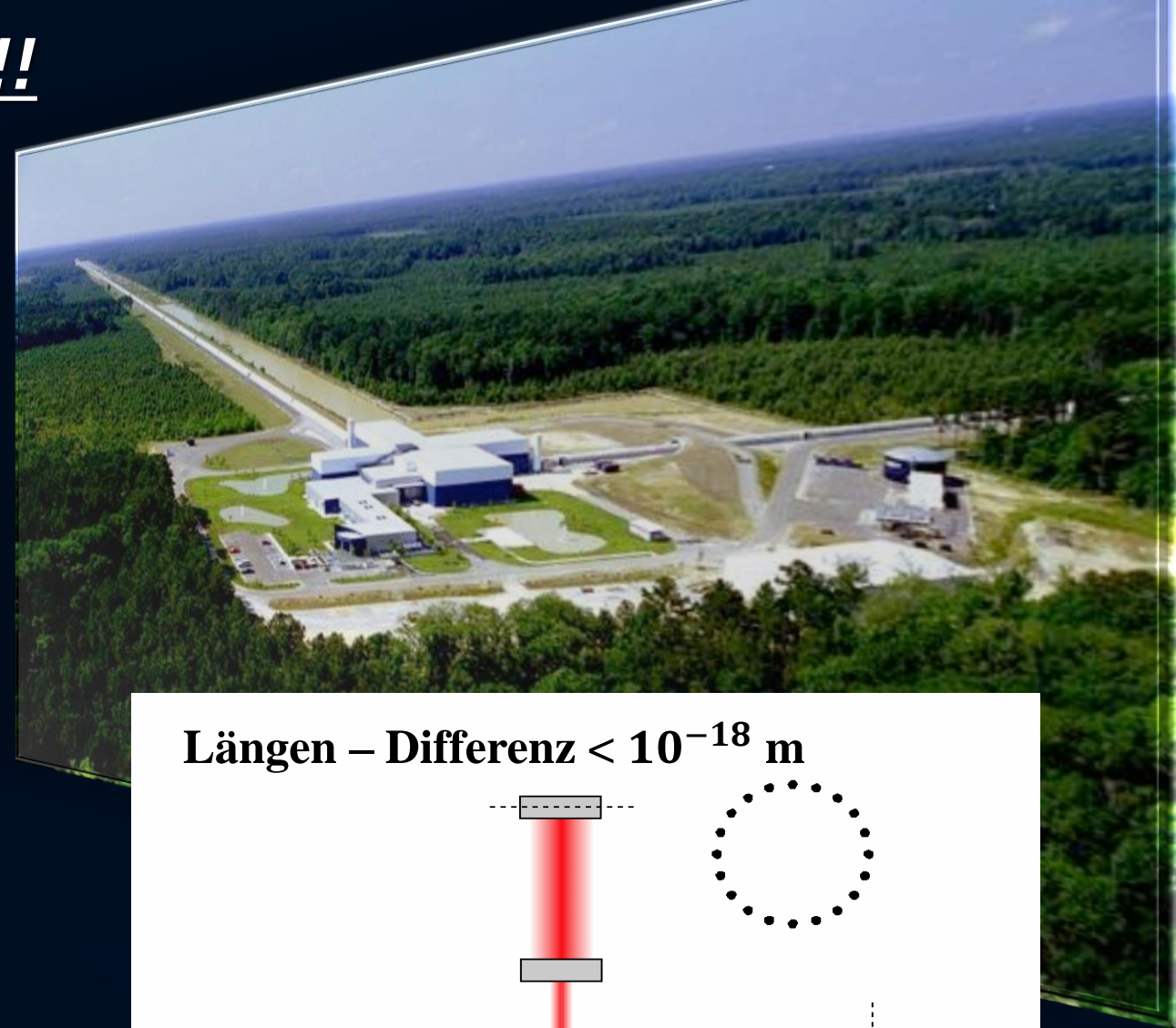
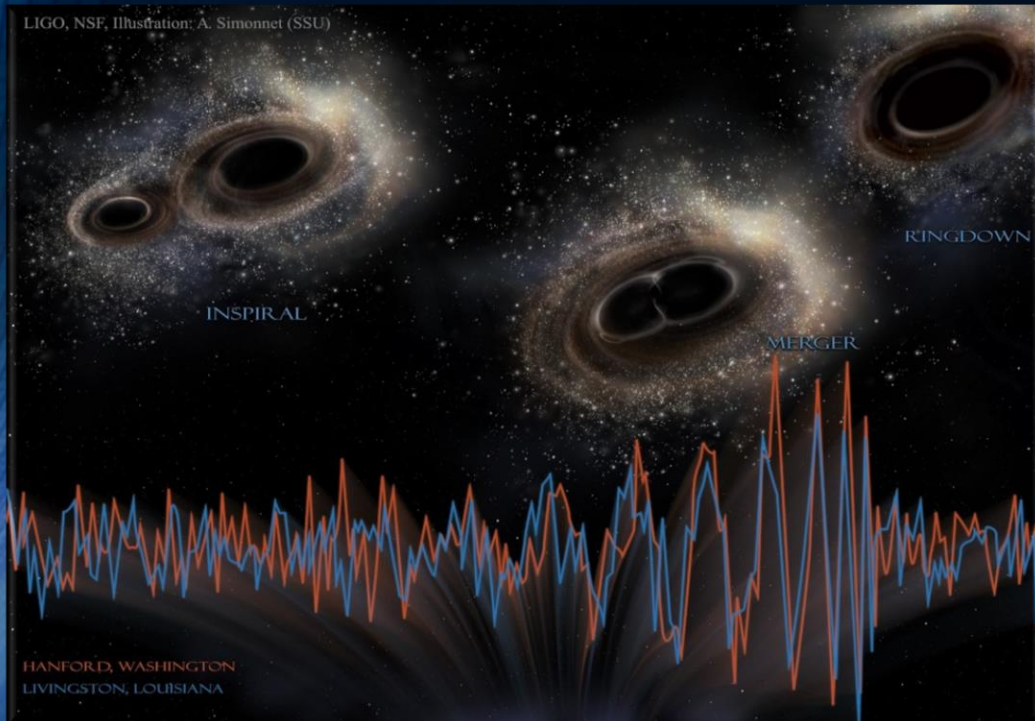
T [MeV]

Gravitational Waves detected!!!

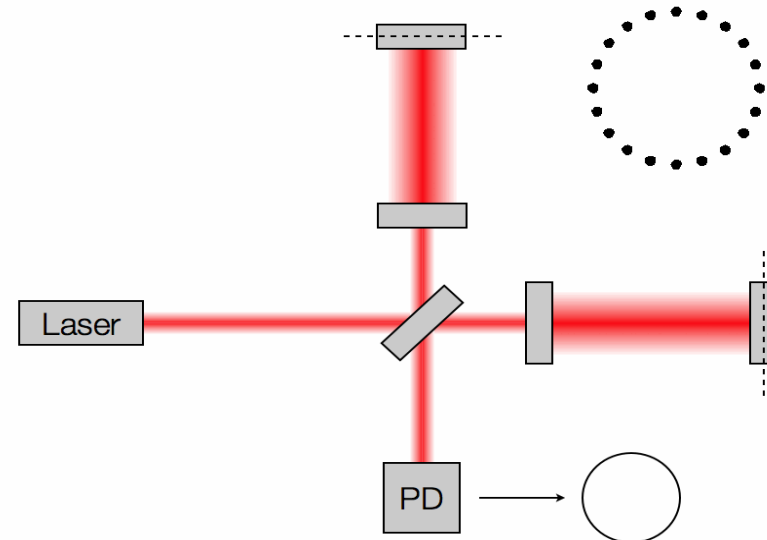
Collision of two Black Holes GW150914

Masses: 36 & 29 Sun masses

Distance to the earth 410 Mpc
(1.34 Billion Light Years)



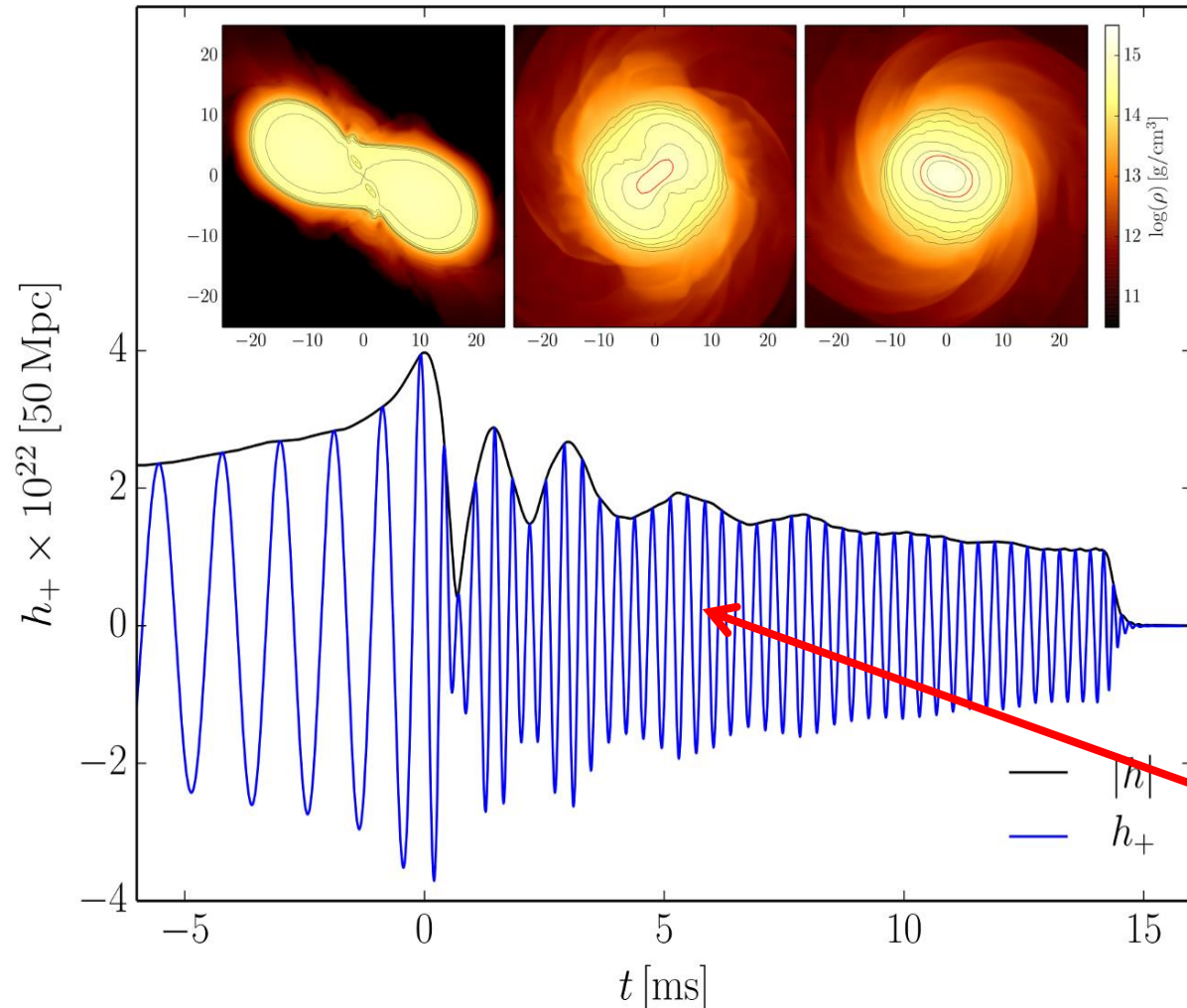
Längen – Differenz $< 10^{-18}$ m



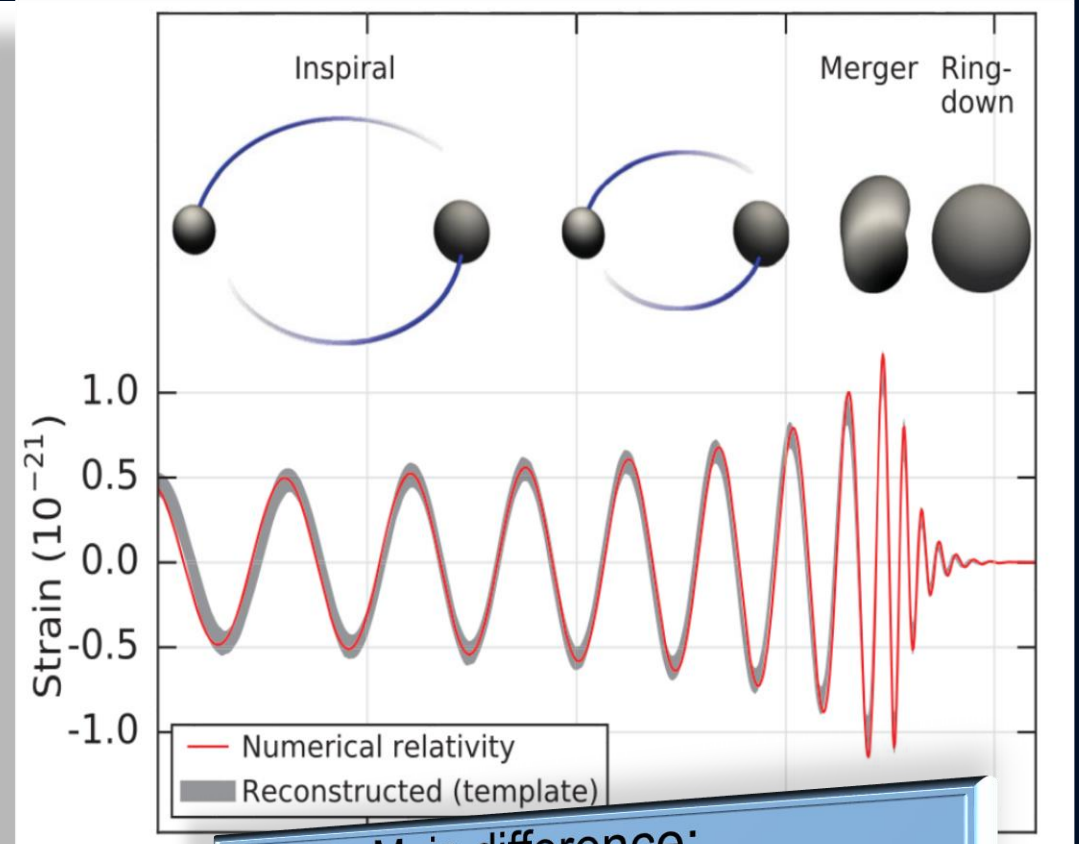
Credit: Les Wade from Kenyon College

Gravitational Waves from Neutron Star Mergers

Neutron Star Collision (Simulation)



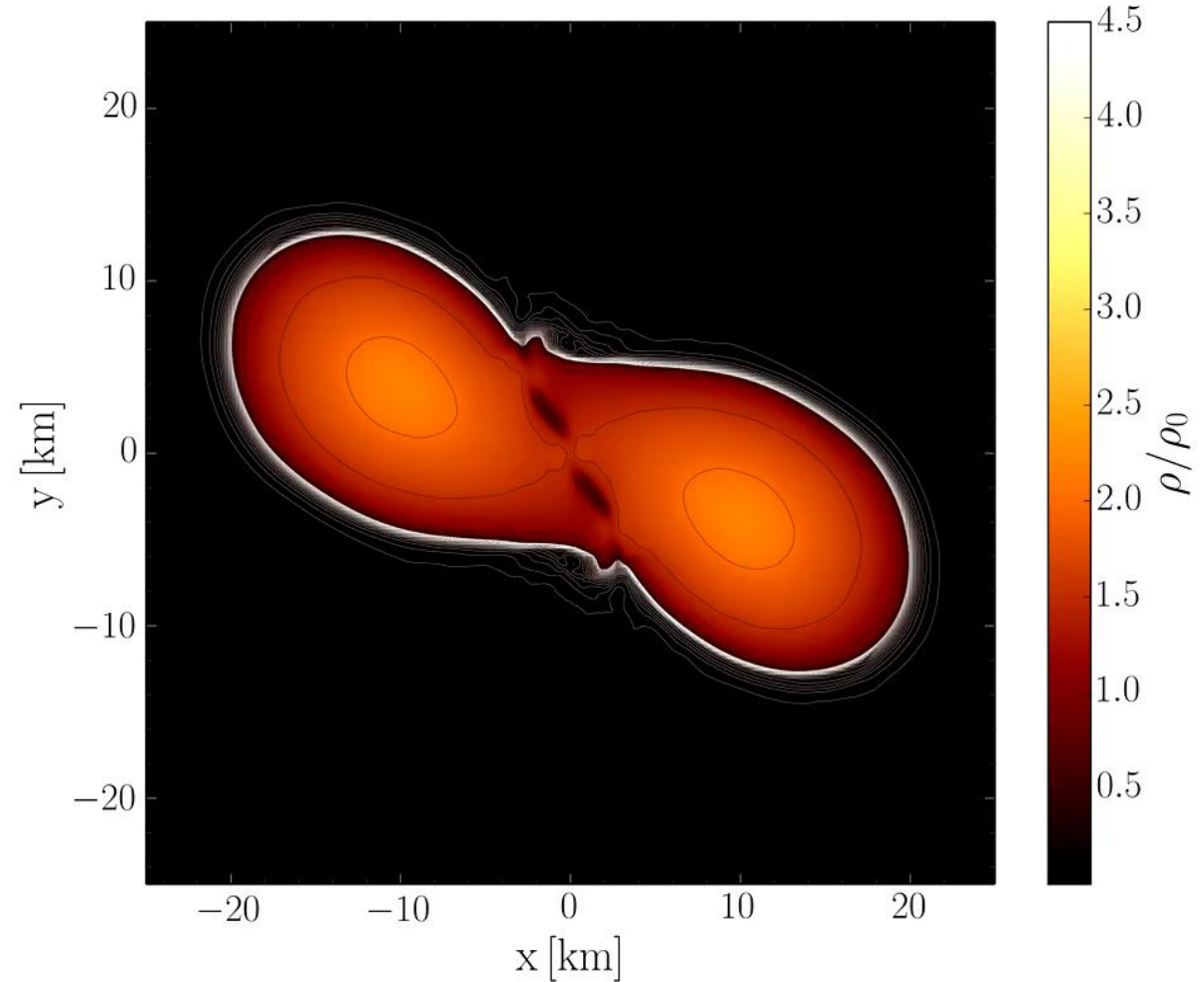
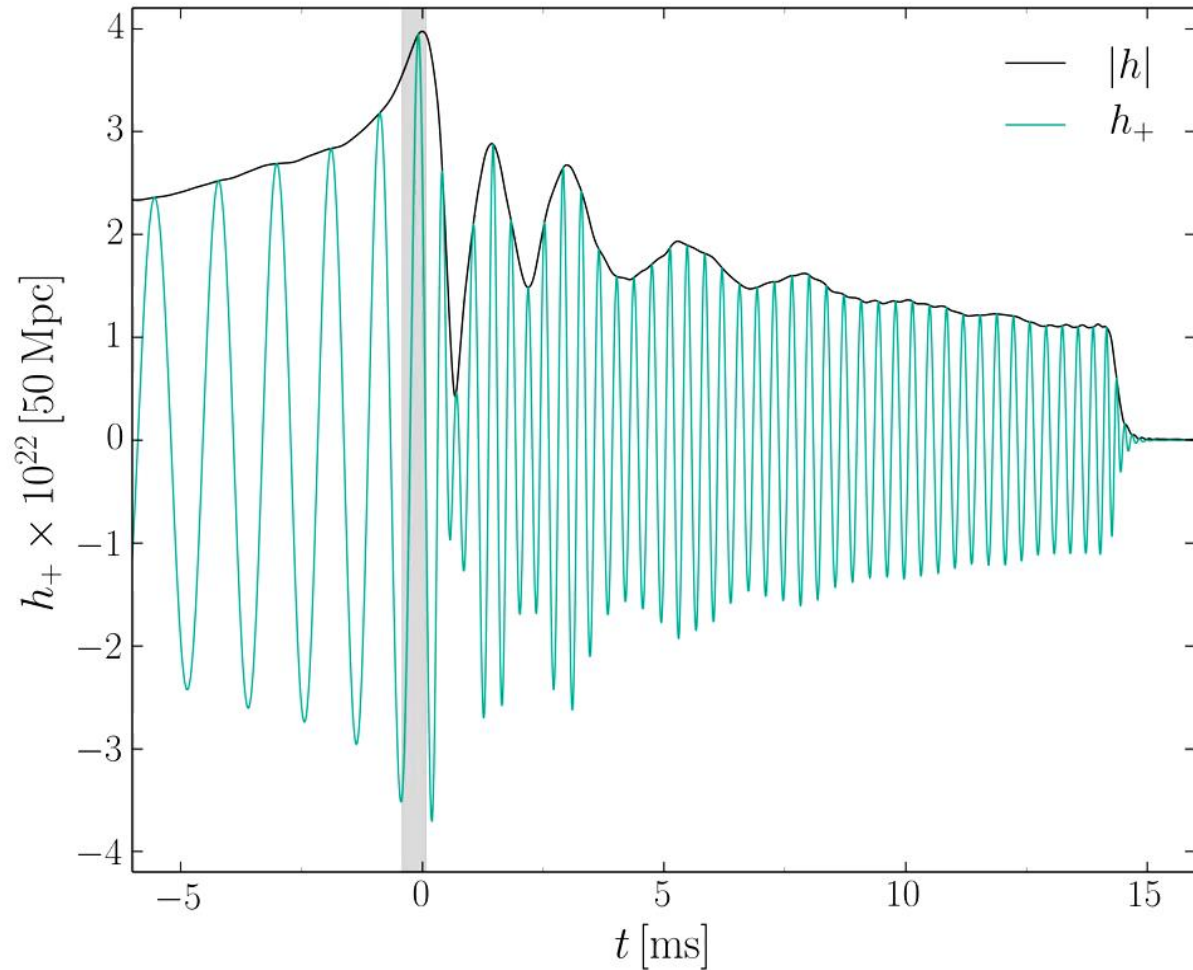
Collision of two Black Holes

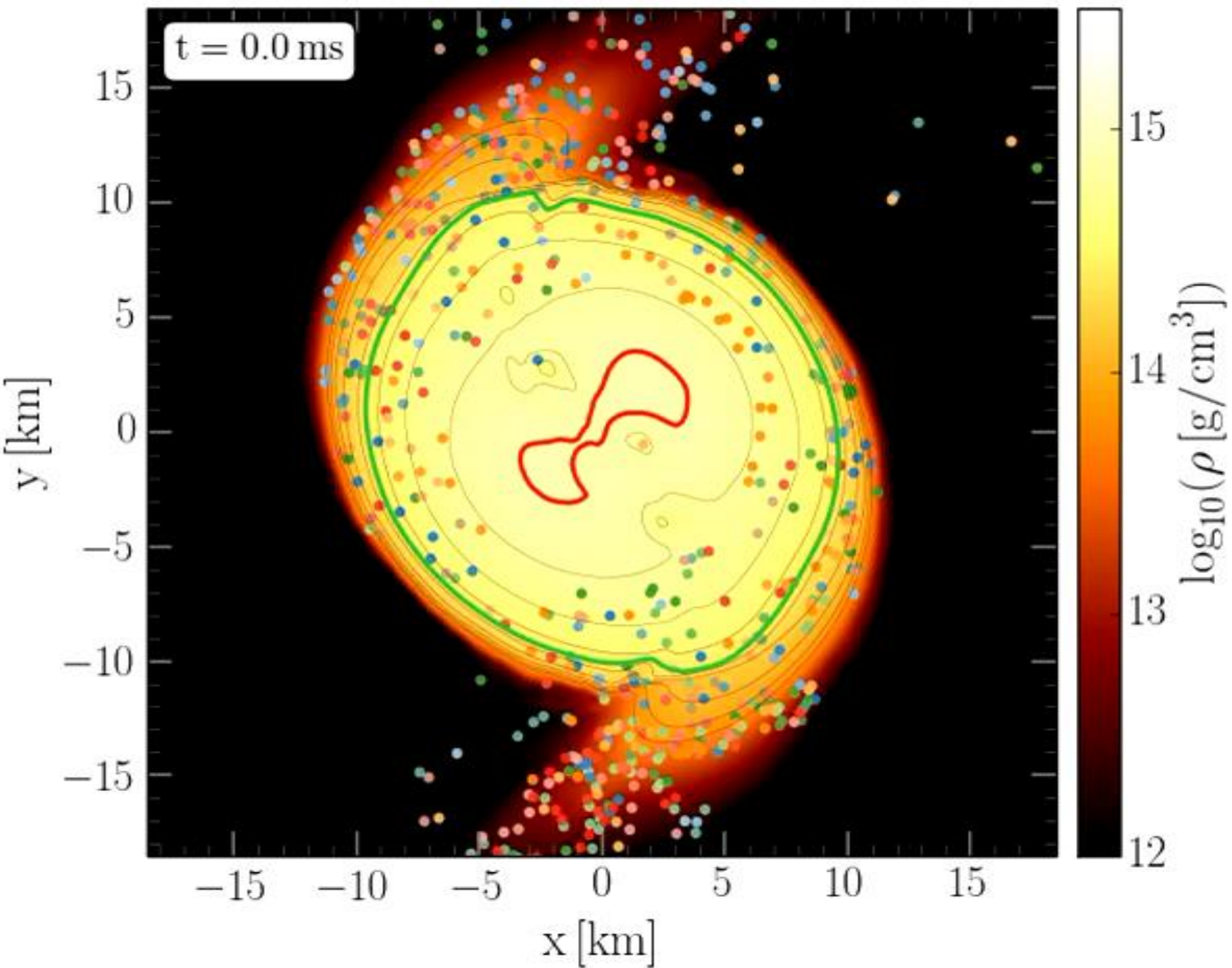


Main difference:
In binary neutron star mergers a **Post-Merger Phase** often exists

Chapter III

Gravitational Waves from colliding Compact Star Binaries in the context of Strange/Exotic Matter



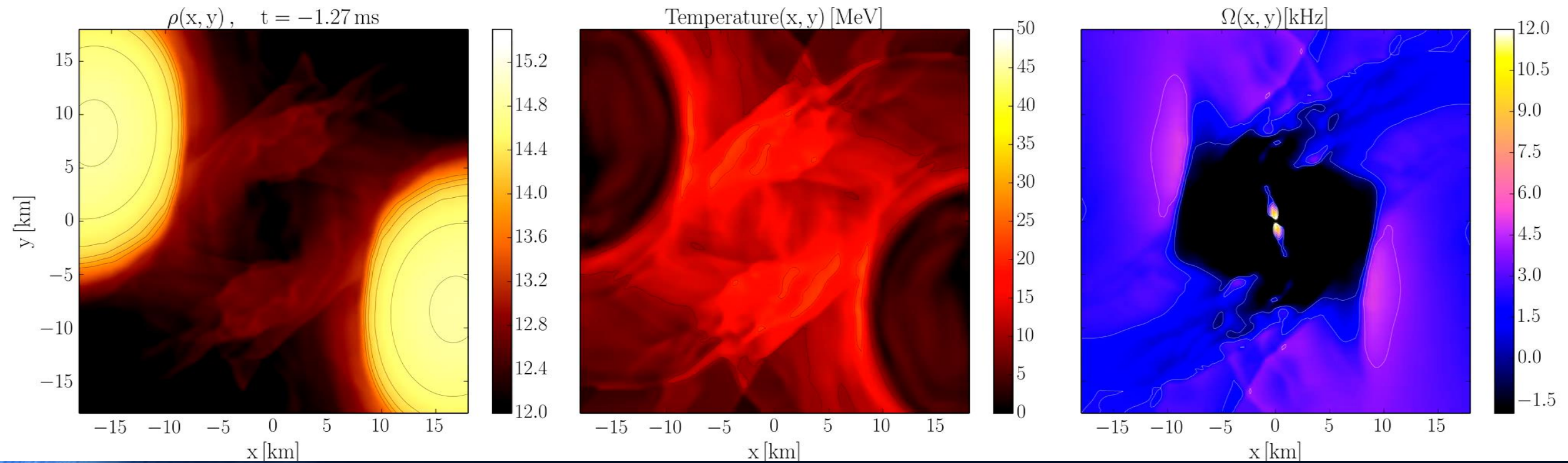


Chapter III

*Gravitational Waves from
colliding Compact Star Binaries
in the context of
Strange/Exotic Matter*

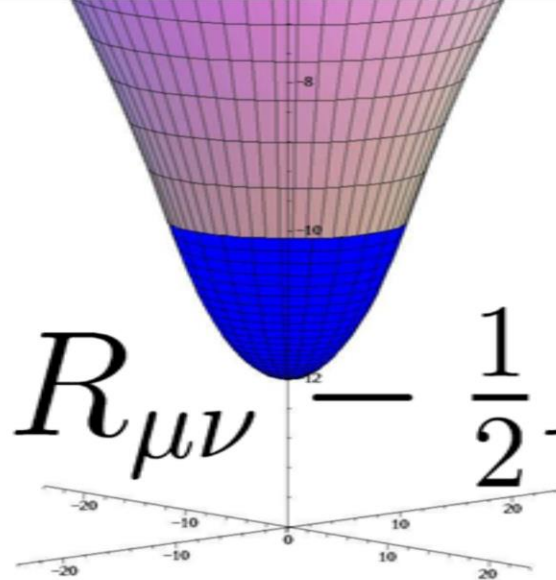
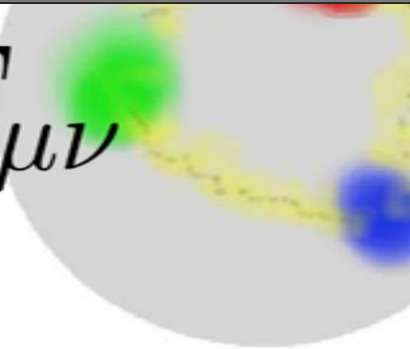
Chapter III

Gravitational Waves from colliding Compact Star Binaries in the context of Strange/Exotic Matter



The Theory of General Relativity

A little more than 100 years ago (1915), Albert Einstein presented his new theory of gravity „General Relativity“ (GR) to the public.

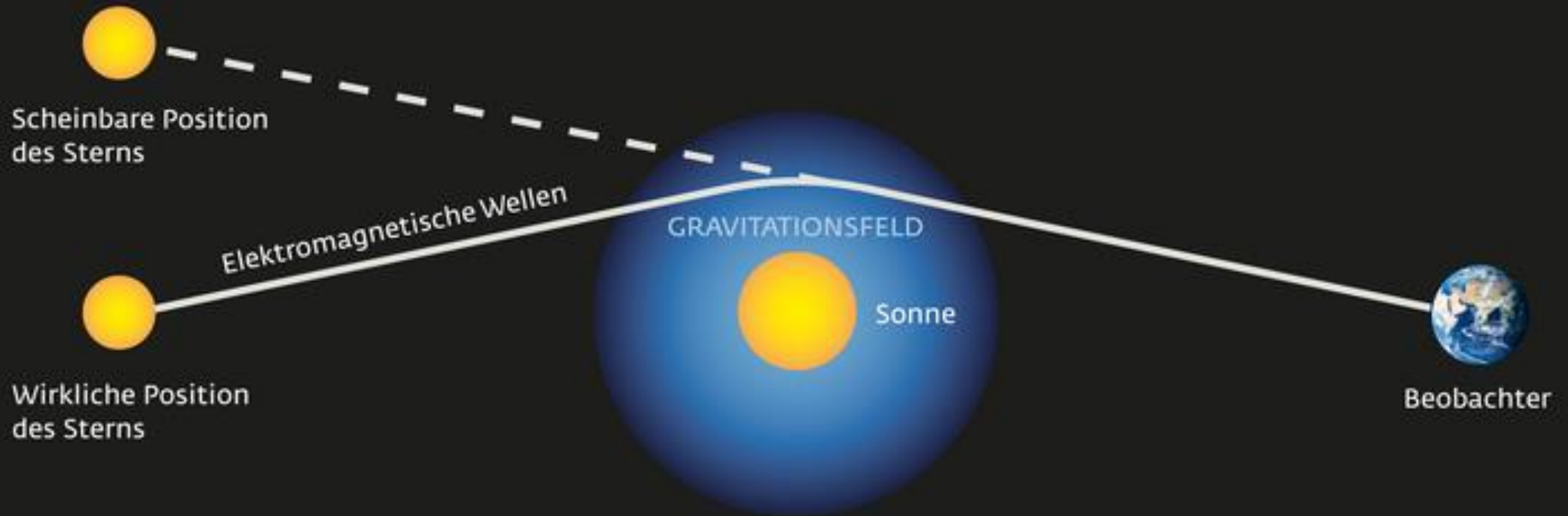

$$R_{\mu\nu} - \frac{1}{2}R g_{\mu\nu} = \frac{8\pi G}{c^4} T_{\mu\nu}$$


GR was a very revolutionary theory. The Einstein equation says that all forms of energy and momentum bends the structure of spacetime and this curvature of spacetime is the underlying reason of the gravitational force. -> Curvature of spacetime = Energy

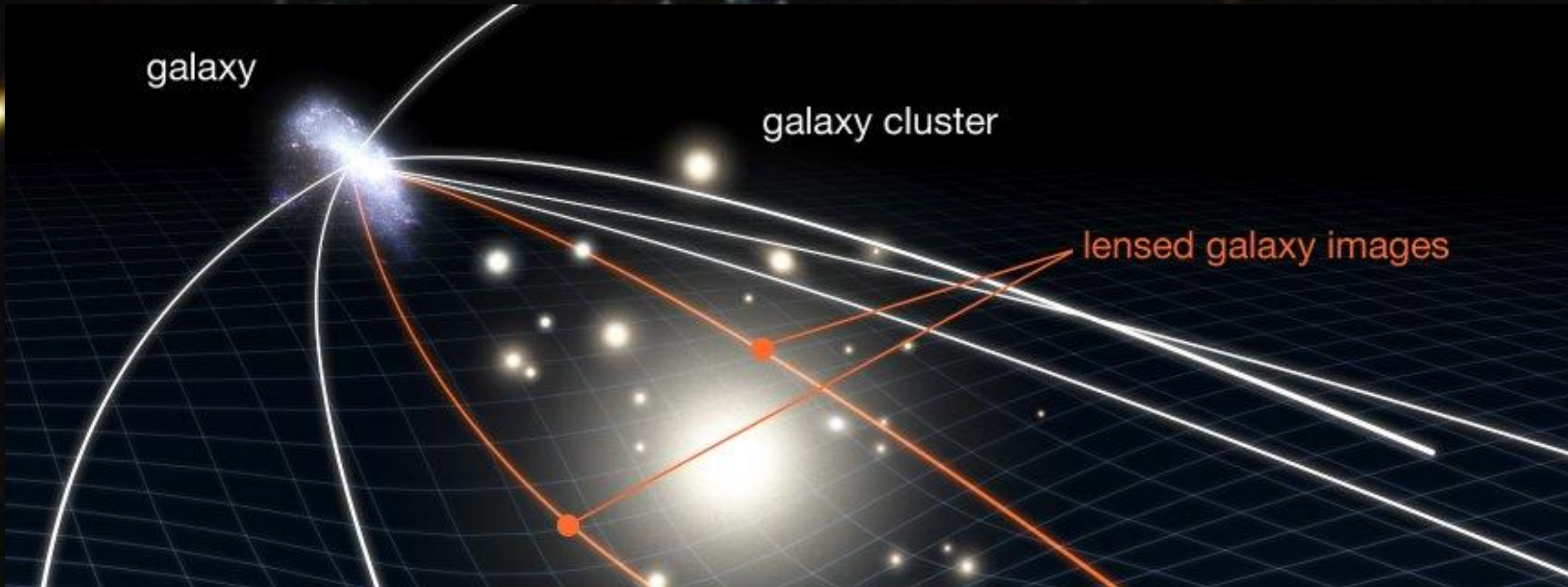
The First Experimental Validation of GR

The Solar Eclipse in the Year 1919

Unfortunately, not many physicists believed in Einsteins Theory. This changed abruptly after the solar eclipse in the year 1919:



Gravitational Lensing

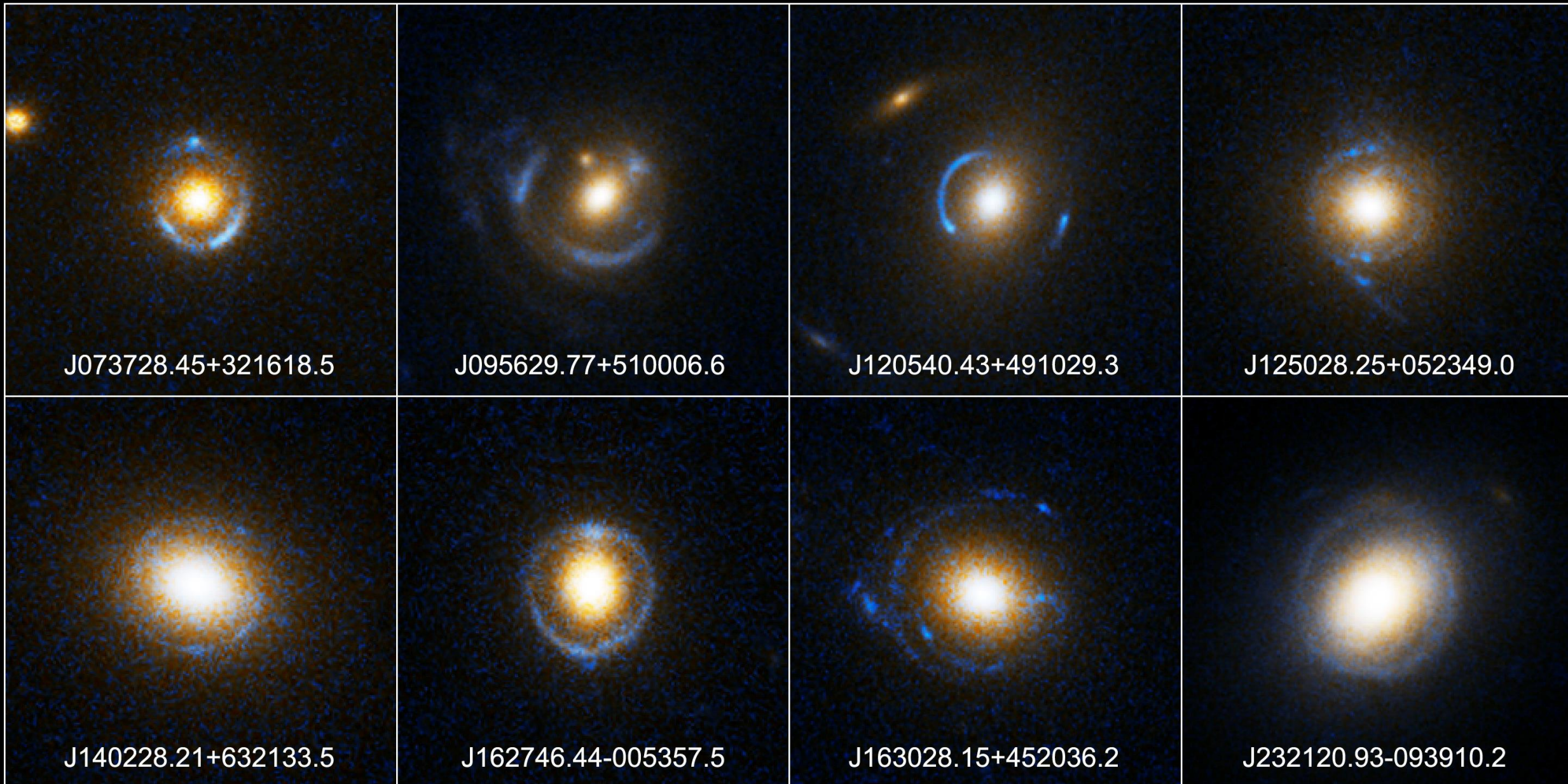


The Einstein-Ring



LRG 3-757: Observed with the Hubble Telescope in the year 2007

Other Einstein-Rings



The Schwarzschild Solution

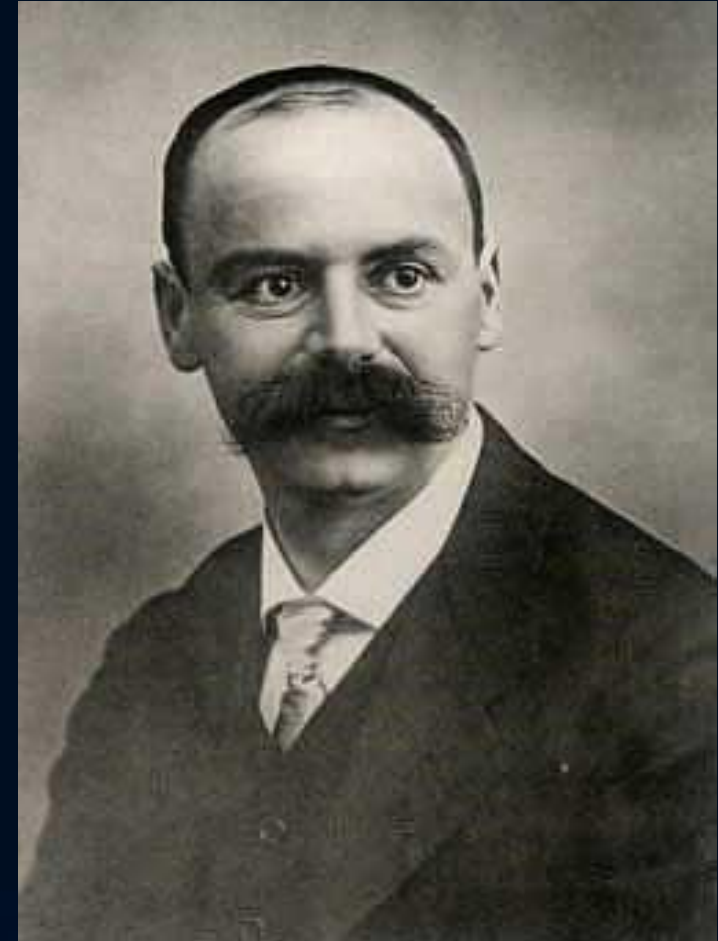
1915 Einsteins Gravitation:

Gravity is curvature of spacetime

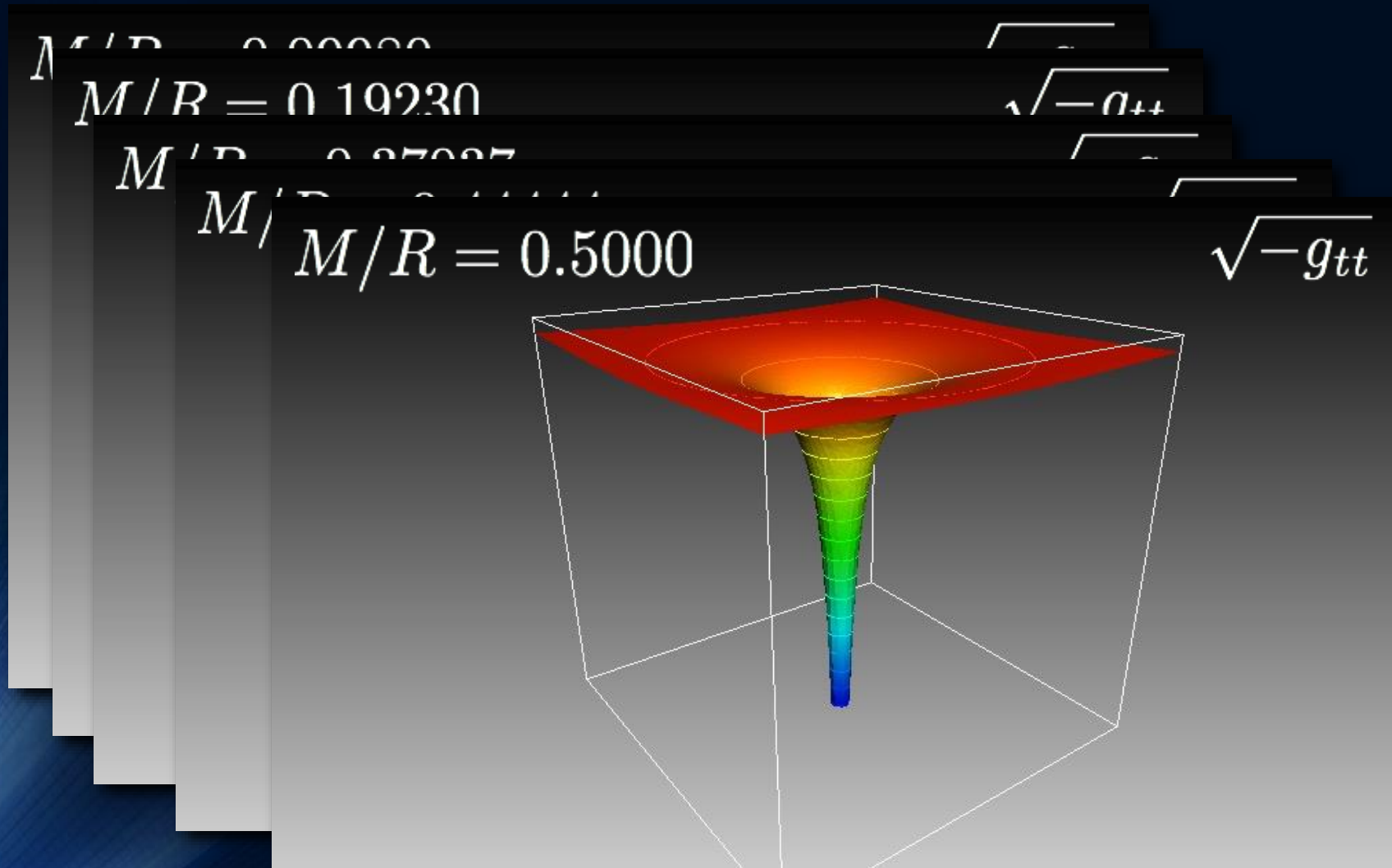
1916 Karl Schwarzschild:

... was born in Frankfurt in the year 1873. First analytic solution of the Einstein equation – only three months after Einsteins article! Metric of spacetime outside a spherically symmetric body (metric of a non-rotating black hole without charge).

Unfortunately, Schwarzschild died only one month later as a soldier in the first world war.



What are Black Holes?



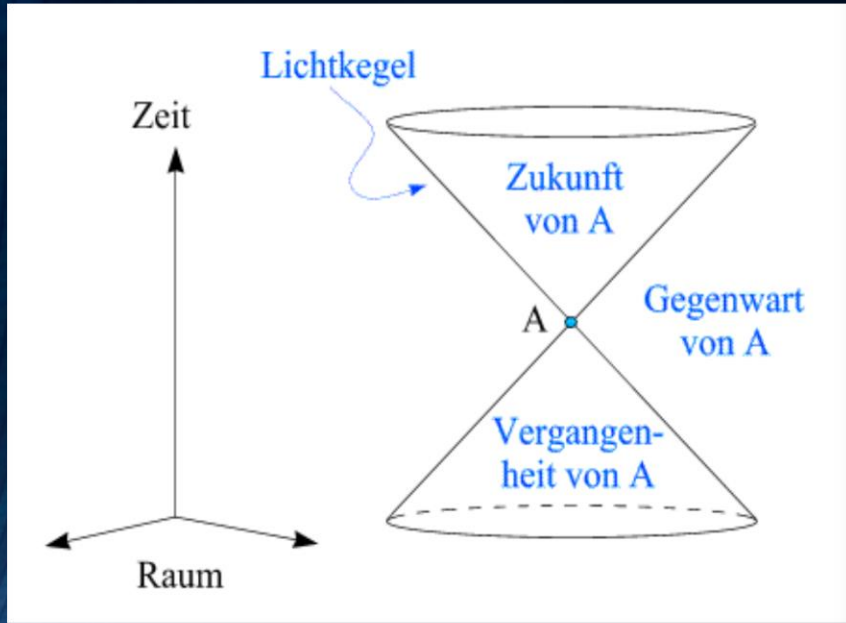
We have overcome a barrier and created a black hole!

Threshold of the curvature: Stable objects (e.g. neutron stars) are no longer possible

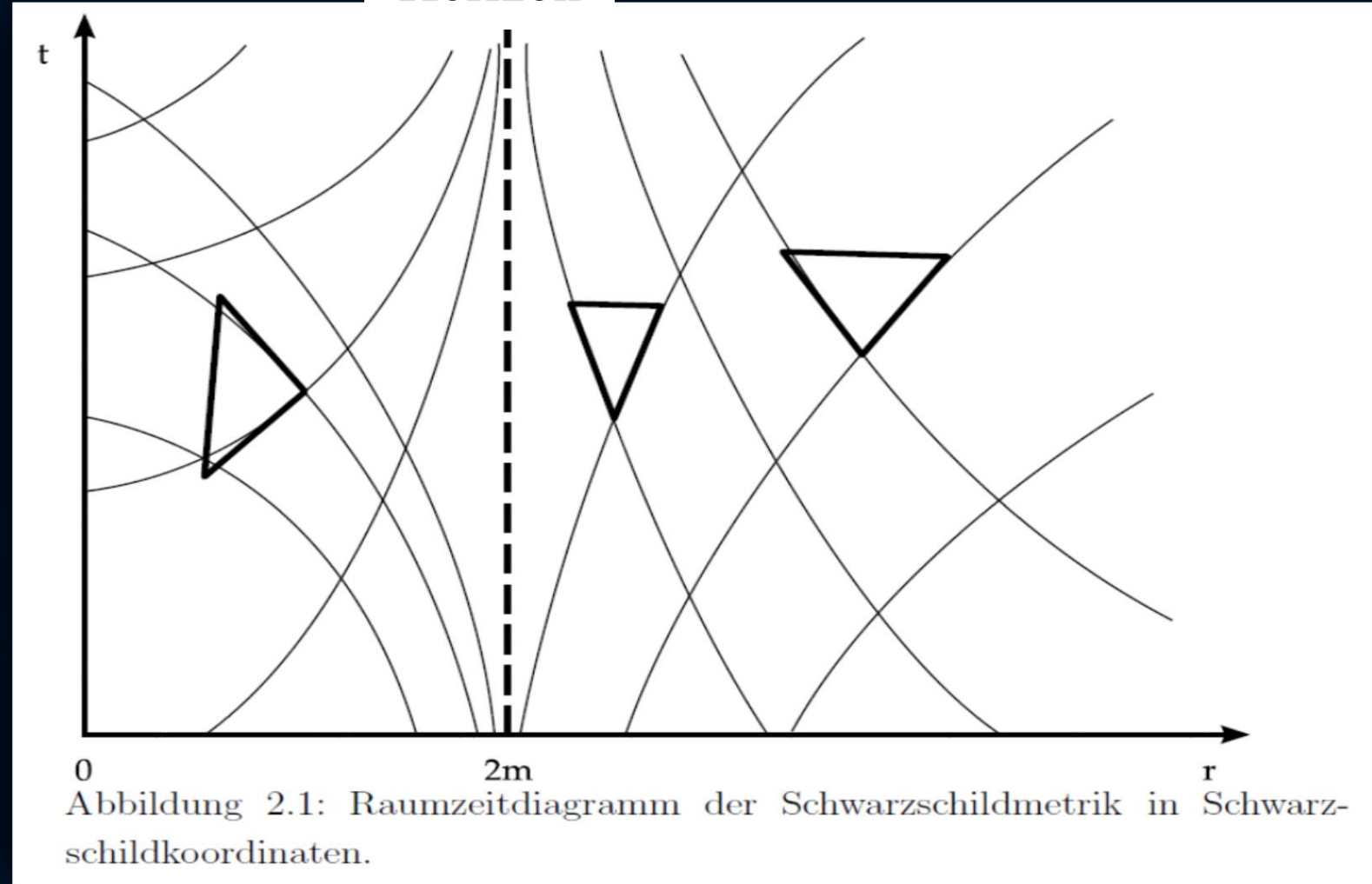
Spacetime Diagram of a Black Hole in Schwarzschild Coordinates

(Viewpoint from an observer which is at infinity at rest)

Event
Horizon



Spacetime structure is flat



Curvature of the structure of spacetime around a black hole

Spacetime Diagram of a Black Hole

in infalling Eddington-Finkelstein coordinates

(Viewpoint from an observer which falls with the speed of light into the black hole)

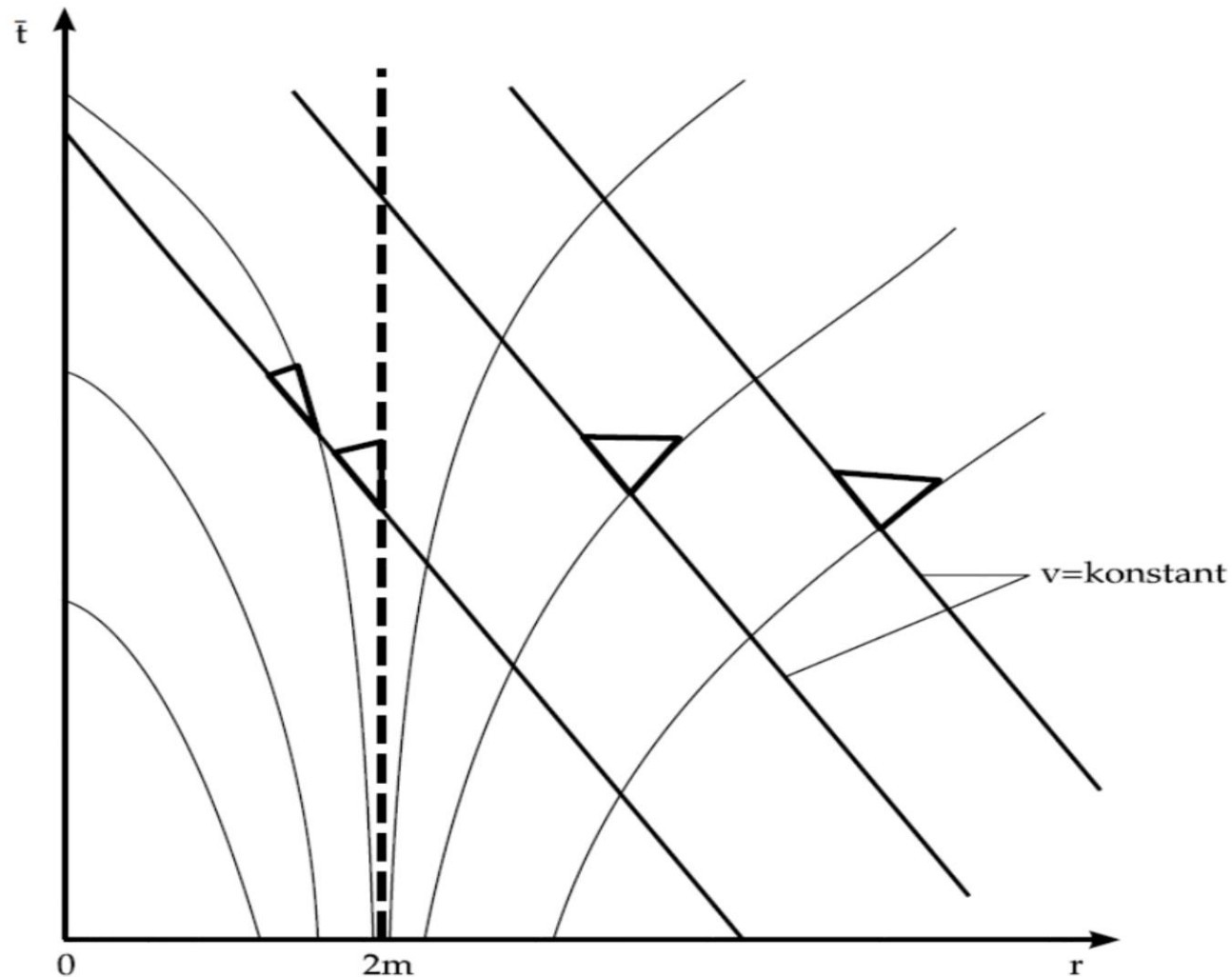
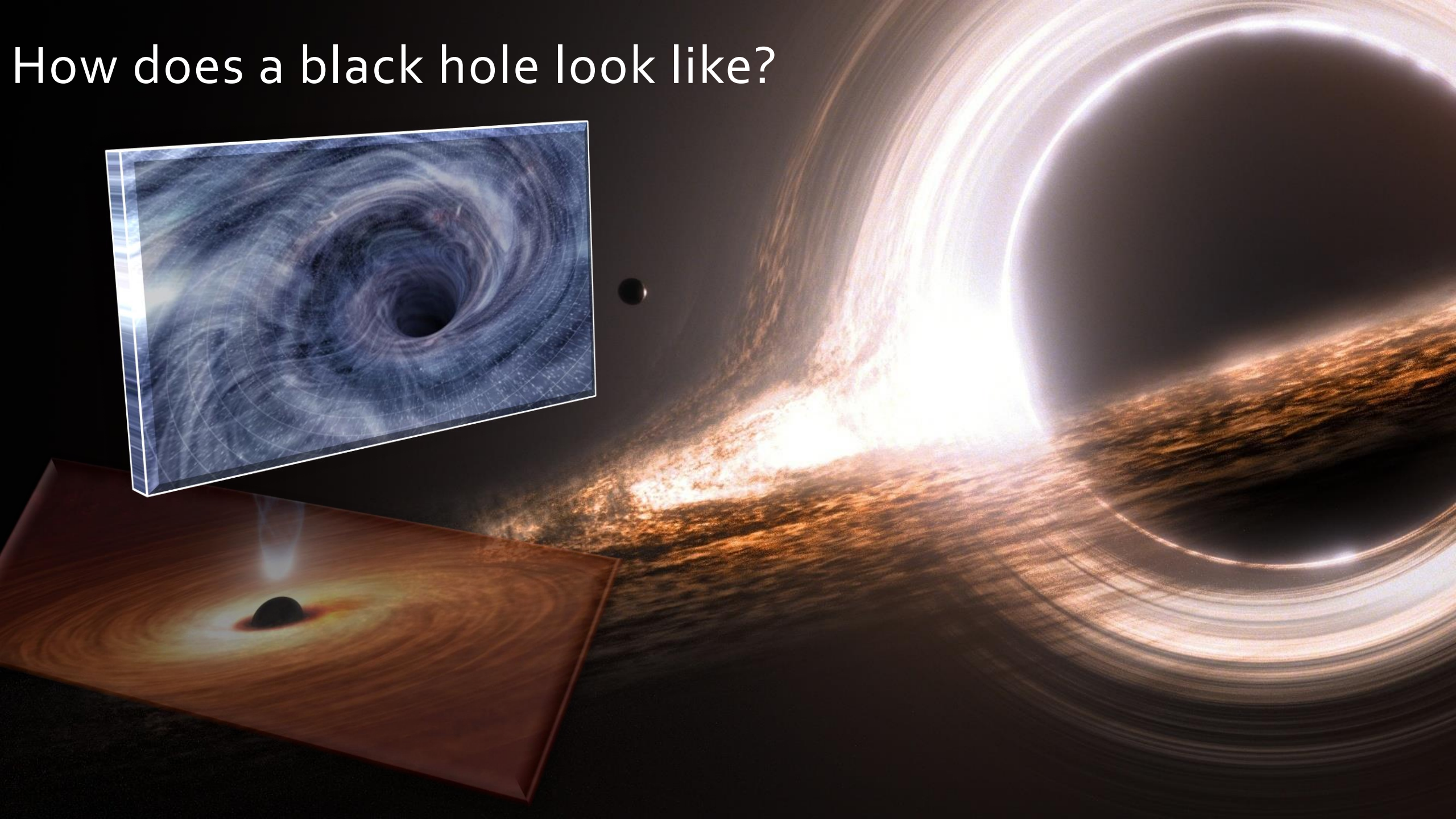
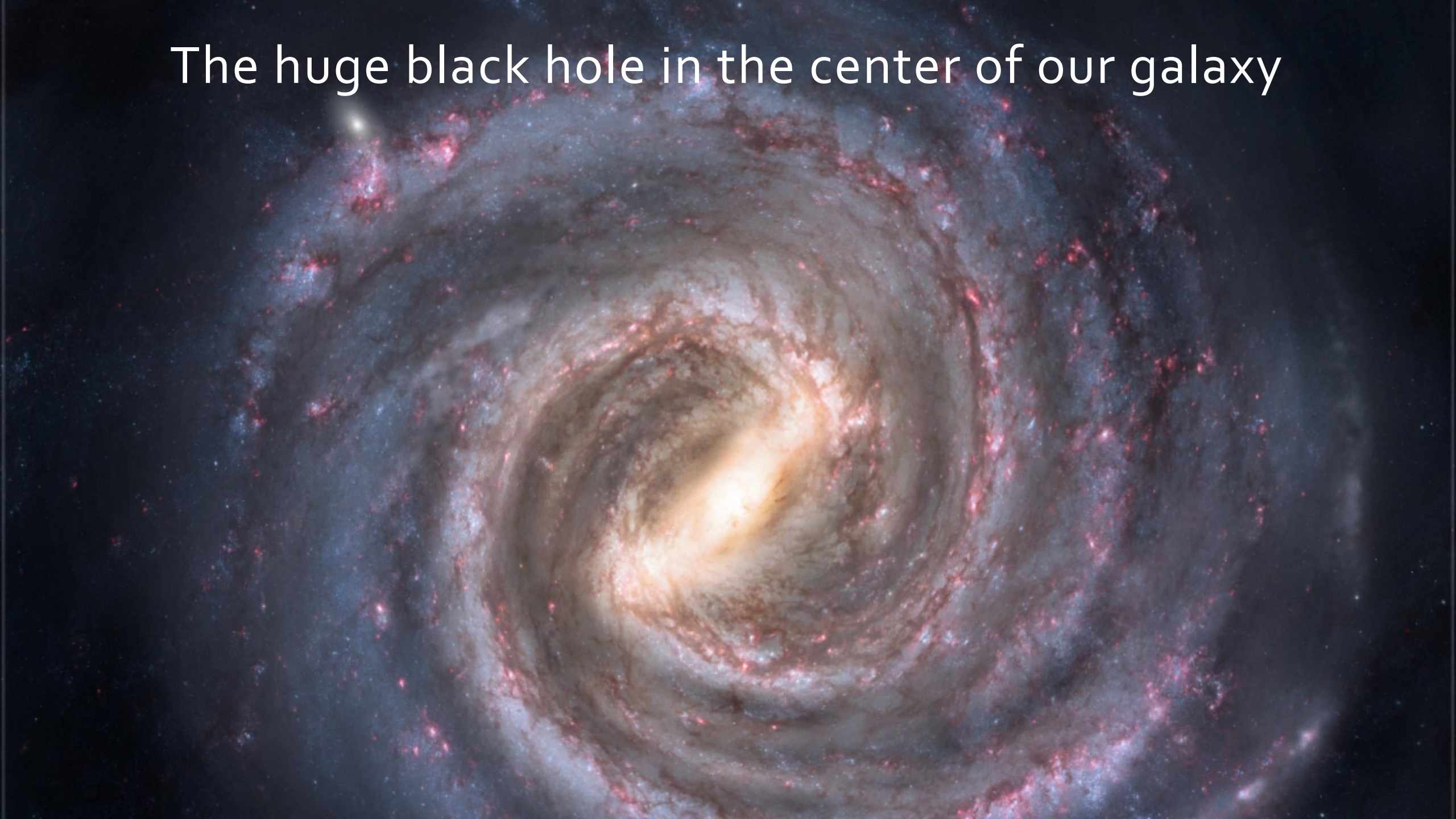


Abbildung 2.2: Raumzeitdiagramm der Schwarzschildmetrik in avancierten Eddington-Finkelstein Koordinaten.

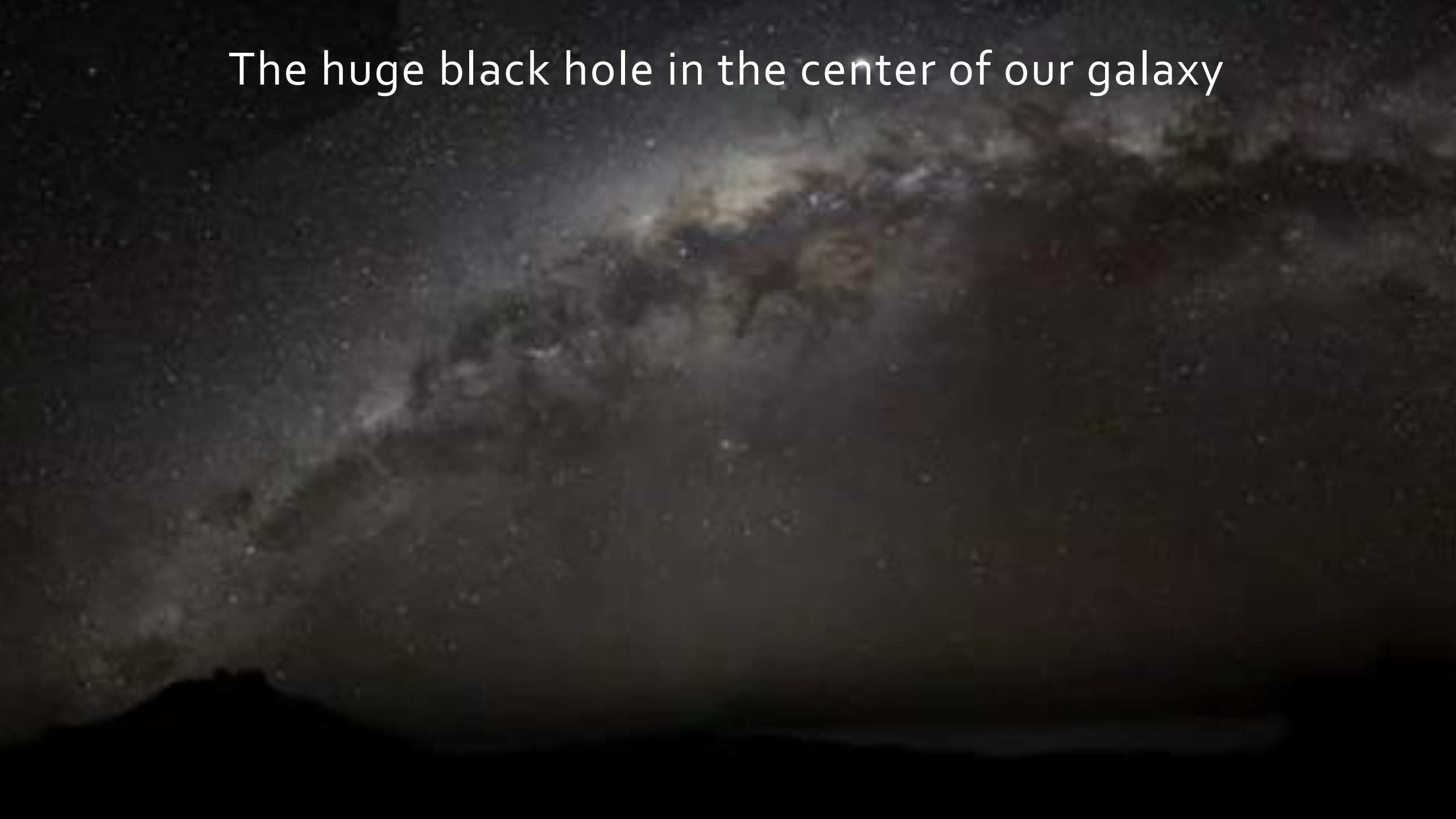
How does a black hole look like?



The huge black hole in the center of our galaxy



The huge black hole in the center of our galaxy





2009

Cloud of dust falls into the black hole

We will soon see the first picture of the black hole!

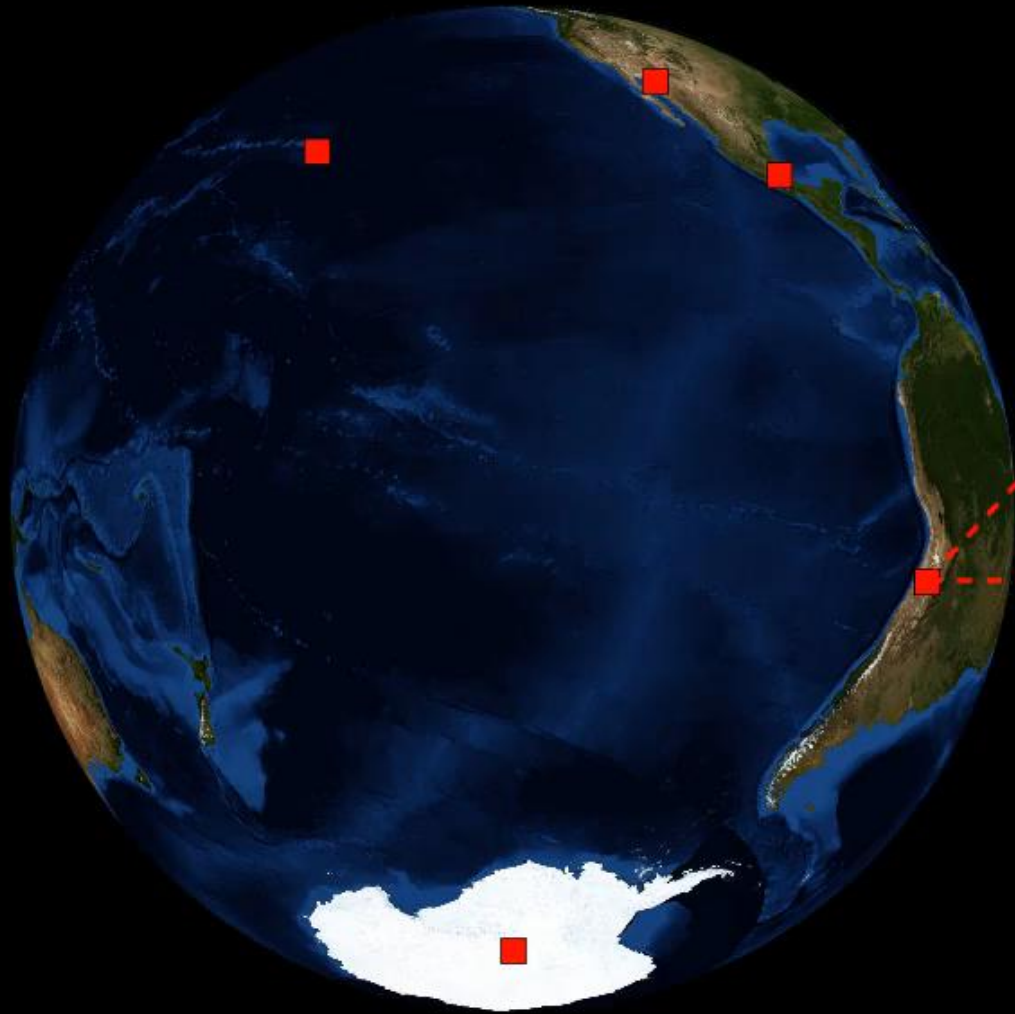


EU-Project **BlackHoleCam**

L.Rezzolla, H.Falke und M.Kramer

Black hole cam is a European funded project, which is a partner in the Event Horizon Telescope and not a separate network!

Event Horizon Telescope



Atacama Large
Millimeter Array (ALMA)



Coordinates: $23^{\circ} 01' 09''\text{S}$, $67^{\circ} 45' 12''\text{W}$

Diameter: 12m

Create a virtual radio telescope
the size of the earth, using the
shortest wavelength

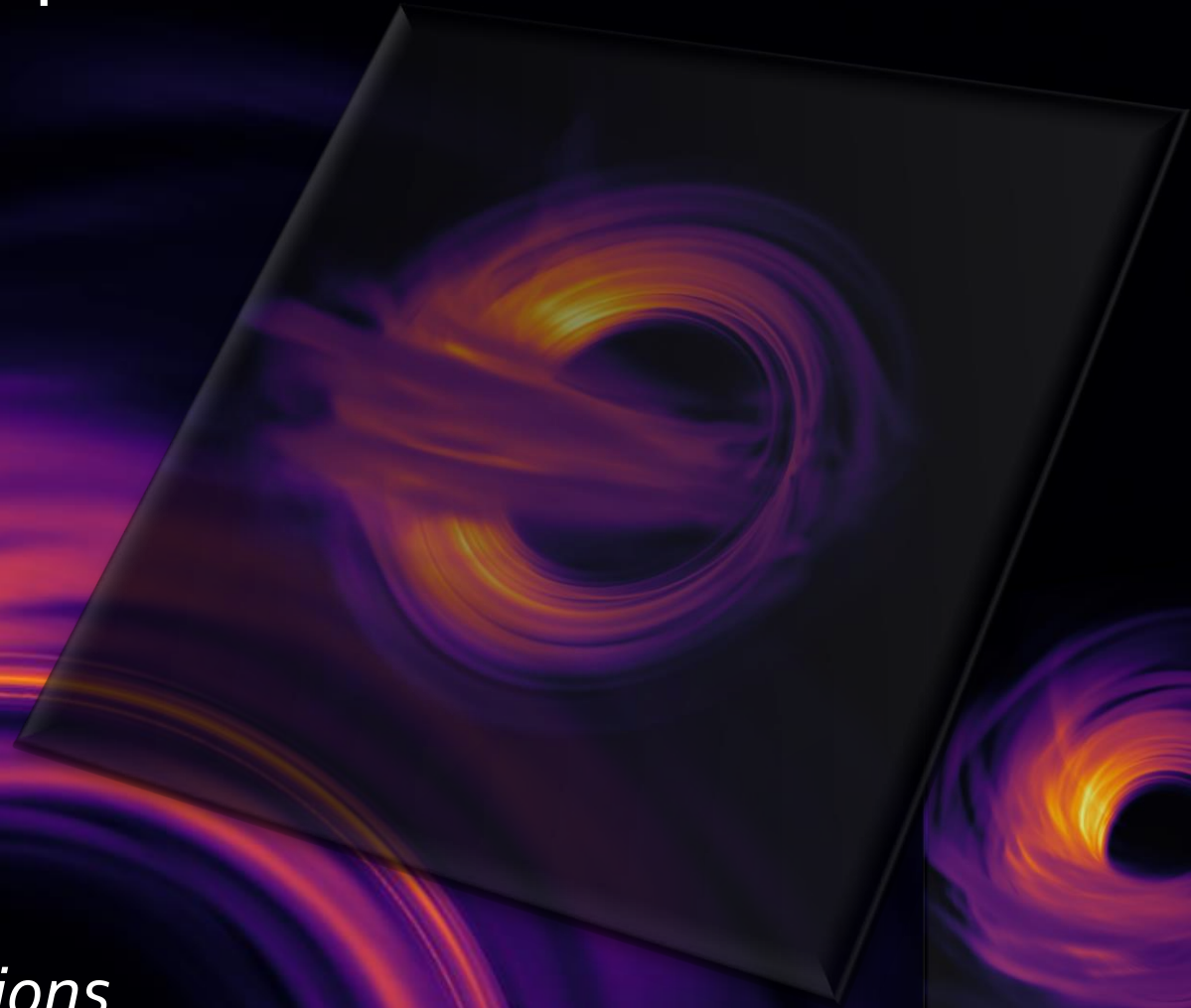
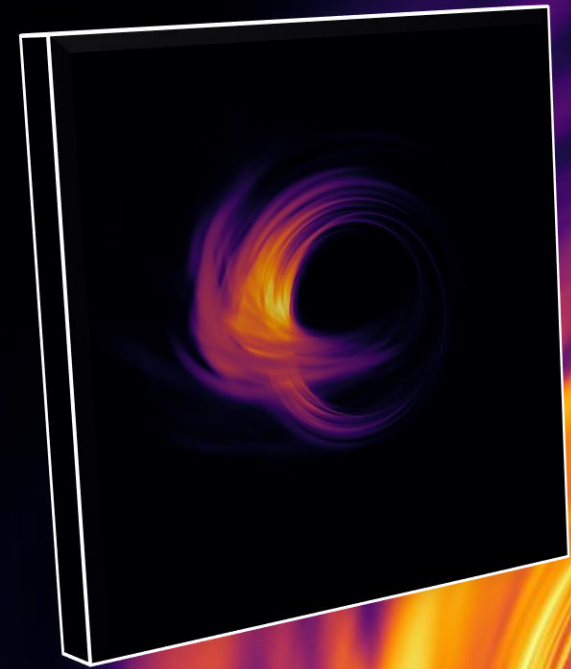
International collaboration project of Very Long Baseline Interferometry (VLBI)
at mm (sub-mm) wavelength

*Python-Animation from
Dr. Christian Fromm*

Bilder von zwei schwarzen Löchern werden erwartet

	M87	Sgr A*
Mass (M_{sun})	$3-6 \times 10^9$ (?)	4×10^6
Distance	16 Mpc	8.5 kpc
Luminosity	10^{44} erg/s	10^{36} erg/s
Mdot (M_{edd})	10^{-4}	10^{-8}
BH Spin Axis	Gal disk?	10-25 deg los
@ the BH?	Maybe	Yes
B field @ BH	60-130 G	10-100 G
Scattered?	No	yes
Shadow Size	640 AU	0.5 AU
Shadow Angle	20-40 μas	52 μas
GM/c ³	8 hrs	20 sec
Jet Power	$10^{42}-10^{43}$ erg/s	?

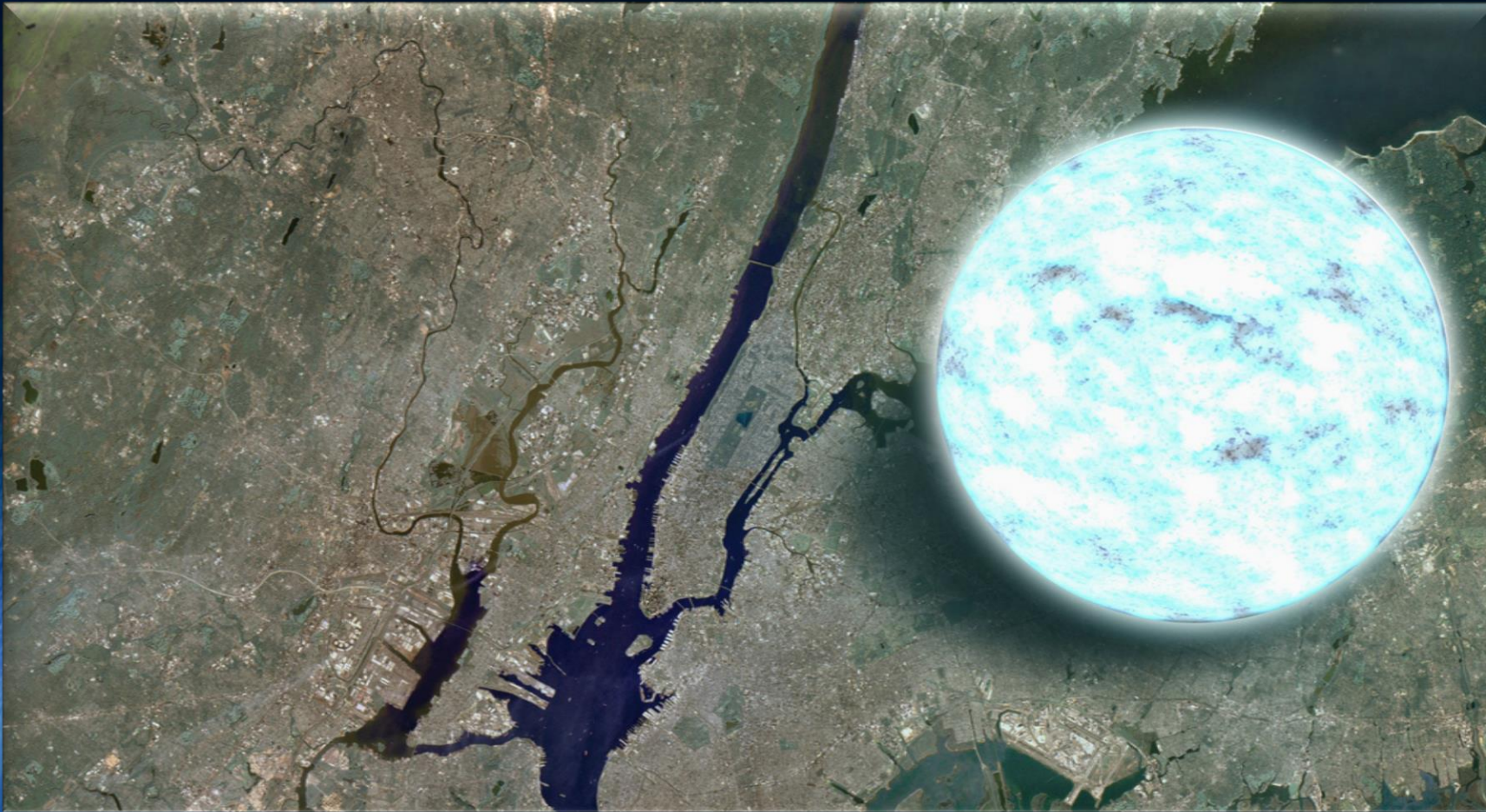
The simulated picture of the black hole



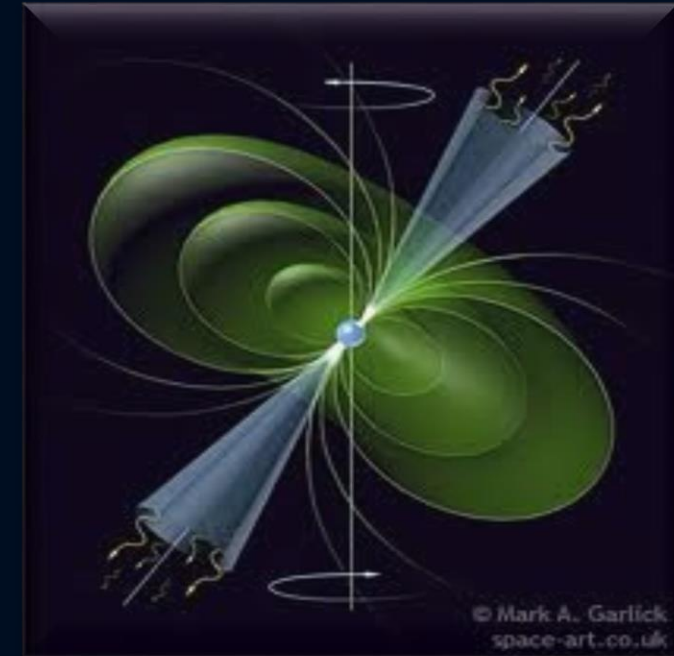
*Simulations
from
Dr. Ziri Younsi*

Properties of Neutron Stars

radius ~ 10 km, mass ~ 1-2 Sun masses, large magnetic fields ~ 10^{11} Tesla,
high rotation (up to 716 Hz)

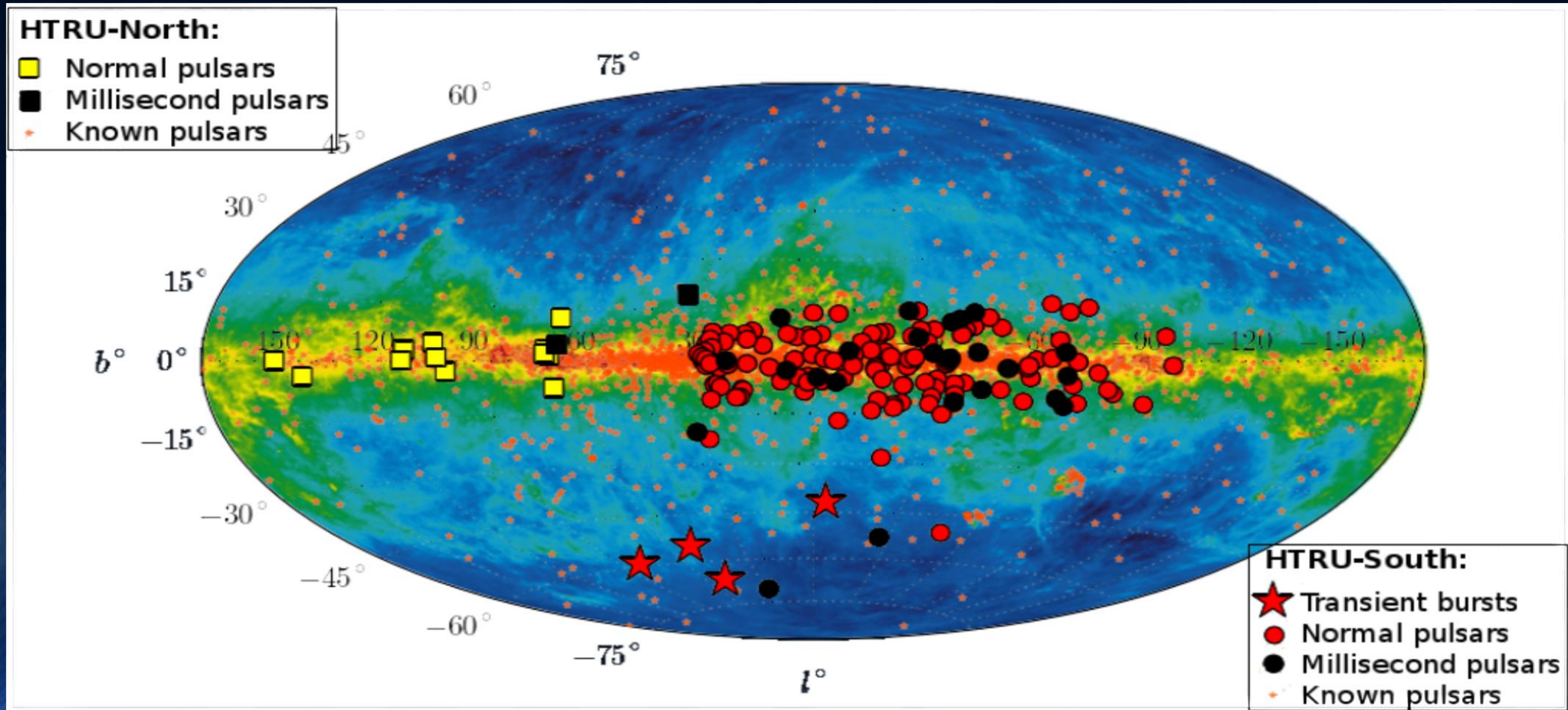


NASA/Goddard Space Flight Center



Pulsars are Rotating Neutron Stars

Currently we know about 2500 Neutron Stars



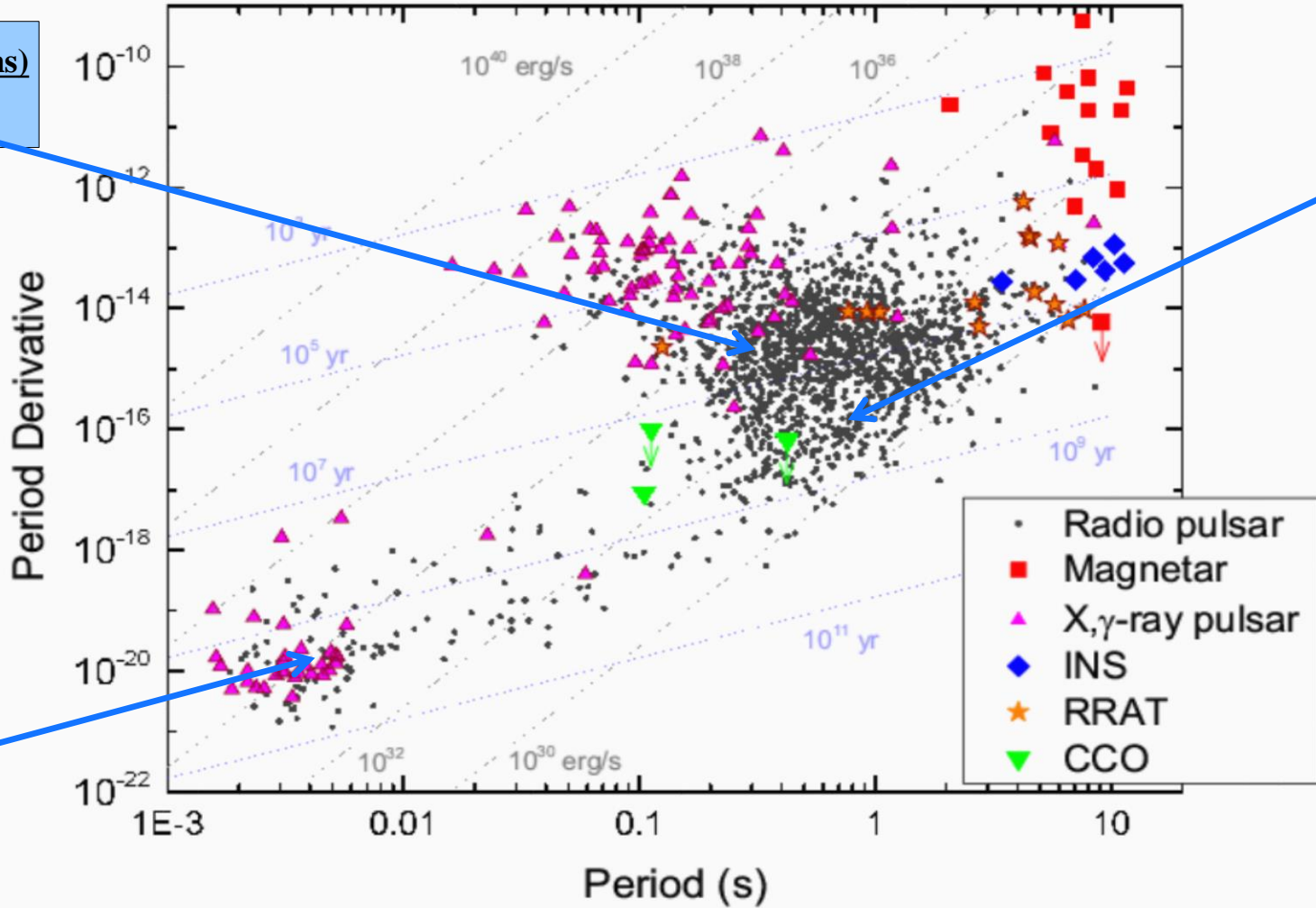
Millisecond and Second Pulsars



PSR B0531+21 (33.5 ms)
Crab Pulsar



PSR B0329+54 (0.715 s)



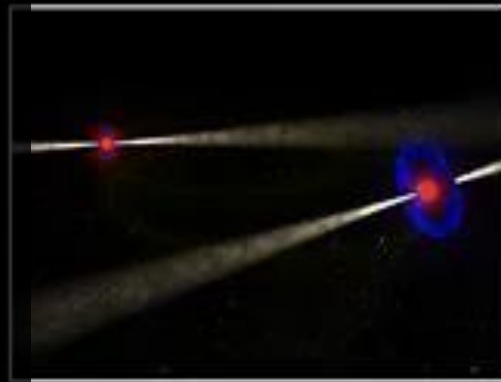
PSR B1937+21 (1.56 ms)

Binary Neutron Star Systems

Kramer, Wex, Class. Quantum Grav. 2009

The Double Pulsar (PSR J0737-3039A/B):
Observed in 2003
Eccentricity: 0.088
Pulsar A: $P=23$ ms, $M=1.3381(7)$
Pulsar B: $P=2.7$ s, $M=1.2489(7)$
Only separated 800,000 km from each other
Orbital period: 147 Minuten
Pulsar A is eclipsed by Pulsar B
(30 s for each orbit)

Distance shrinks
due to Gravitational Wave emission
→ They will collide in 85 Million Years!



Observed Masses in Binary Neutron Star Systems

Some of the known Neutron Stars (NS) are in binary systems:

NS-Planet, NS-(white dwarf) or NS-NS binary

PSR J1906+0746

144-ms Pulsar, observed in 2004

Orbital Period: 3.98 hours,

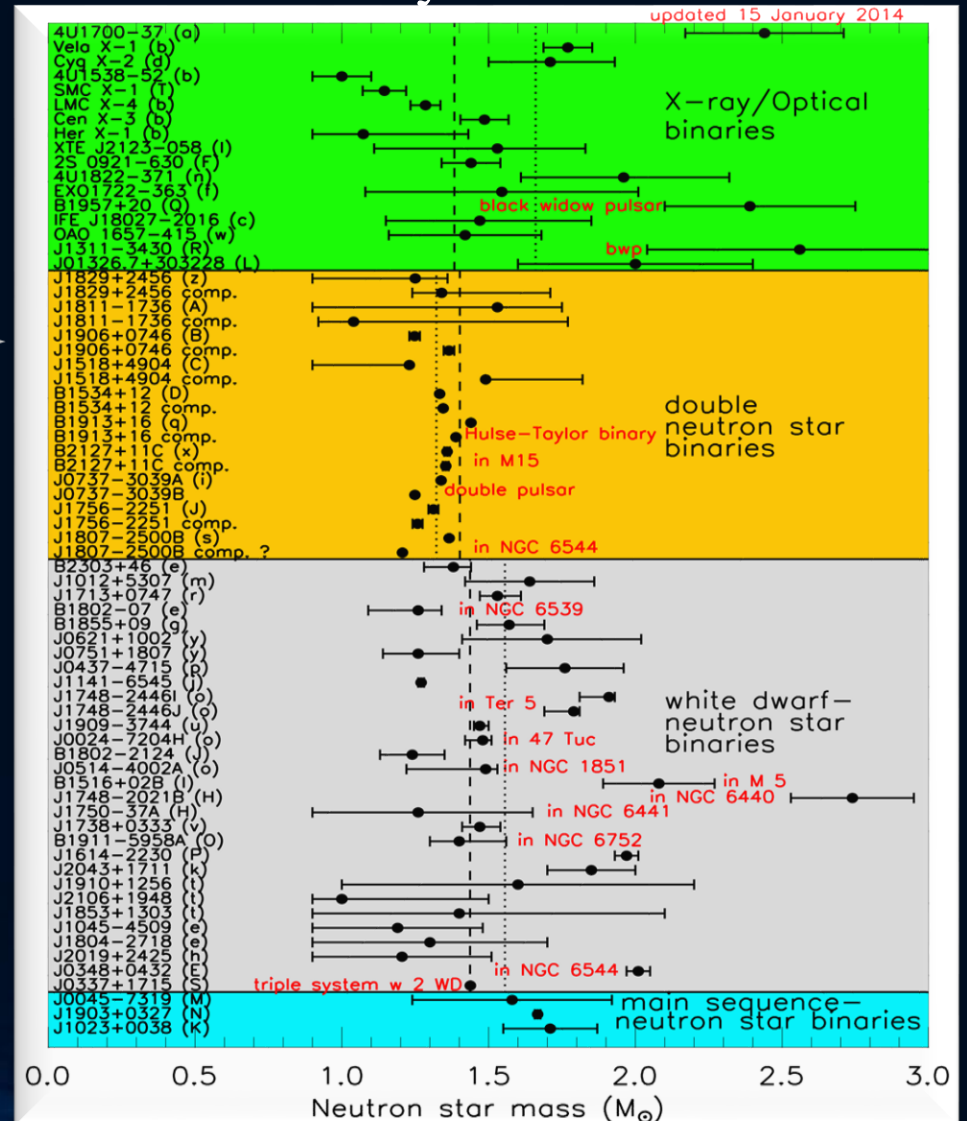
Eccentricity: 0.085

Pulsar Mass: 1.291(11)

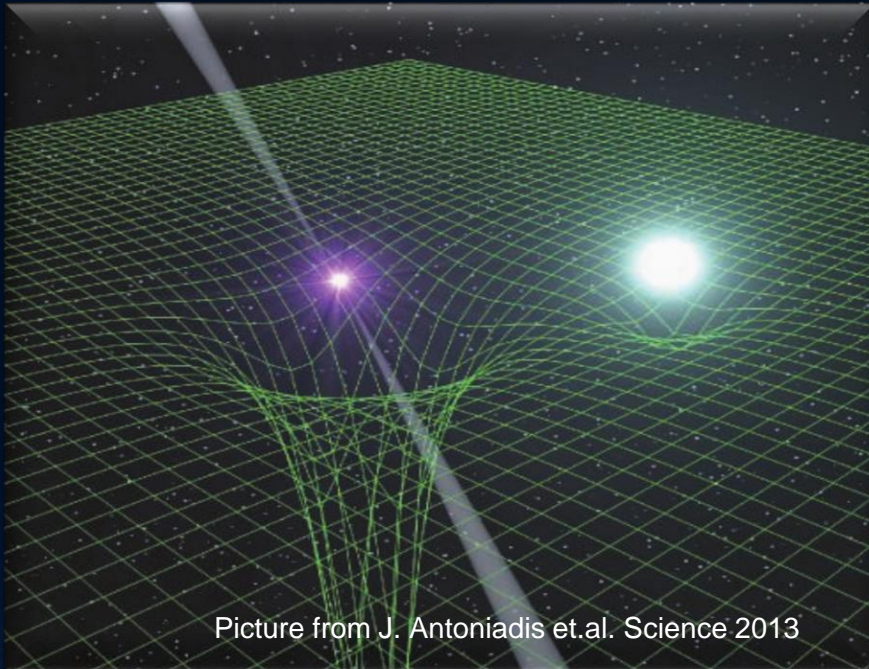
Mass Companion: 1.322(1)

Observed between 1998-2009,
after 2009, the pulsar disappeared
because of spin precession

Van Leeuwen et al, arXiv:1411.1518



A Two Solarmass Neutron Star



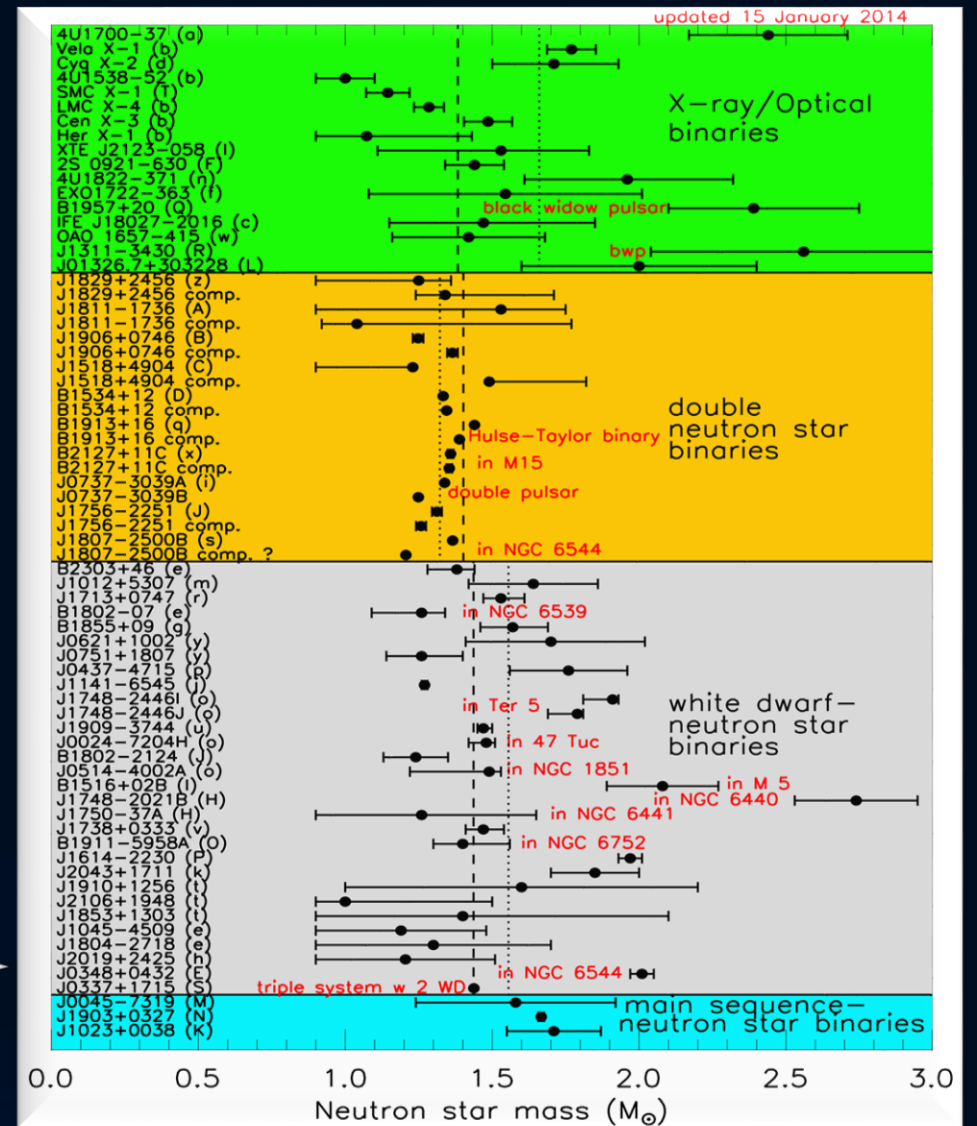
PSR J0348+0432

Orbital Period: 2.46 hours

Pulsar mass: 2.01 ± 0.04

Mass of the white dwarf:

$M = 0.172 \pm 0.003$



Die Einstein Gleichung

100 years ago, Albert Einstein presented the main equation of General Relativity: **The Einstein-Equation**

$$R_{\mu\nu} - \frac{1}{2}R g_{\mu\nu} = \frac{8\pi G}{c^4} T_{\mu\nu}$$

Spacetime curvature
Properties of the
Spacetime metric

Mass, Energy and Momentum of the System
Equation of State of elementary matter
(density, temperature)

From the Einstein Equation to the TOV equation

$$g_{\mu\nu} = \begin{pmatrix} e^{\nu(r)} & 0 & 0 & 0 \\ 0 & -e^{\lambda(r)} & 0 & 0 \\ 0 & 0 & -r^2 & 0 \\ 0 & 0 & 0 & -r^2 \sin^2 \theta \end{pmatrix} . \quad (2.45)$$

Das Einsetzen dieses Ansatzes der Metrik in die Einsteingleichung

$$G^\mu{}_\nu = R^\mu{}_\nu - \frac{1}{2} R g^\mu{}_\nu = 8\pi\kappa T^\mu{}_\nu \quad (2.46)$$

liefert das folgende System von Differentialgleichungen:

$$\begin{aligned} G^t{}_t &= -e^{-\lambda} \left(\frac{1}{r^2} - \frac{\lambda'}{r} \right) + \frac{1}{r^2} &= 8\pi\kappa T^t{}_t \\ G^r{}_r &= -e^{-\lambda} \left(\frac{1}{r^2} + \frac{\nu'}{r} \right) + \frac{1}{r^2} &= 8\pi\kappa T^r{}_r \\ G^\theta{}_\theta &= -\frac{e^{-\lambda}}{2} \left(\nu'' - \frac{\lambda'\nu'}{2} + \frac{(\nu')^2}{2} + \frac{\nu' - \lambda'}{r} \right) &= 8\pi\kappa T^\theta{}_\theta \\ G^\phi{}_\phi &= G^\theta{}_\theta &= 8\pi\kappa T^\phi{}_\phi \end{aligned} \quad (2.47)$$

The Energie-Momentum Tensor

1..3, $i \neq j$) vernachlässigen. Der Energieimpulstensor $T^{\mu\nu}$ einer solchen idealen Flüssigkeit, lokal betrachtet an seinem Ort, kann wie folgt geschrieben werden

$$T^{\mu\nu} = (\epsilon + P)u^\mu u^\nu - g^{\mu\nu} P \quad \text{mit: } u^\mu = \frac{dx^\mu}{d\tau} \quad , \quad (2.48)$$

wobei u^μ die 4er Geschwindigkeit der Materie ist, τ die lokale Eigenzeit an einem betrachteten Materiepunkt beschreibt ($d\tau = \sqrt{ds^2} = \sqrt{g_{tt}} dt$, t ist die Koordinatenzeit eines unendlich entfernten Beobachters), ϵ die Energiedichte und P der Druck der Materie ist.

The Tolman-Oppenheimer-Volkoff Equation

als die **Tollman-Oppenheimer-Volkoff (TOV) Gleichungen**

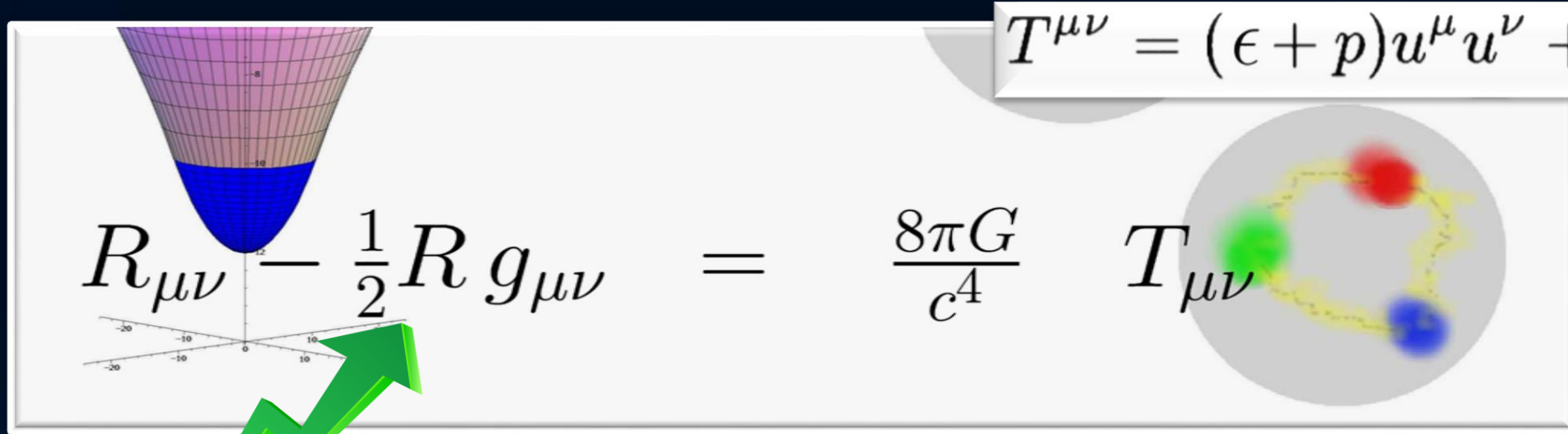
$$\begin{aligned}\frac{dP}{dr} &= -\frac{(\epsilon + P)4\pi r^3 + m}{r(r - 2m)} \\ m(r) &= \int_0^r 4\pi \tilde{r}^2 \epsilon(\tilde{r}) d\tilde{r} \\ \frac{d\nu}{dr} &= \frac{8\pi P r^3 + 2m}{r(r - 2m)} \quad ,\end{aligned}\tag{2.61}$$

wobei die raumzeitliche Struktur durch die folgenden Ausdrücke bestimmt ist

$$g_{\mu\nu} = \begin{pmatrix} e^{\nu(r)} & 0 & 0 & 0 \\ 0 & -\left(1 - \frac{2m(r)}{r}\right)^{-1} & 0 & 0 \\ 0 & 0 & -r^2 & 0 \\ 0 & 0 & 0 & -r^2 \sin^2\theta \end{pmatrix}$$
$$ds^2 = e^{\nu(r)} dt^2 + \left(1 - \frac{2m(r)}{r}\right)^{-1} dr^2 - r^2 (d\theta^2 + \sin^2\theta d\phi^2) .$$

Neutron Stars

(Simplest model: Nonrotating, spherical symmetric, static, ideal fluid)



$$R_{\mu\nu} - \frac{1}{2}R g_{\mu\nu} = \frac{8\pi G}{c^4} T_{\mu\nu}$$

$$T^{\mu\nu} = (\epsilon + p)u^\mu u^\nu + pg^{\mu\nu}$$

Space-Time Metric

$$g_{\mu\nu} = \begin{pmatrix} e^{\nu(r)} & 0 & 0 & 0 \\ 0 & -\left(1 - \frac{2m(r)}{r}\right)^{-1} & 0 & 0 \\ 0 & 0 & -r^2 & 0 \\ 0 & 0 & 0 & -r^2 \sin^2\theta \end{pmatrix}$$

Tolman-Oppenheimer-Volkoff Equation

$$\frac{dP}{dr} = -\frac{(\epsilon + P)4\pi r^3 + m}{r(r - 2m)}$$

$$m(r) = \int_0^r 4\pi \tilde{r}^2 \epsilon(\tilde{r}) d\tilde{r}$$

$$\frac{d\nu}{dr} = \frac{8\pi P r^3 + 2m}{r(r - 2m)},$$

The Einstein Equation

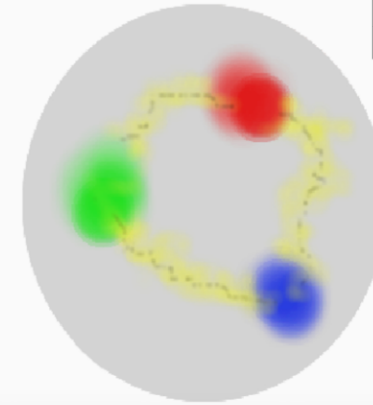
ART	<u>Yang-Mills-Theories</u>
$D_\beta v^\alpha = \partial_\beta v^\alpha + \Gamma_{\sigma\beta}^\alpha v^\sigma$	$D_{\beta a}{}^b = \partial_\beta 1_a{}^b + ig A_{\beta a}{}^b$
$R^\delta{}_{\mu\alpha\beta} v^\mu = [D_\alpha, D_\beta] v^\delta$	$F_{\alpha\beta a}{}^b = \frac{1}{ig} [D_{\alpha a}{}^c, D_{\beta c}{}^b]$
$R^\delta{}_{\mu\alpha\beta} = \Gamma_{\mu\alpha \beta}^\delta - \Gamma_{\mu\beta \alpha}^\delta$ $+ \Gamma_{\nu\beta}^\delta \Gamma_{\mu\alpha}^\nu + \Gamma_{\nu\alpha}^\delta \Gamma_{\mu\beta}^\nu$	$= A_{\beta a}{}^b _\alpha - A_{\alpha a}{}^b _\beta$ $+ \frac{1}{ig} [A_{\alpha a}{}^c, A_{\beta c}{}^b]$
$\mathcal{L}_G = R + \underbrace{(c_1 R_{\mu\nu} R^{\mu\nu} + \dots)}_{\equiv 0 \text{ for ART}}$	$\mathcal{L}_{YM} = \frac{1}{4} F_{\mu\nu a}{}^b F^{\mu\nu}{}_a{}^b$

Quantum ChromoDynamic:

($SU(3)_{(c)}$ - Color Yang-Mills-Gauge Theory)

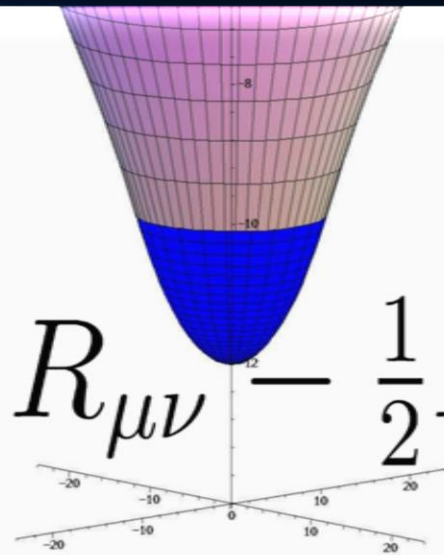
$$D_{\beta A}{}^B = \partial_\beta 1_A{}^B + ig G_{\beta A}{}^B$$

$A, B = \text{red, green, blue}$



$$\psi_A^f = \begin{pmatrix} \psi_r^f \\ \psi_g^f \\ \psi_b^f \end{pmatrix}$$

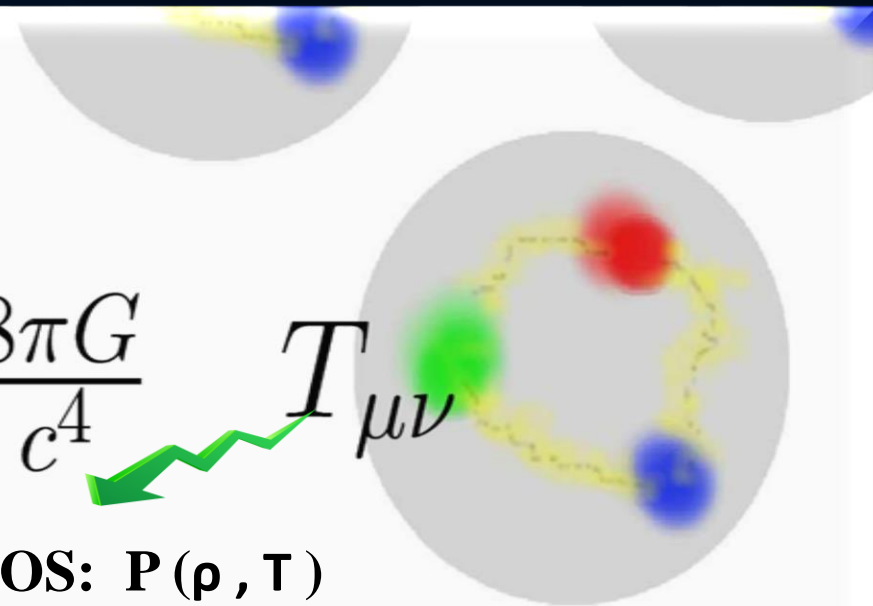
Confinement
chiral symmetry, ...



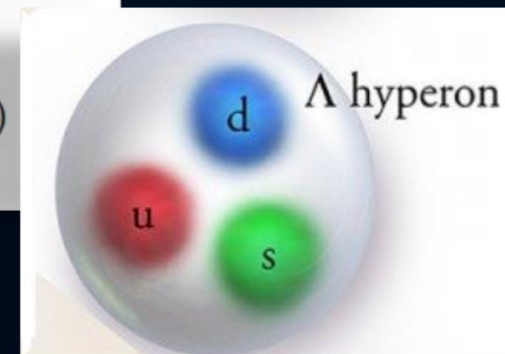
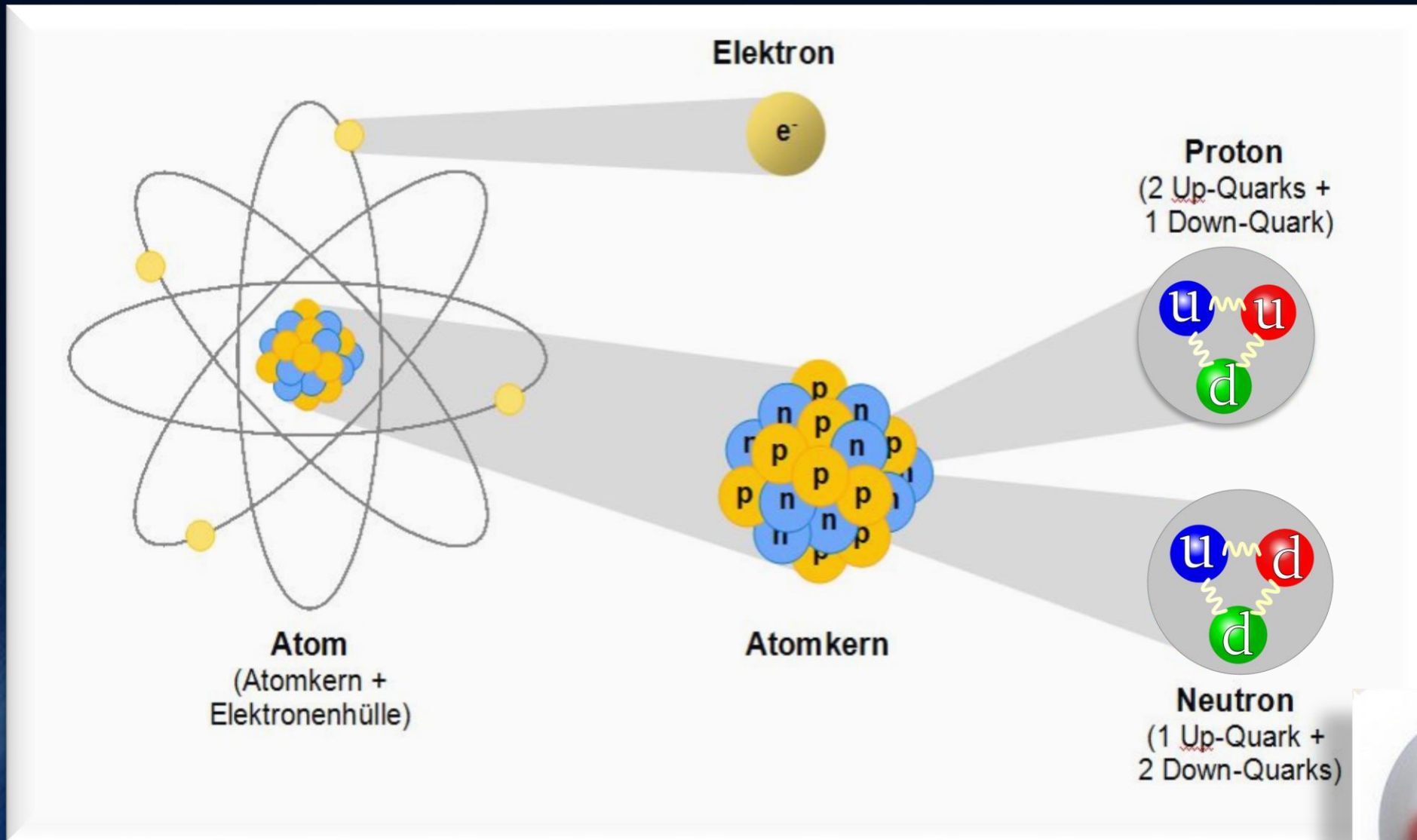
$$R_{\mu\nu} - \frac{1}{2} R g_{\mu\nu} =$$

$$\frac{8\pi G}{c^4} T_{\mu\nu}$$

EOS: $P(\rho, T)$



Elementary Matter



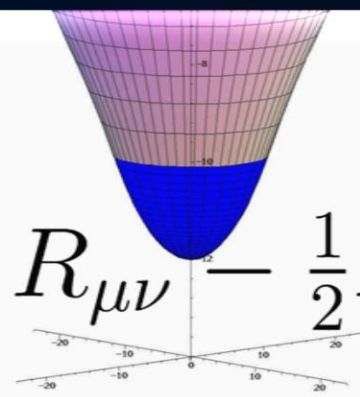
If the densities or temperatures are very high, additional Hyperonic Particles can occur

Einordnungshierarchie			Teilchen		Ladung	Spin	Masse	Quarkinhalt
HADRONEN	MESONEN	(pseudo)-skalare Mesonen	Pion	π^0	0	0	135	$(u\bar{u} - d\bar{d})/\sqrt{2}$
				π^+	1	0	139.6	$u\bar{d}$
				π^-	-1	0	139.6	$\bar{u}d$
			Kaon	K^0	0	0	497.7	$d\bar{s}$
				K^+	1	0	493.6	$u\bar{s}$
				K^-	-1	0	493.6	$\bar{u}s$
		Eta-Meson	η	0	0	548.8	$c_1(u\bar{u} + d\bar{d}) + c_2s\bar{s}$	
		Vektor Mesonen	Rho-Meson	ρ^0	0	1	770	$u\bar{u}$
				ρ^+	1	1	770	$u\bar{d}$
				ρ^-	-1	1	770	$d\bar{u}$
	Omega		ω	0	1	782	$d\bar{d}$	
	Phi		ϕ	0	1	1020	$s\bar{s}$	
	Tensor Mesonen		A_2	0	2	1310	-	
		f-Meson	f	0	2	1271	-	
	Mesonen Resonanzen	Mesonen	J/Psi	J/ψ	0	1	3096.9	$c\bar{c}$
			Psi-Meson	ψ	0	1	3685	$c\bar{c}$
Upsilon			Υ	0	1	9460	$b\bar{b}$	
BARIONEN	Nukleonen	Neutron	n	0	1/2	939.57	udd	
		Proton	p	1	1/2	938.27	uud	
	Hyperonen	Lambda	Λ	0	1/2	1115.6	uds	
			Sigma	Σ^0	0	1/2	1192.6	uds
				Σ^+	1	1/2	1189.4	uus
		Σ^-		-1	1/2	1197.4	dds	
		Xi	Ξ^0	0	1/2	1314.9	uss	
			Ξ^-	-1	1/2	1321.3	dss	
		Omega	Ω^-	-1	3/2	1672.4	sss	
	Barionische Resonanzen	Delta	Δ^0	0	3/2	1232	udd	
			Δ^+	1	3/2	1232	uud	
			Δ^-	-1	3/2	1232	ddd	

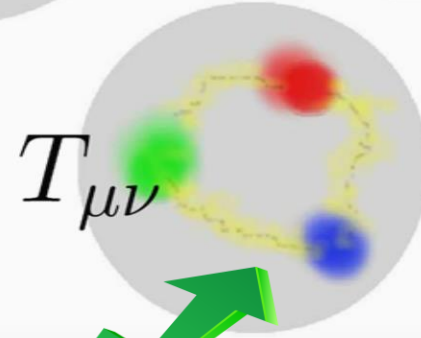
Hadronic Particles (Barions and Mesons)

Neutron Stars (NS)

 \sum_B
 $(p, n, \Lambda, \Sigma^-, \Sigma^0, \Sigma^+, \Xi^-, \Xi^0)$



$$R_{\mu\nu} - \frac{1}{2}R g_{\mu\nu} = \frac{8\pi G}{c^4} T_{\mu\nu}$$



Relativistic Mean-Field Hadronic Models

$$\begin{aligned} \mathcal{L} = & \sum_B \bar{\psi}_B (i\partial - m_B) \psi_B + \frac{1}{2} \partial^\mu \sigma \partial_\mu \sigma - \frac{1}{2} m_\sigma^2 \sigma^2 - \frac{a}{3} \sigma^3 - \frac{b}{4} \sigma^4 - \frac{1}{4} \omega^{\mu\nu} \omega_{\mu\nu} \\ & + \frac{1}{2} m_\omega^2 \omega^\mu \omega_\mu - \frac{1}{4} \vec{\rho}^{\mu\nu} \vec{\rho}_{\mu\nu} + \frac{1}{2} m_\rho^2 \vec{\rho}^\mu \vec{\rho}_\mu + \sum_B \bar{\psi}_B (g_\sigma \sigma + g_\omega \omega^\mu \gamma_\mu + g_\rho \vec{\rho}^\mu \gamma_\mu \vec{T}_B) \psi_B \end{aligned}$$

$$\begin{aligned} \mathcal{L}^{YY} = & \frac{1}{2} (\partial^\mu \sigma^* \partial_\mu \sigma^* - m_{\sigma^*}^2 \sigma^{*2}) - \frac{1}{4} \phi^{\mu\nu} \phi_{\mu\nu} + \frac{1}{2} m_\phi^2 \phi^\mu \phi_\mu \\ & + \sum_Y \bar{\psi}_Y (g_{\sigma^* Y} \sigma^* + g_{\phi Y} \phi^\mu \gamma_\mu) \psi_Y \quad , \end{aligned}$$

$$\mathcal{L}_{\text{lep}} = \sum_{l=e,\mu} \bar{\psi}_l [i\gamma_\mu \partial^\mu - m_l] \psi_l$$

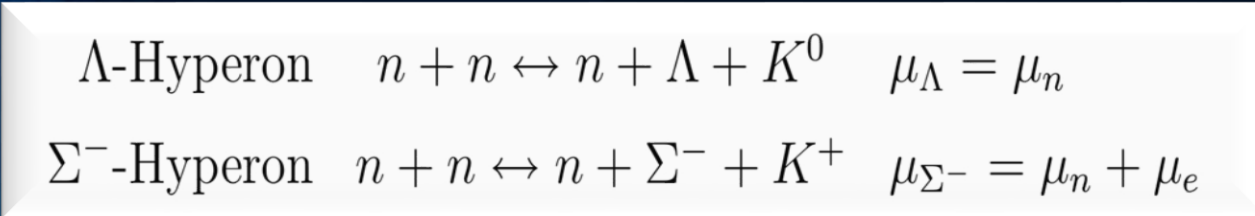
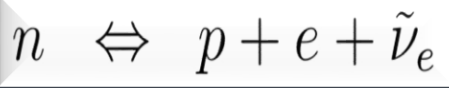
Composition of Neutron Star Matter

Neutron star matter conditions:

Charge Neutrality

β -equilibrium

Strangeness production

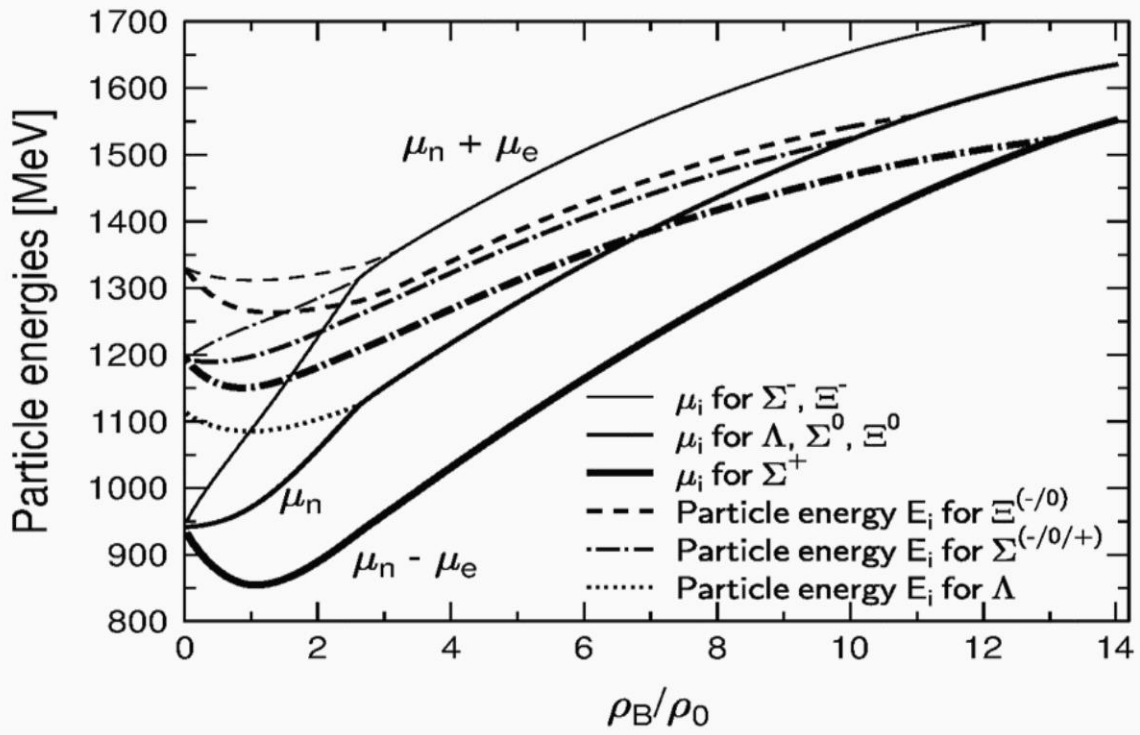
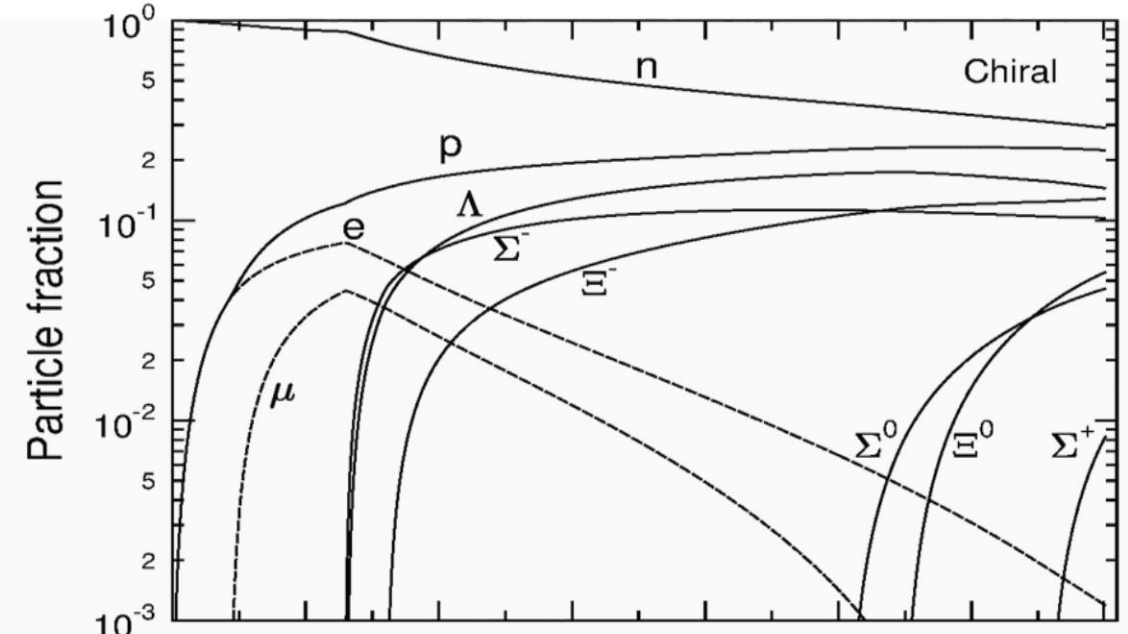


$$E_i(k) = E_i^*(k) + g_{i\omega}\omega_0 + g_{i\phi}\phi_0 + g_{i\rho}I_{3i}\rho_0$$

$$E_i^*(k) = \sqrt{k_i^2 + m_i^{*2}}$$

$$\mu_i = b_i\mu_n - q_i\mu_e$$

Particle composition vs baryonic density ➔



M. Hanauske, D. Zschiesche, S. Pal, S. Schramm, H. Stöcker, and W. Greiner, *Astrophys. J.* 537, 958 (2000)

Nuklear and Neutron Star Matter

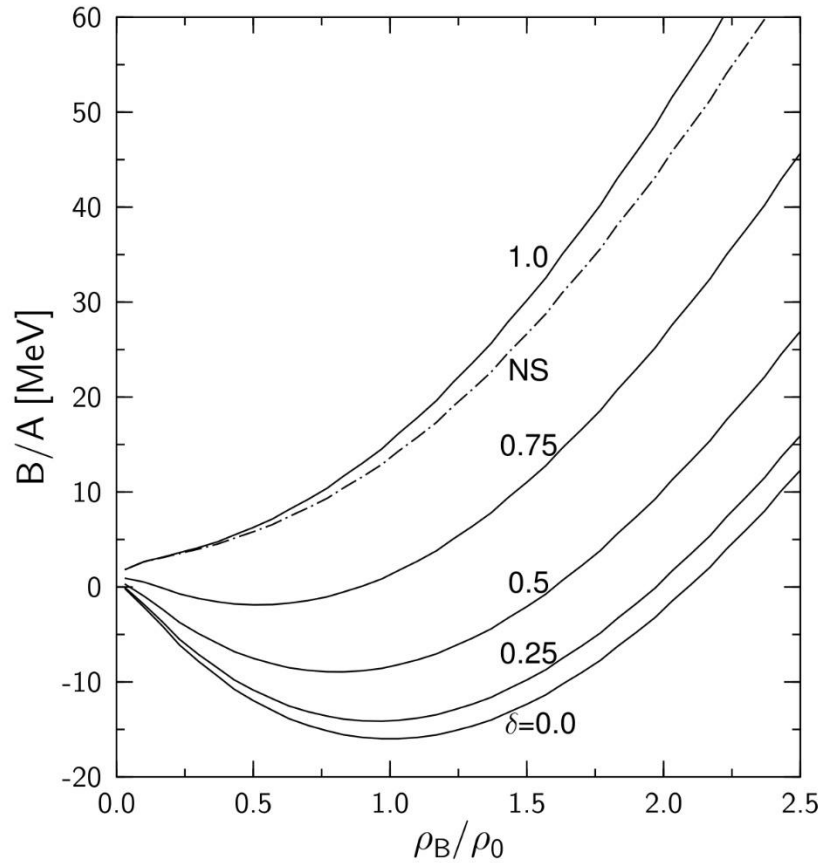
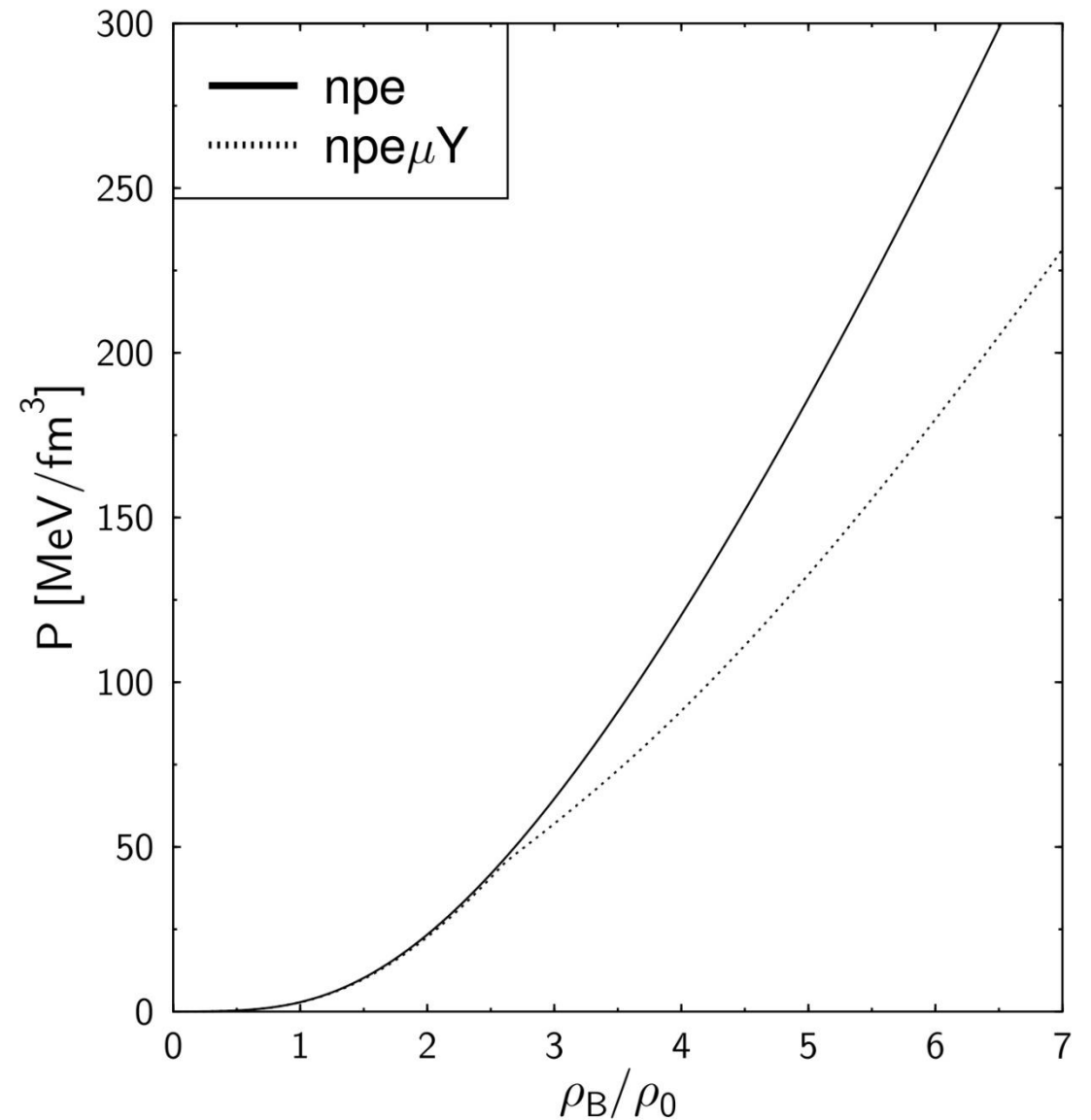
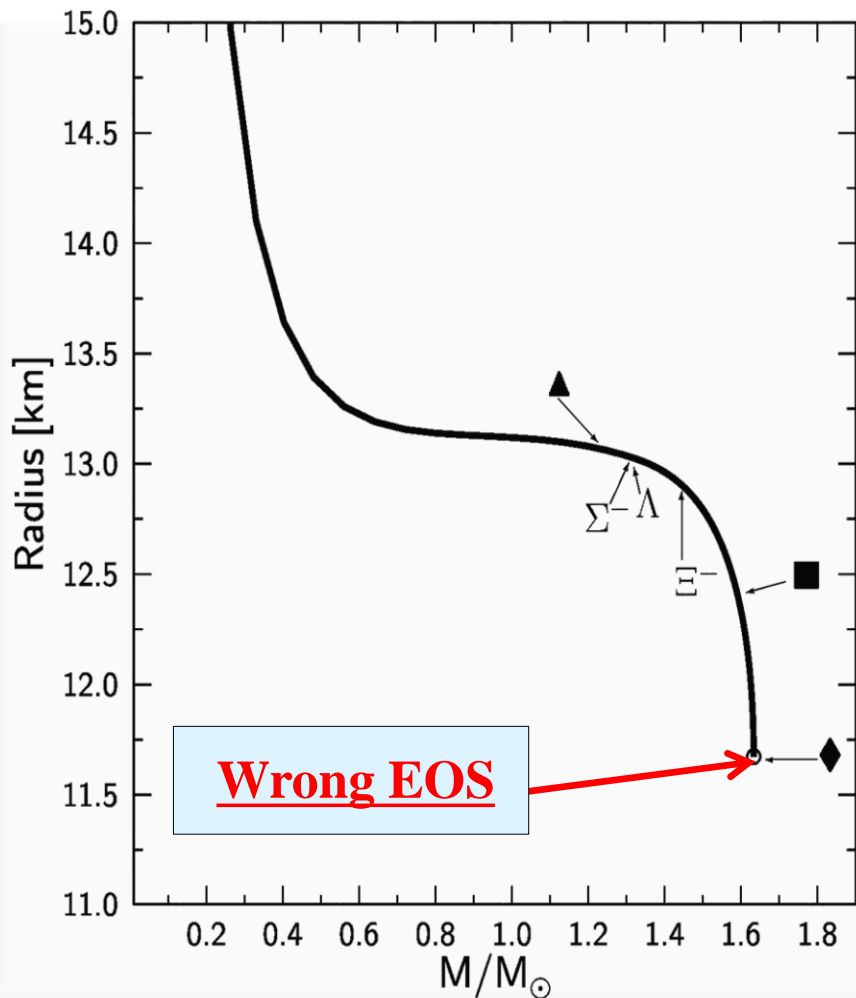


Abbildung 3.1: Bindungsenergie pro Nukleon B/A in Abhängigkeit der baryonischen Dichte ρ_B/ρ_0 ($\rho_0 = 0.15 \text{ fm}^{-3}$) für unterschiedliche Werte der Neutron-Proton-Asymmetrie ($\delta = (\rho_n - \rho_p)/\rho_B$) berechnet im hadronischen chiralen Modell. Die mit 'NS' bezeichnete Kurve beschreibt ladungsneutrale Neutronensternmaterie im β -Gleichgewicht bestehend aus Nukleonen und Elektronen.

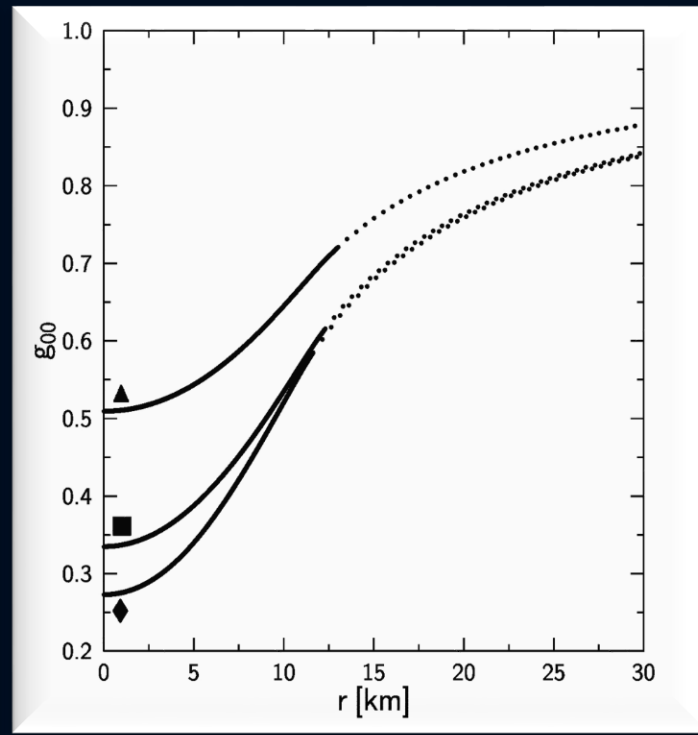
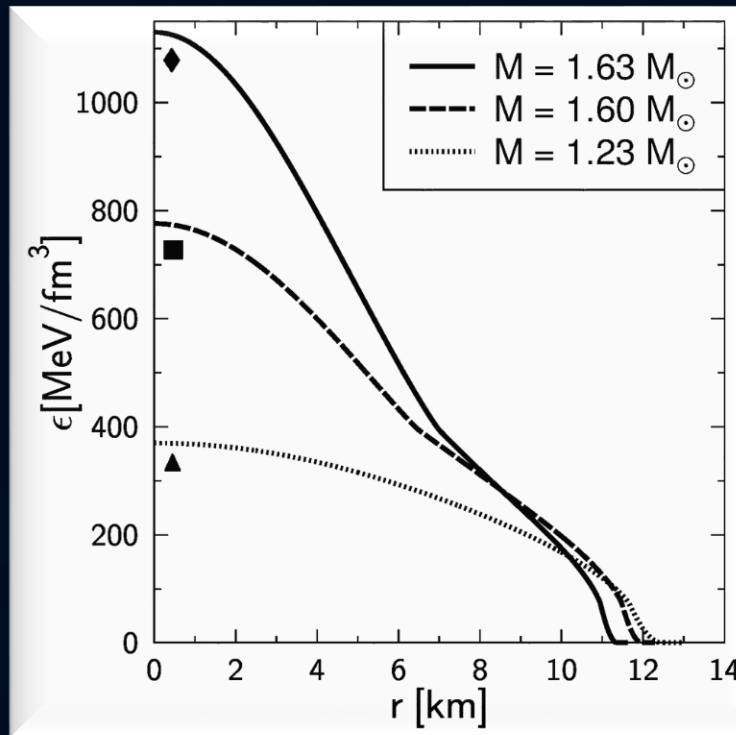


Neutron Star Properties

Left: The neutron star radius as a function of its mass. A low, middle and high density star is shown. Additionally the onset of hyperonic particles is visualized.

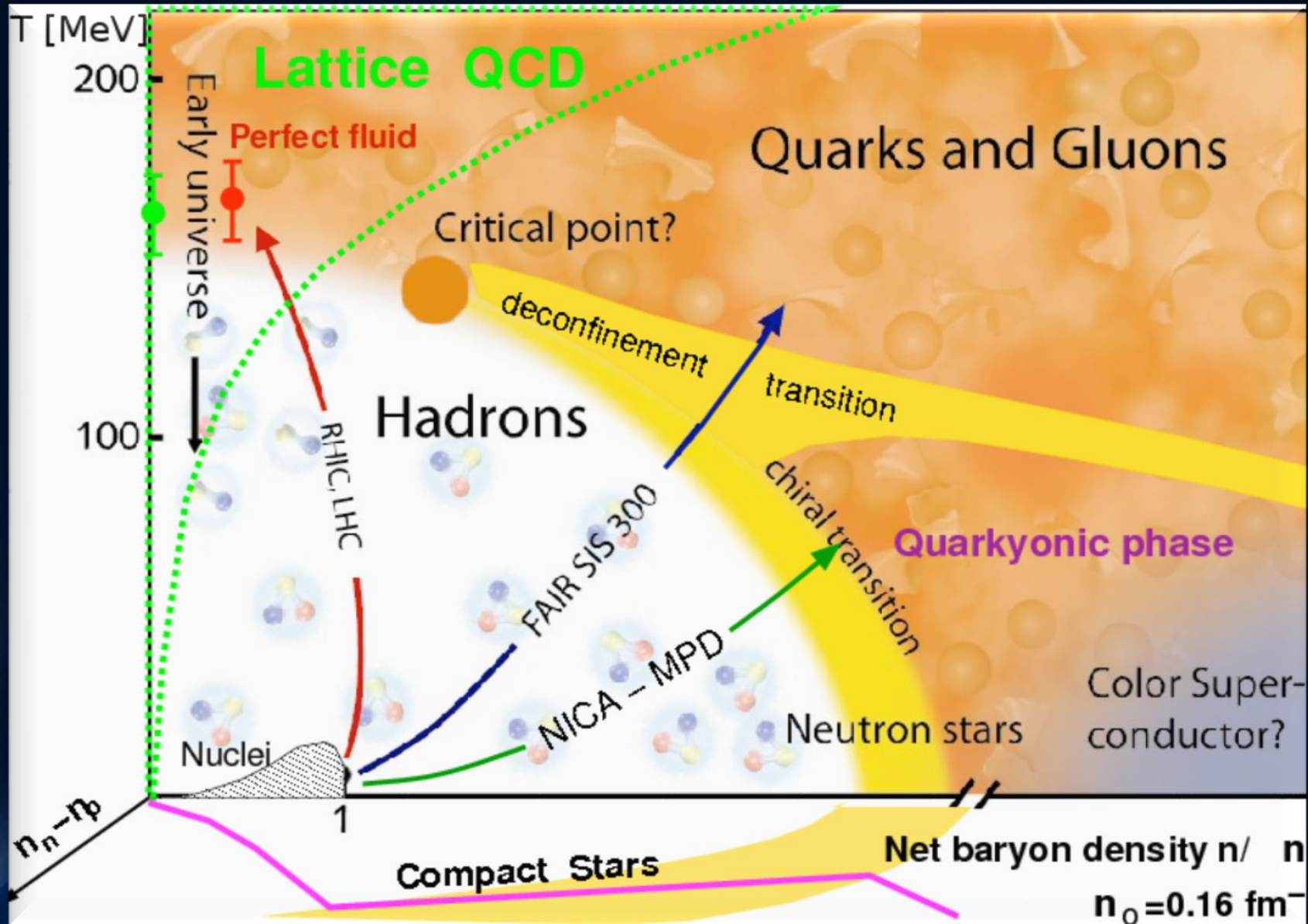


Middle: Energy density profiles of three neutron stars with different central densities and masses. The low density stars do not contain any hyperons, whereas the other two stars do have hyperons in their inner core.

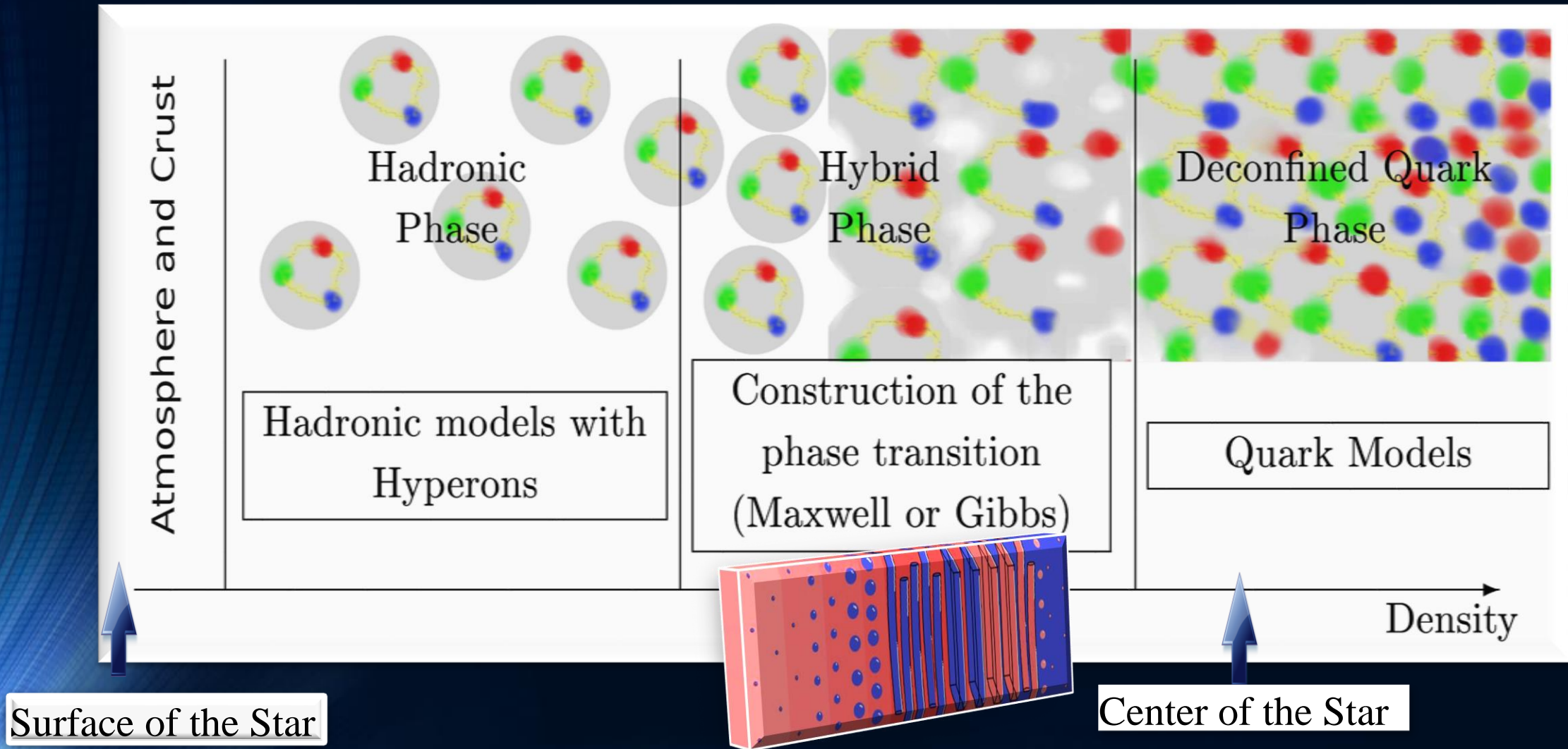


Right: Time-time component of the metric tensor as a function of the radial coordinate. The solid line corresponds to the inner TOV-solution, whereas the dotted curve depicts the outer Schwarzschild part.

The Hadron-Quark Phase Transition

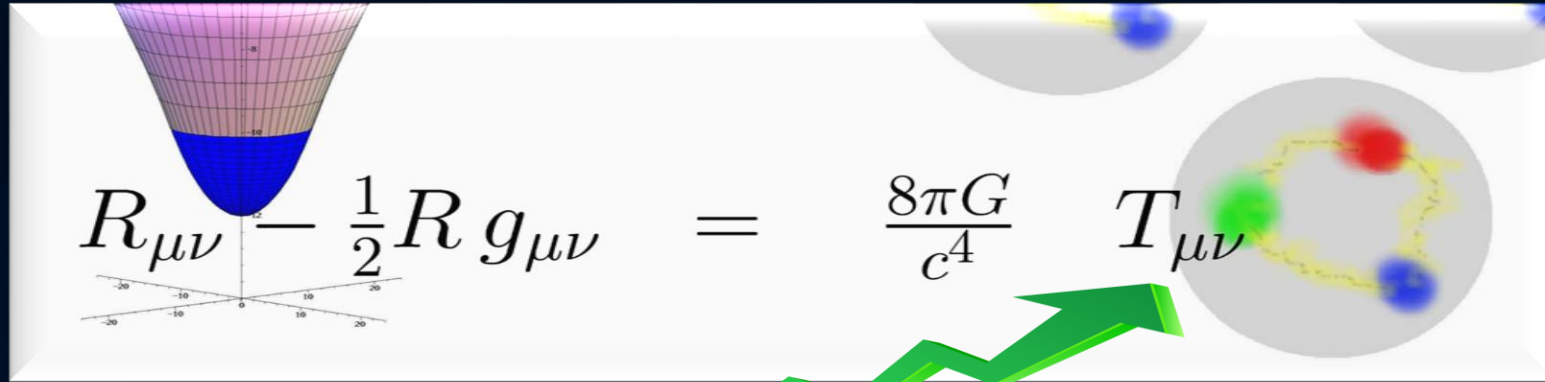


The QCD – Phase Transition and the Interior of a Hybrid Star



See: *Stable hybrid stars within a SU(3) Quark-Meson-Model*,
A.Zacchi, M.Hanuske, J.Schaffner-Bielich, PRD 93, 065011 (2016)

Hybrid Stars



Hadronic Model + Quark Model (eg. NJL model or MIT-Bag model)

Lagrangian density of the NJL model

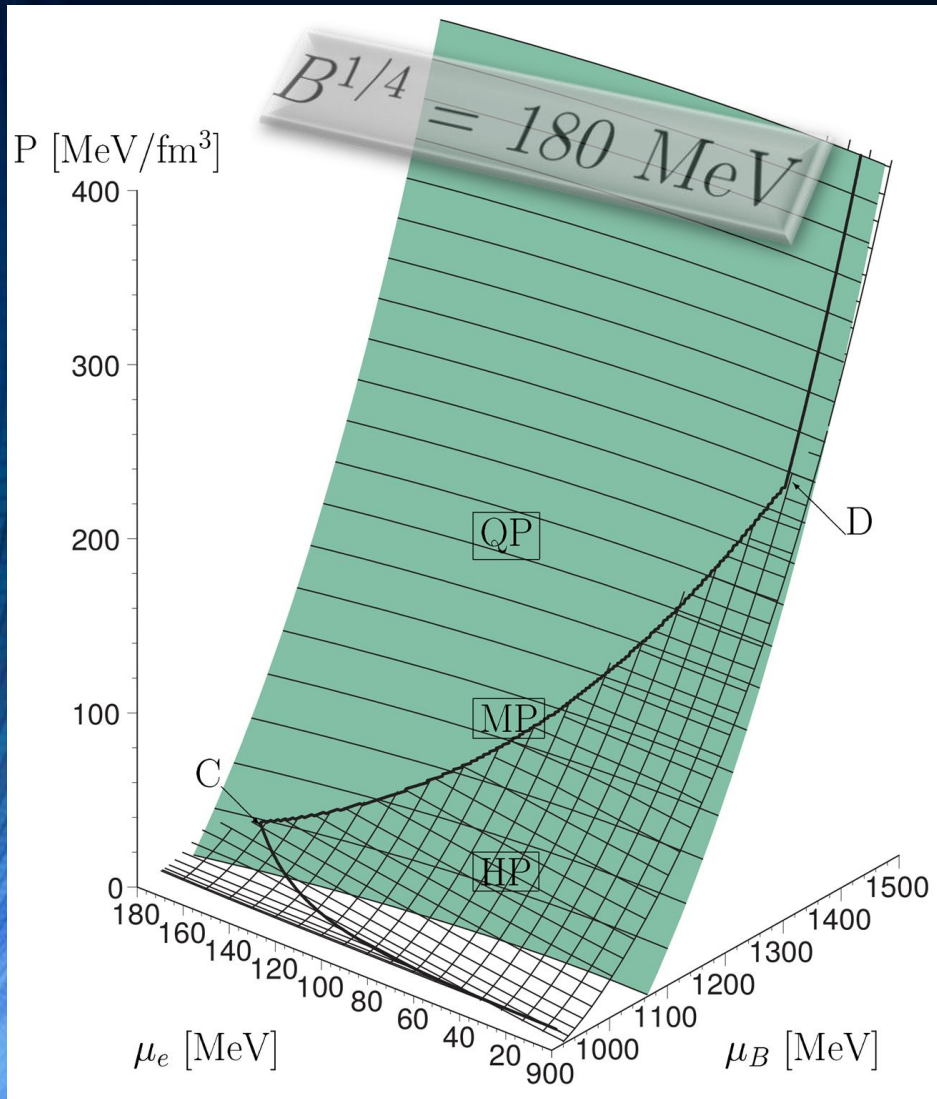
$$\begin{aligned}
 \mathcal{L} = & \underbrace{\bar{\psi} (i \not{\partial} - \hat{m}_0) \psi}_{\text{Kinetic and mass contributions}} + G_S \underbrace{\sum_{j=0}^8 \left[\left(\bar{\psi} \frac{\lambda_j}{2} \psi \right)^2 + \left(\bar{\psi} \frac{i \gamma_5 \lambda_j}{2} \psi \right)^2 \right]}_{\text{Scalar interaction}} \\
 & - G_V \underbrace{\sum_{j=0}^8 \left[\left(\bar{\psi} \gamma_\mu \frac{\lambda_j}{2} \psi \right)^2 + \left(\bar{\psi} \gamma_\mu \frac{\gamma_5 \lambda_j}{2} \psi \right)^2 \right]}_{\text{Vectorial interaction}} \quad \psi \equiv \psi_{Aa}^f \\
 & - K \underbrace{[\det_f (\bar{\psi} (1 - \gamma_5) \psi) + \det_f (\bar{\psi} (1 + \gamma_5) \psi)]}_{\text{Flavour mixing terms}} + \underbrace{\mathcal{L}_L}_{\text{Lepton contributions}}
 \end{aligned}$$

MIT-Bag model

$$\begin{aligned}
 \epsilon^Q &= \sum_{f=u,d,s} \frac{\nu_f}{2\pi^2} \int_0^{k_F^f} k^2 \sqrt{m_f^2 + k^2} dk + B \\
 P^Q &= \sum_{f=u,d,s} \frac{\nu_f}{6\pi^2} \int_0^{k_F^f} \frac{k^4}{\sqrt{m_f^2 + k^2}} dk - B,
 \end{aligned}$$

The Gibbs Construction

Hadronic and quark surface:

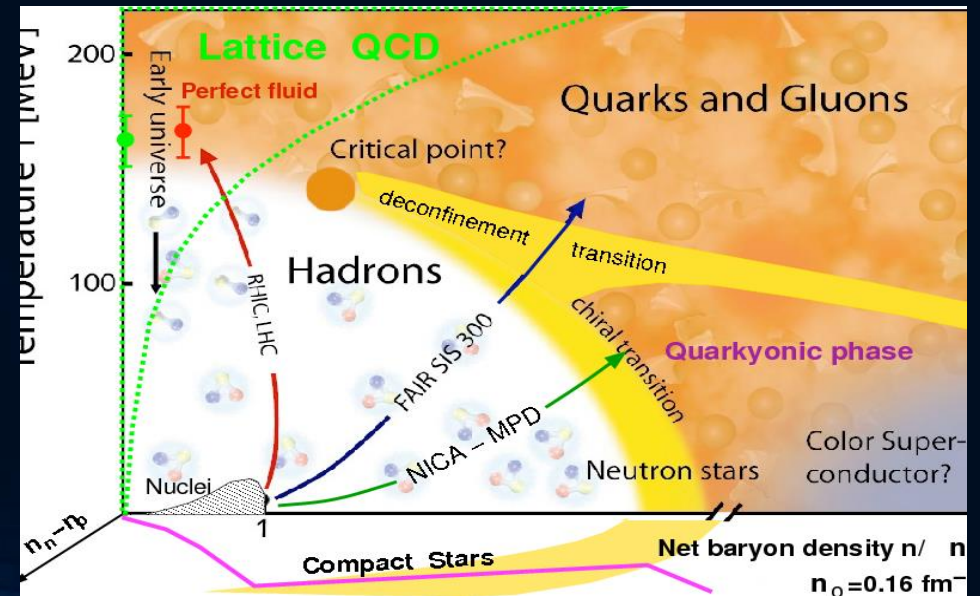


Charge neutrality condition is only globally realized

$$\rho_e := (1 - \chi)\rho_e^H(\mu_B, \mu_e) + \chi\rho_e^Q(\mu_B, \mu_e) = 0.$$

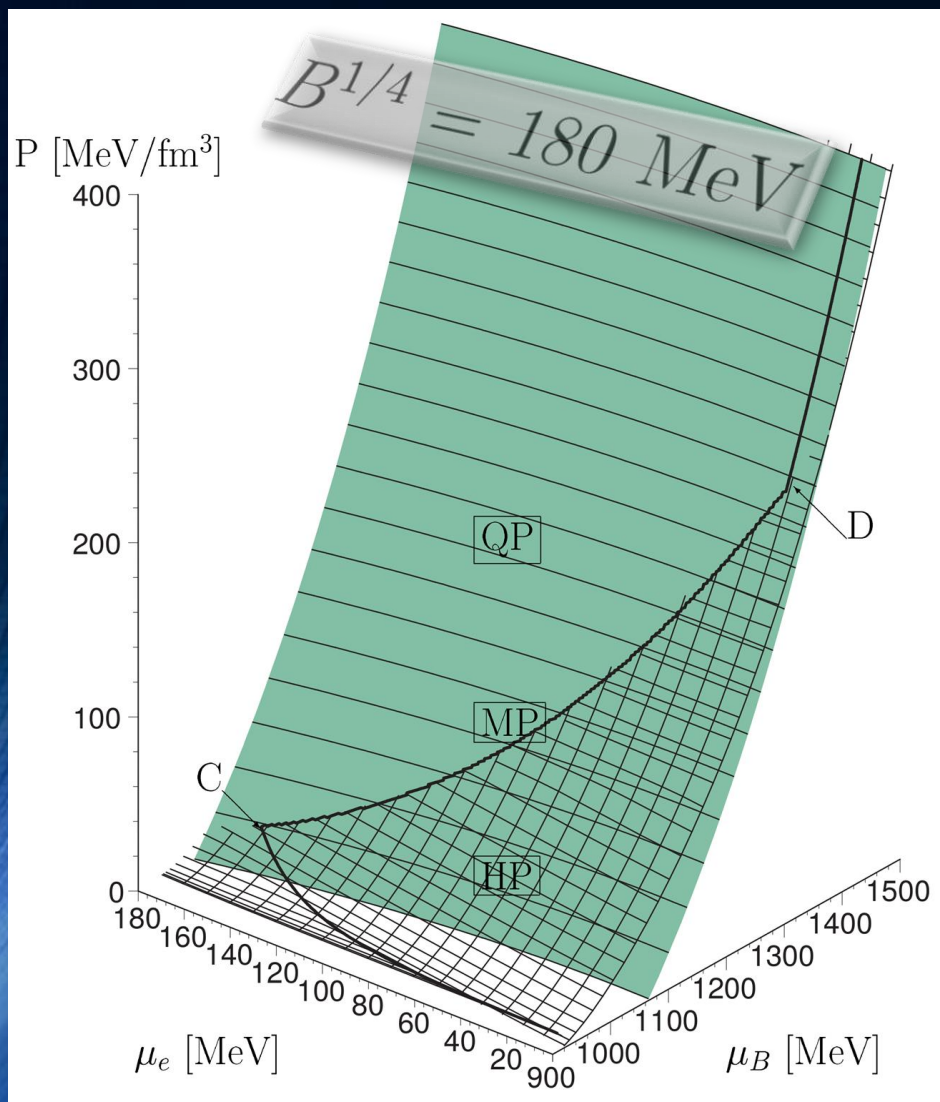
The pressure in the mixed phase depends on two independent chemical potentials

$$\begin{aligned} P^H(\mu_B, \mu_e) &= P^Q(\mu_B, \mu_e), \\ \mu_B &= \mu_B^H = \mu_B^Q, \\ \mu_e &= \mu_e^H = \mu_e^Q \end{aligned}$$

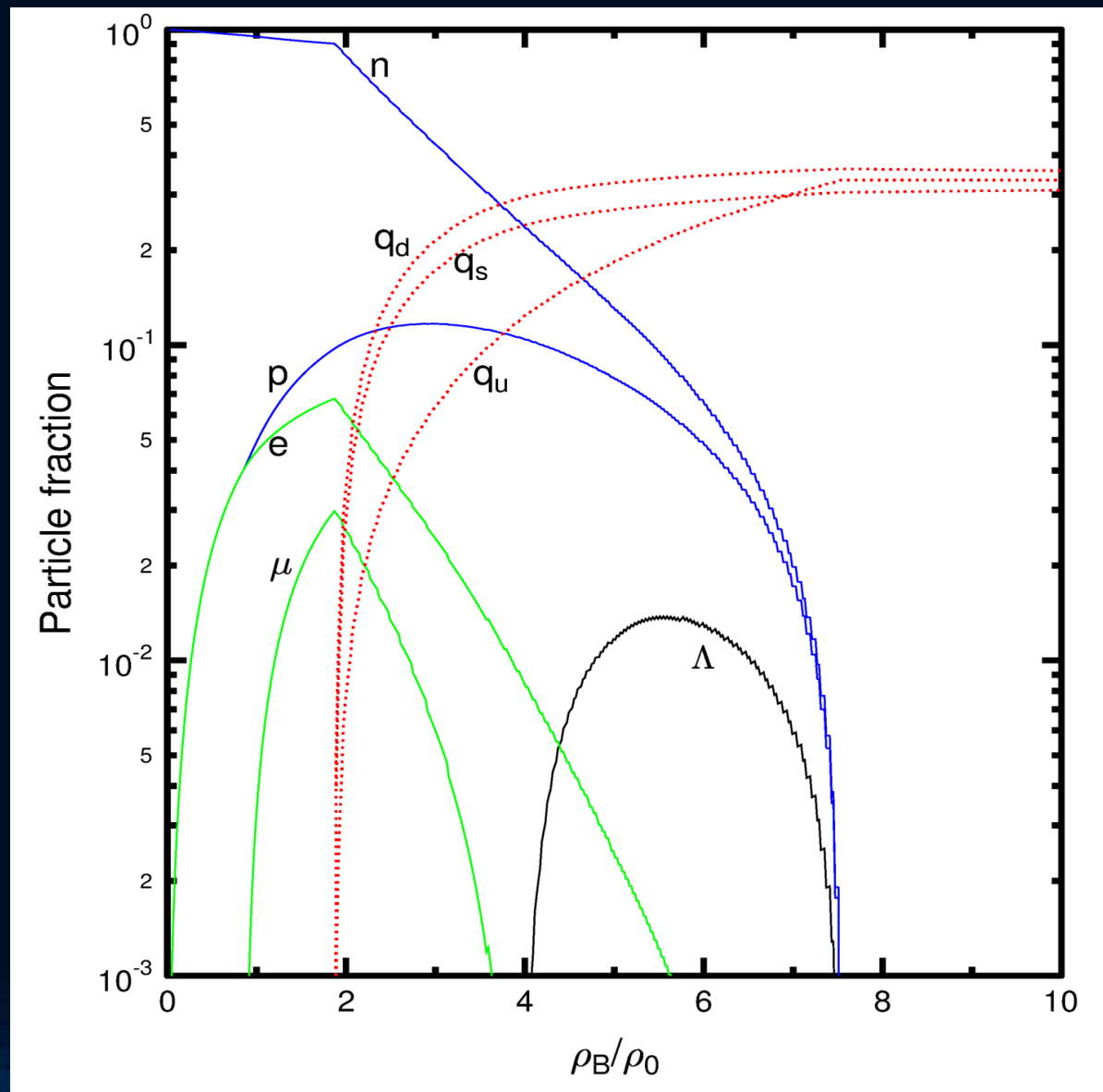


The Gibbs Construction

Hadronic and quark surface:

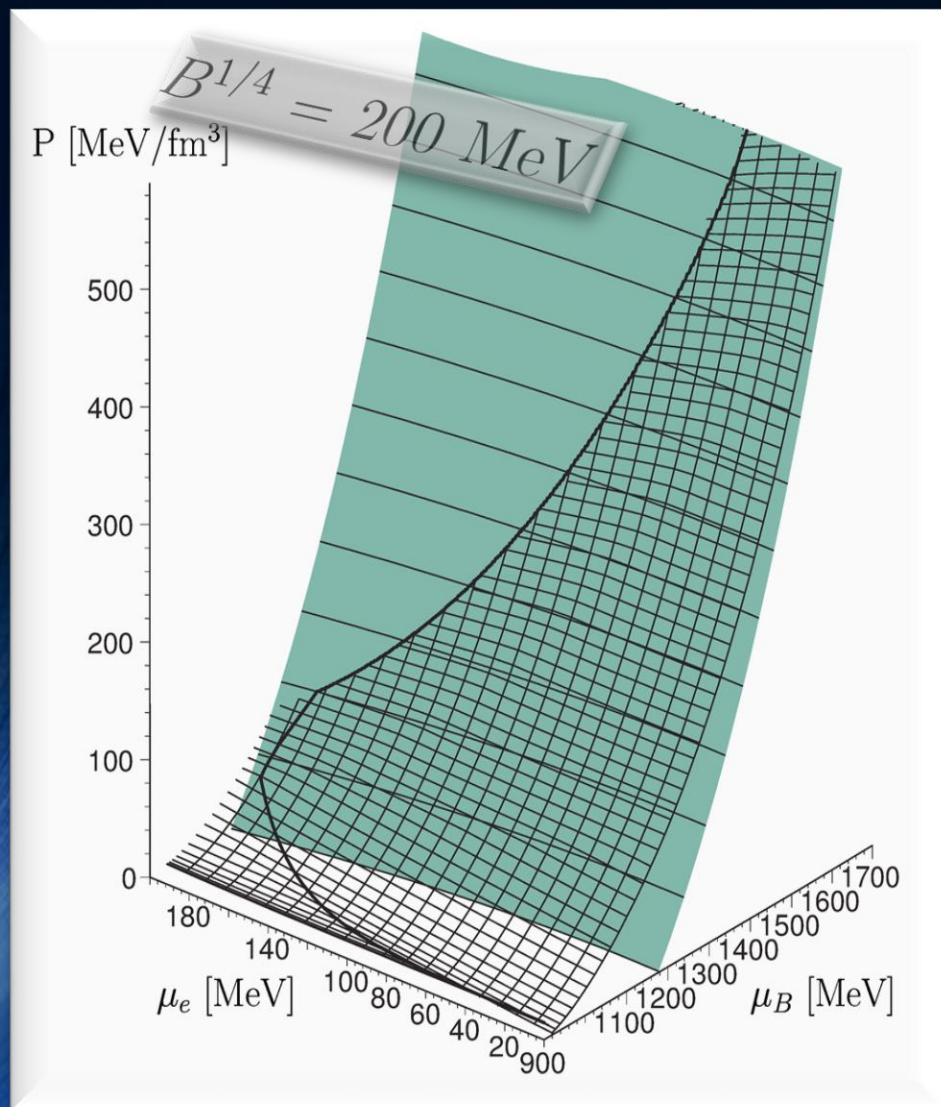


Particle composition:

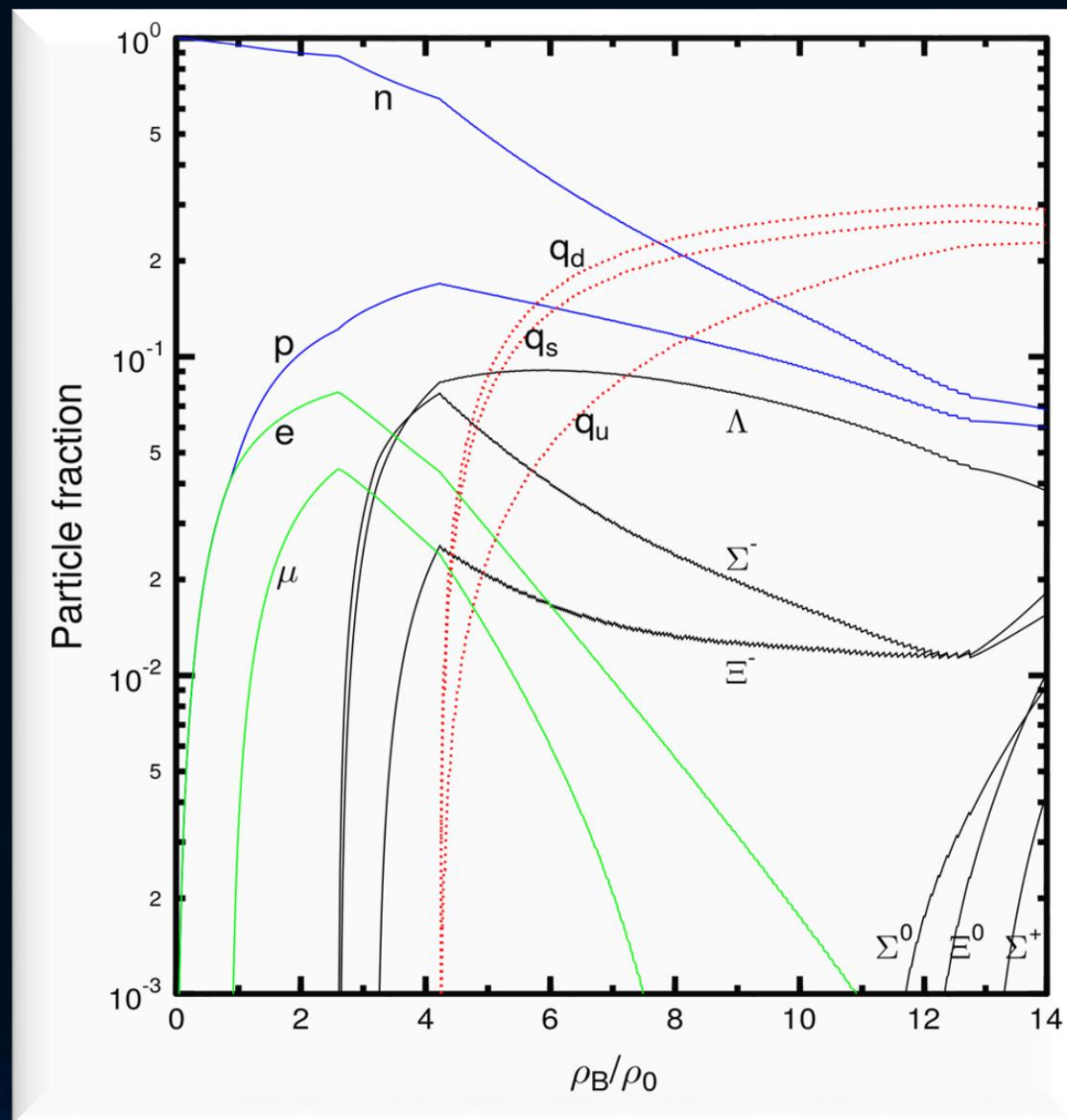


The Gibbs Construction

Hadronic and quark surface:

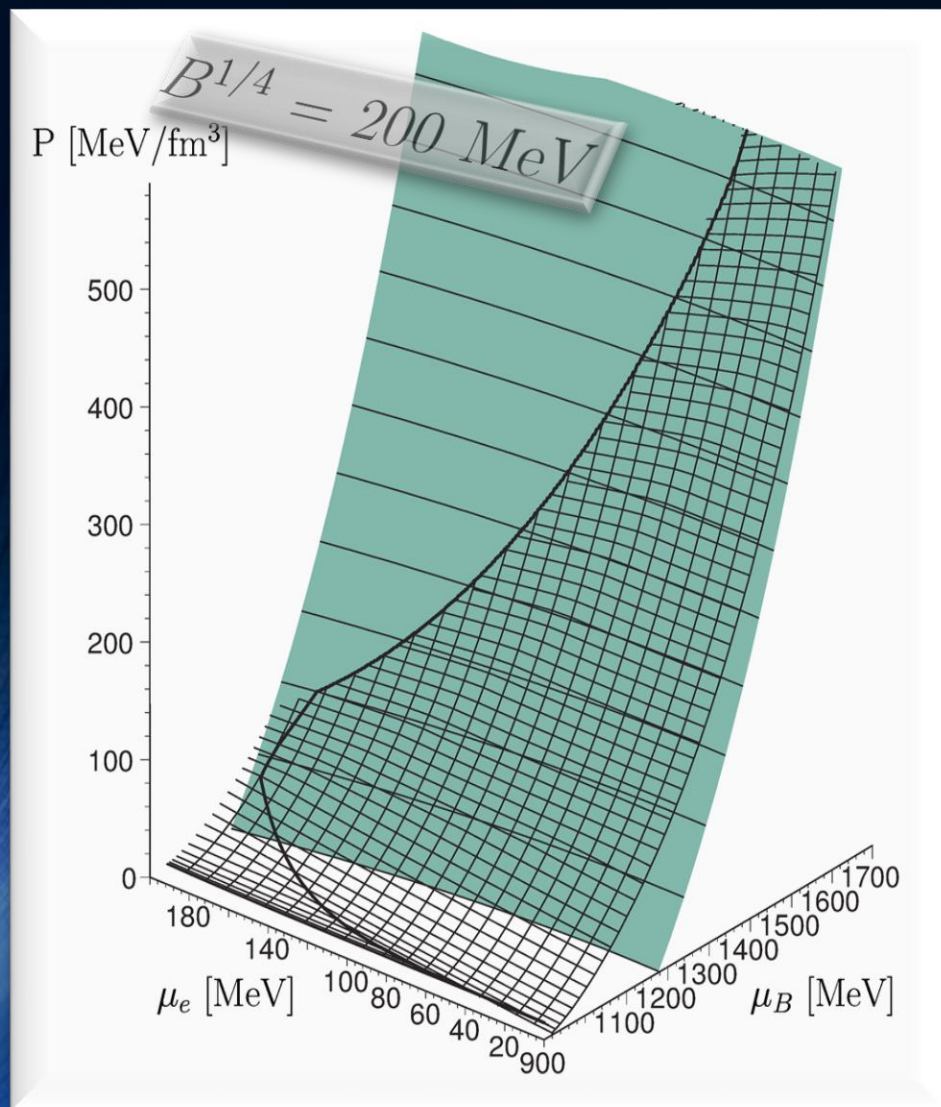


Particle composition:

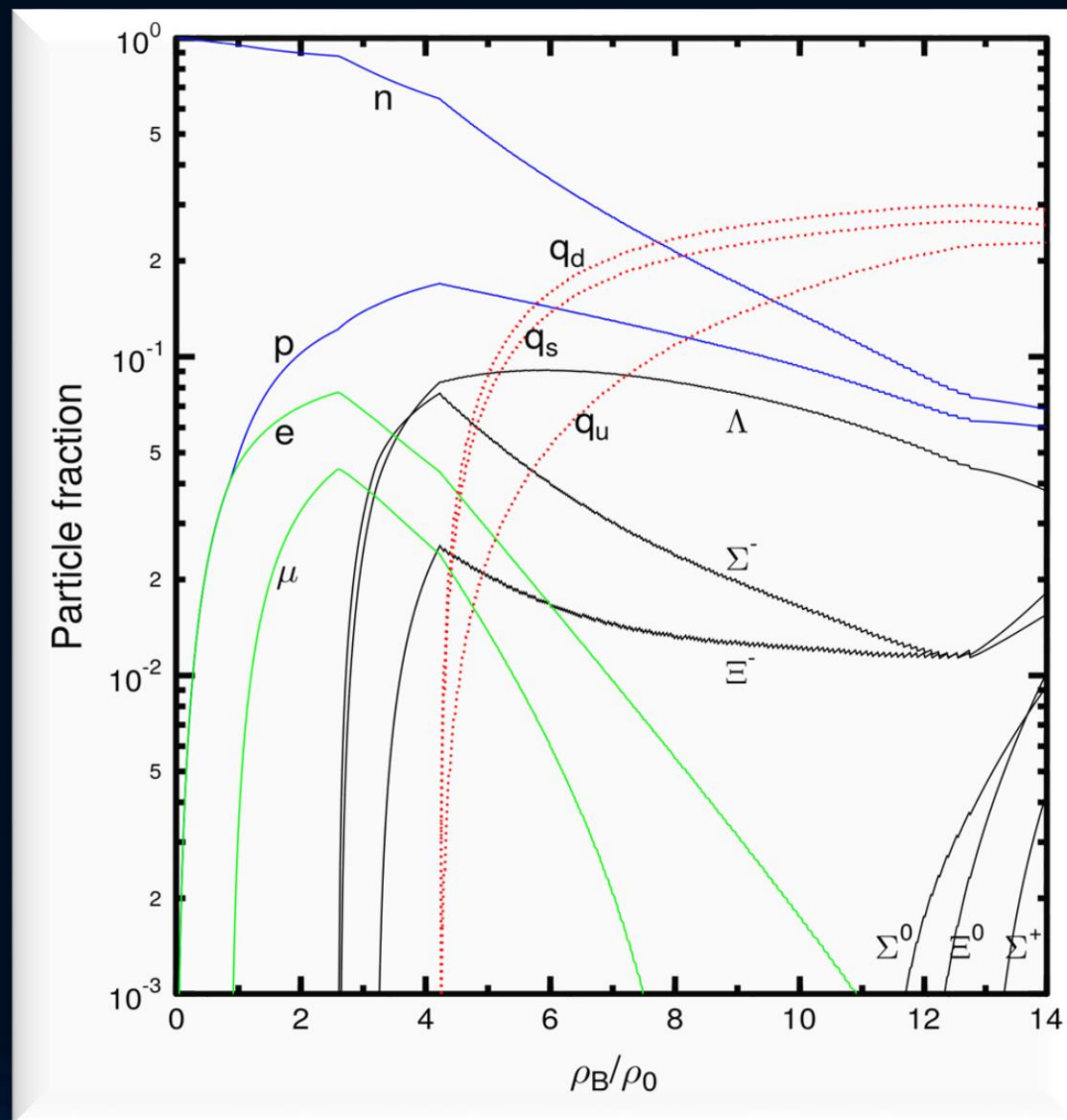


The Gibbs Construction

Hadronic and quark surface:

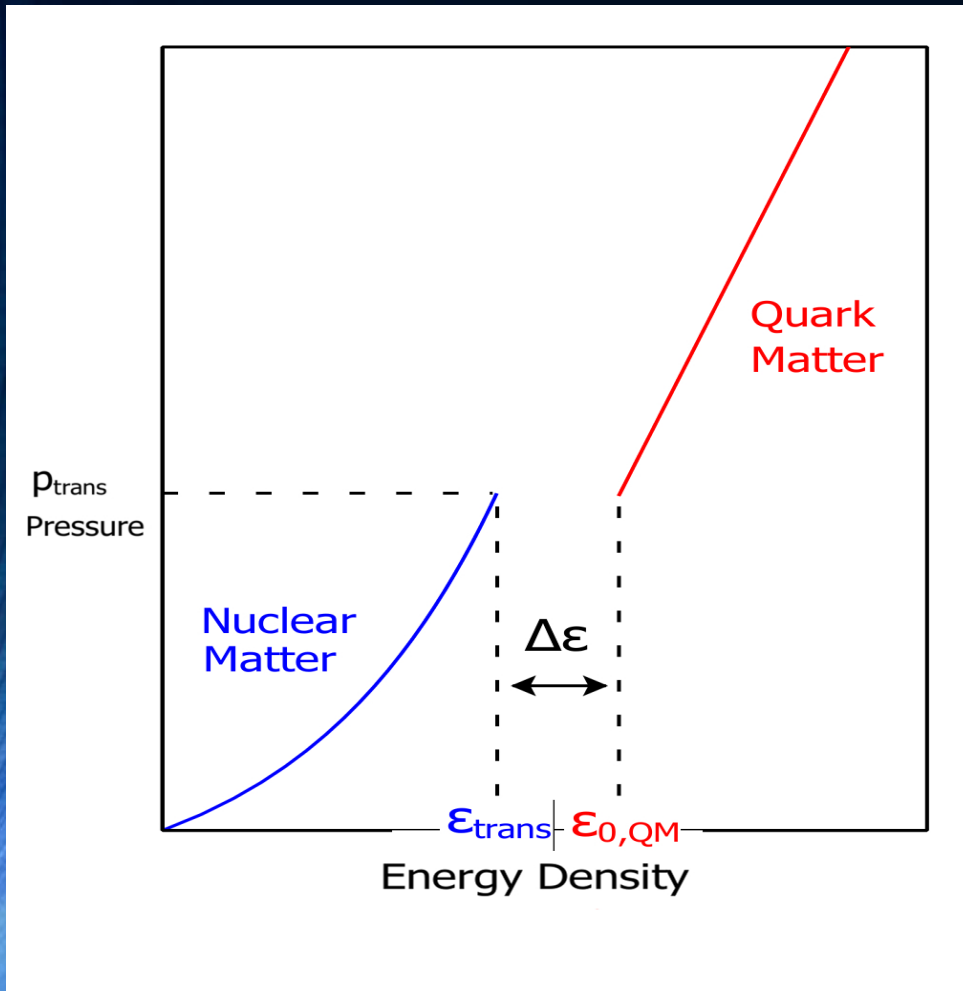


Particle composition:

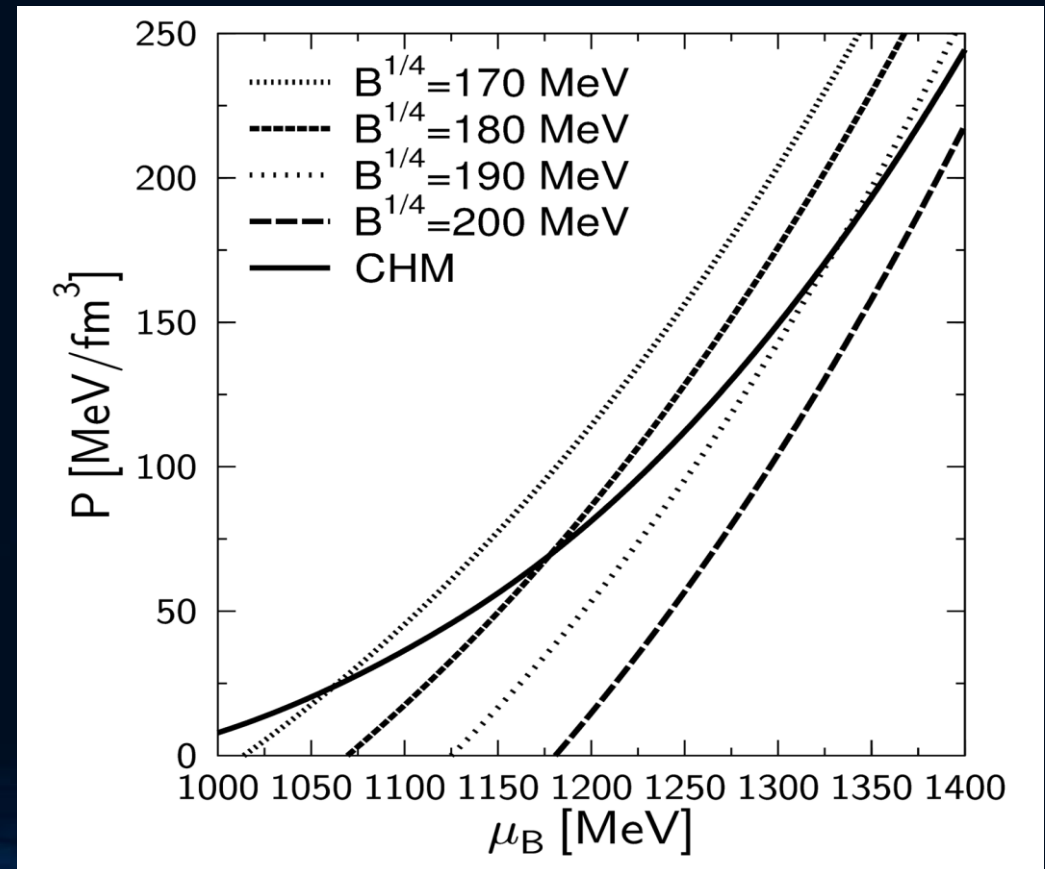


The Maxwell Construction

If the surface tension between the hadron and quark phase is relatively large, the mixed phase could completely disappear, so that a sharp boundary between the two phase exists. The Hadron-quark phase transition is then described using a Maxwell construction.



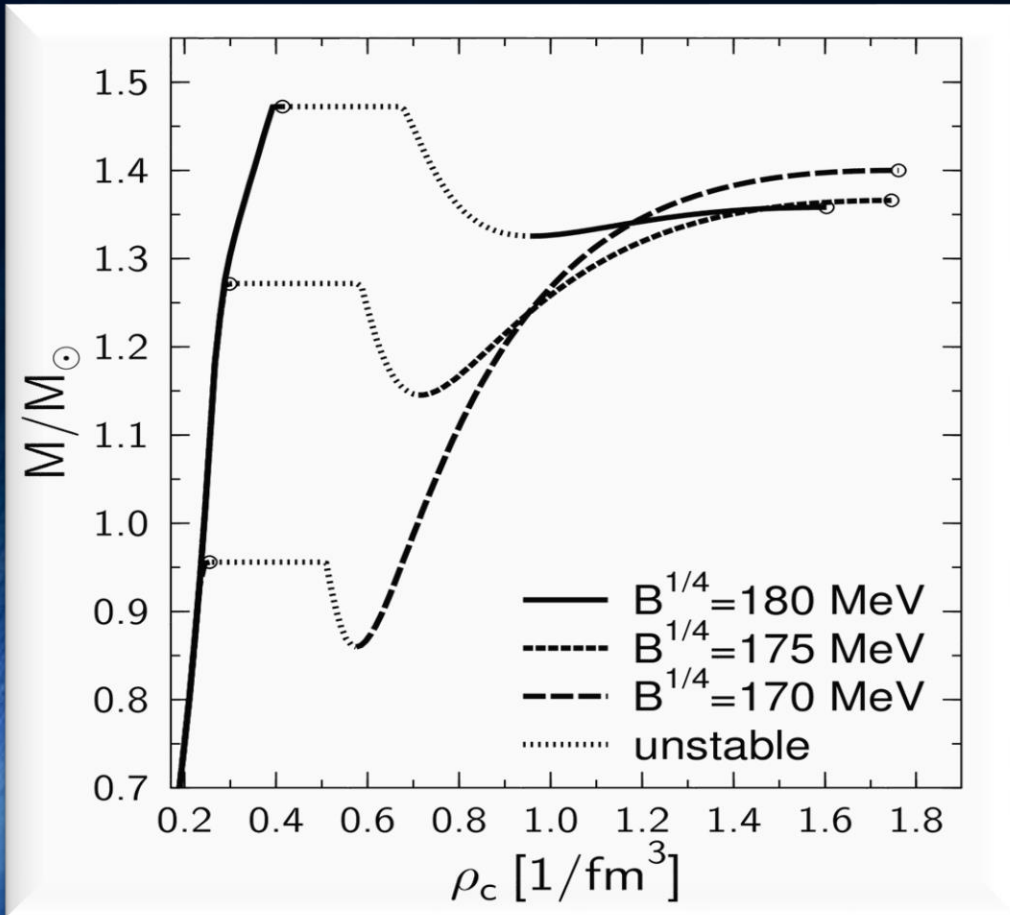
Pressure and baryon chemical potential stays constant, while the density and the charge chemical potential jump discontinuously during the phase transition.



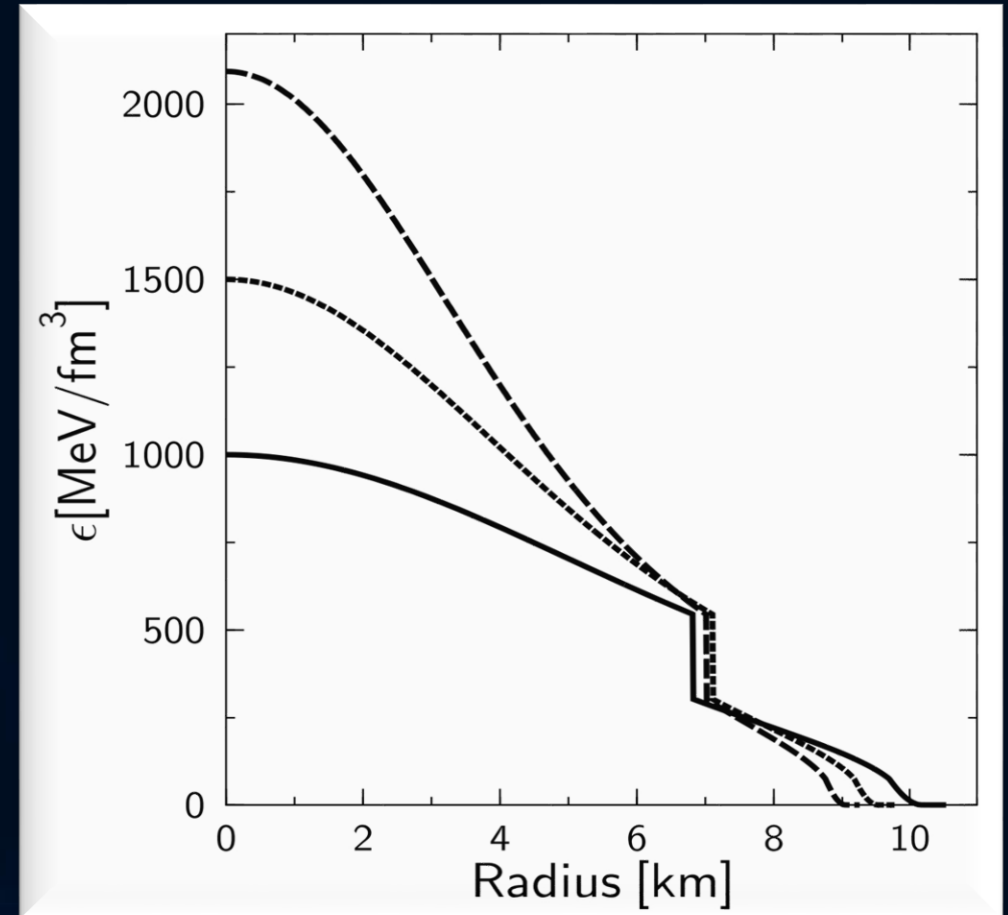
Hybrid Star Properties

In contrast to the Gibbs construction, the star's density profile within the Maxwell construction (see right figure) will have a huge density jump at the phase transition boundary. Twin star properties can be found more easily when using a Maxwell construction.

Mass-Density relation

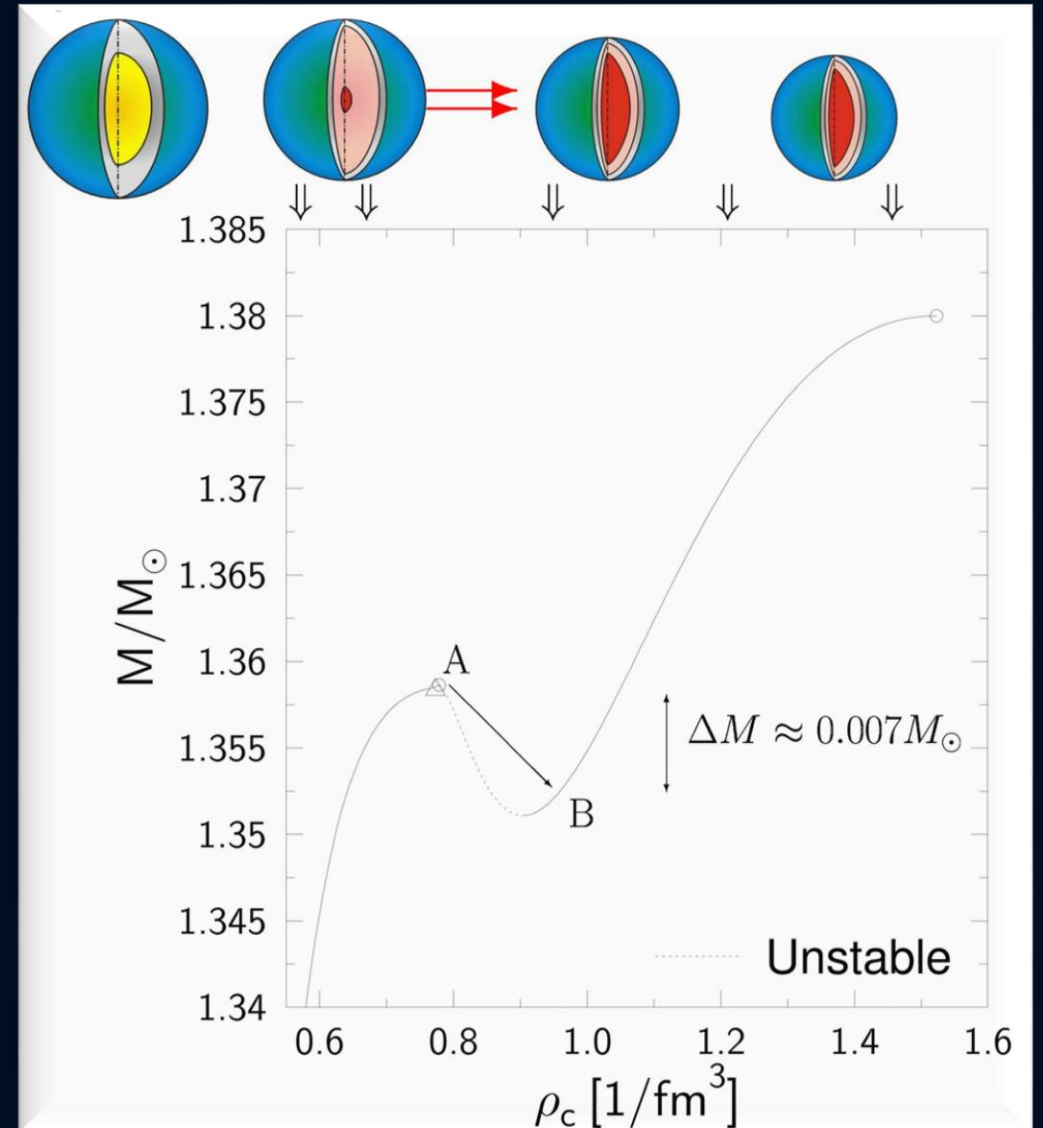
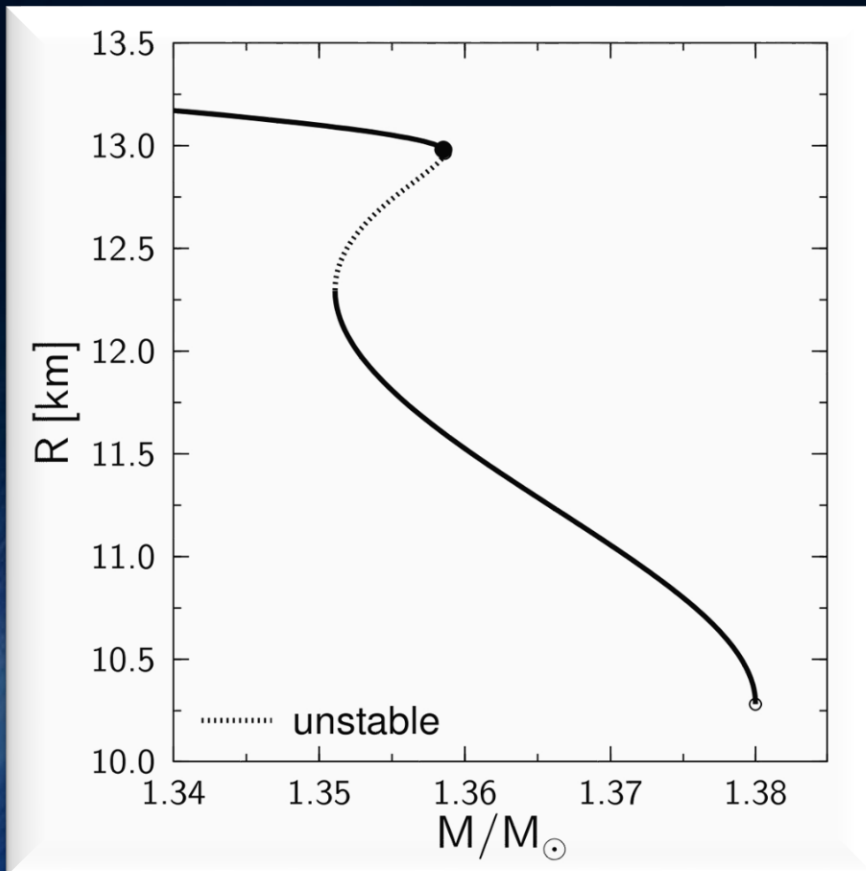


Energy-density profiles



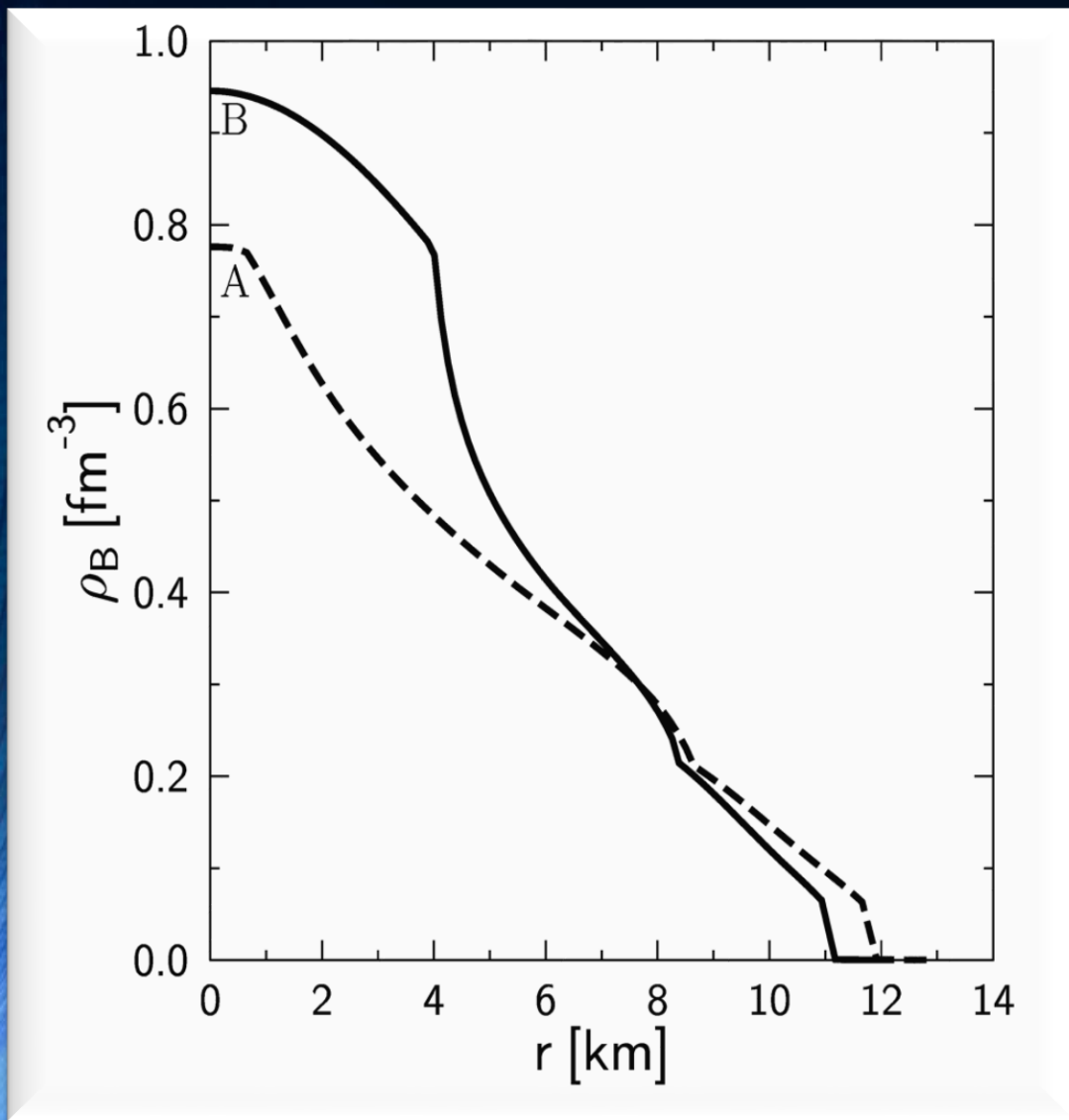
Twin Stars

Usually it is assumed that this loss of stability leads to the collapse into a black hole. However, realistic calculations open another possibility: the collapse into the twin star on the second sequence.

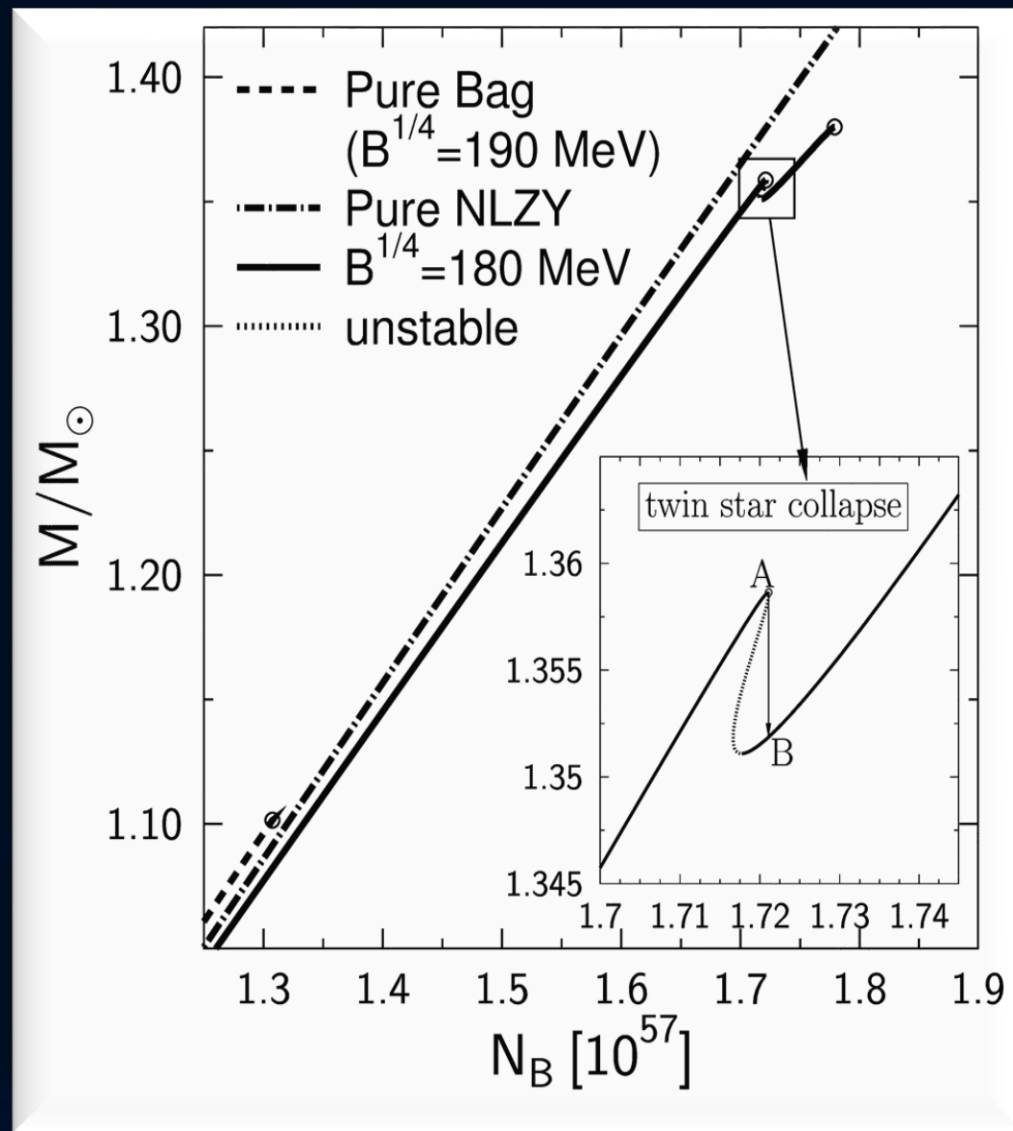


The Twin Star Collapse

Density profiles of the two twins



Conservation of total baryonic mass

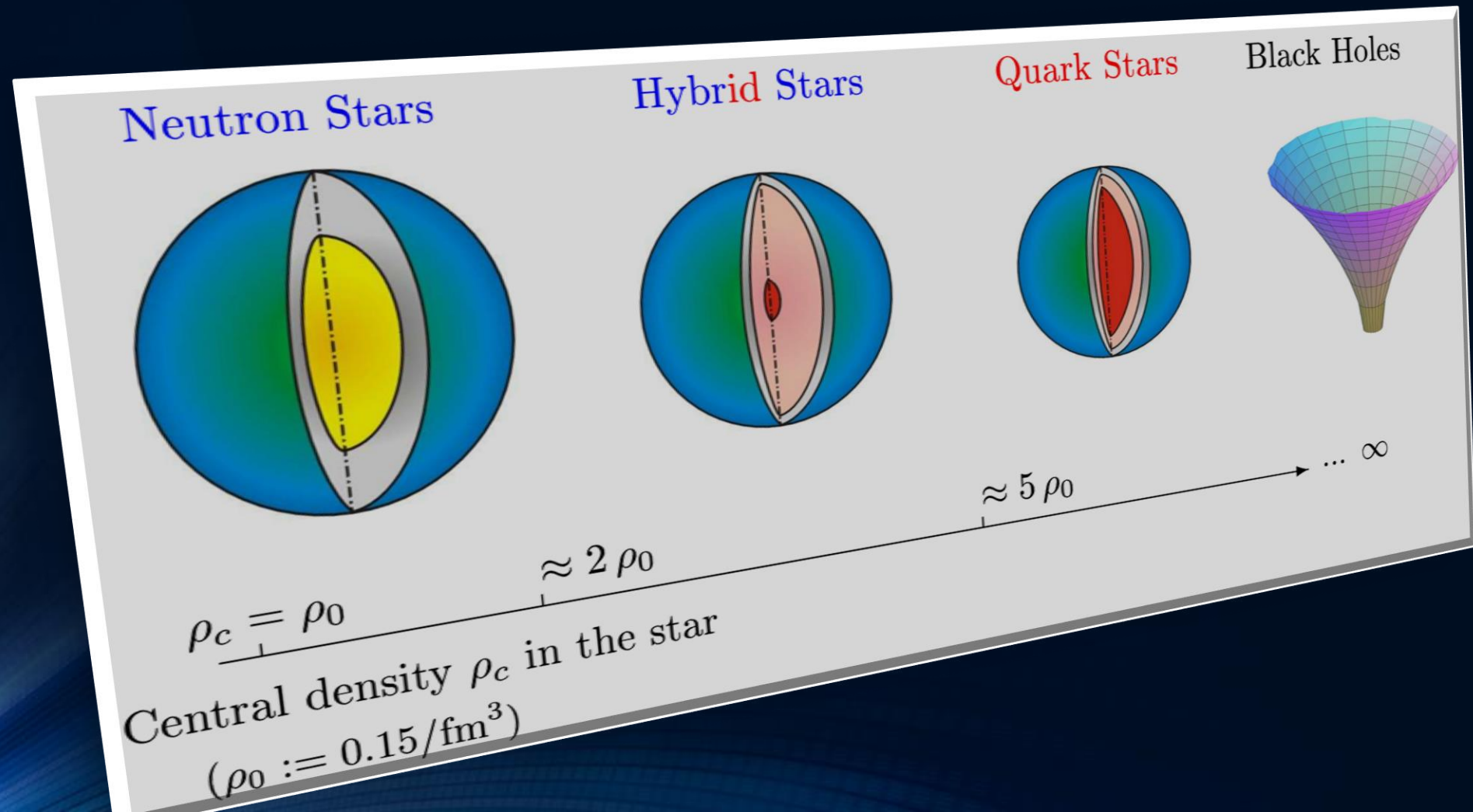


I.N. Mishustin, M. Hanauske, A. Bhattacharyya, L.M. Satarov, H. Stöcker, and W. Greiner,

“Catastrophic rearrangement of a compact star due to quark core formation”, Physics Letters B 552 (2003) p.1-8

Neutron Stars, Hybrid Stars, Quark Stars and Black Holes

At which density the phase transition to the Quark-Gluon-Plasma appears and a detailed analysis of the properties of this transition is still somewhat uncertain. The theoretical modelling is often still based on effective theories of the QCD interaction and therefore different species of compact stars are possible..



Neutron Star

Black Hole

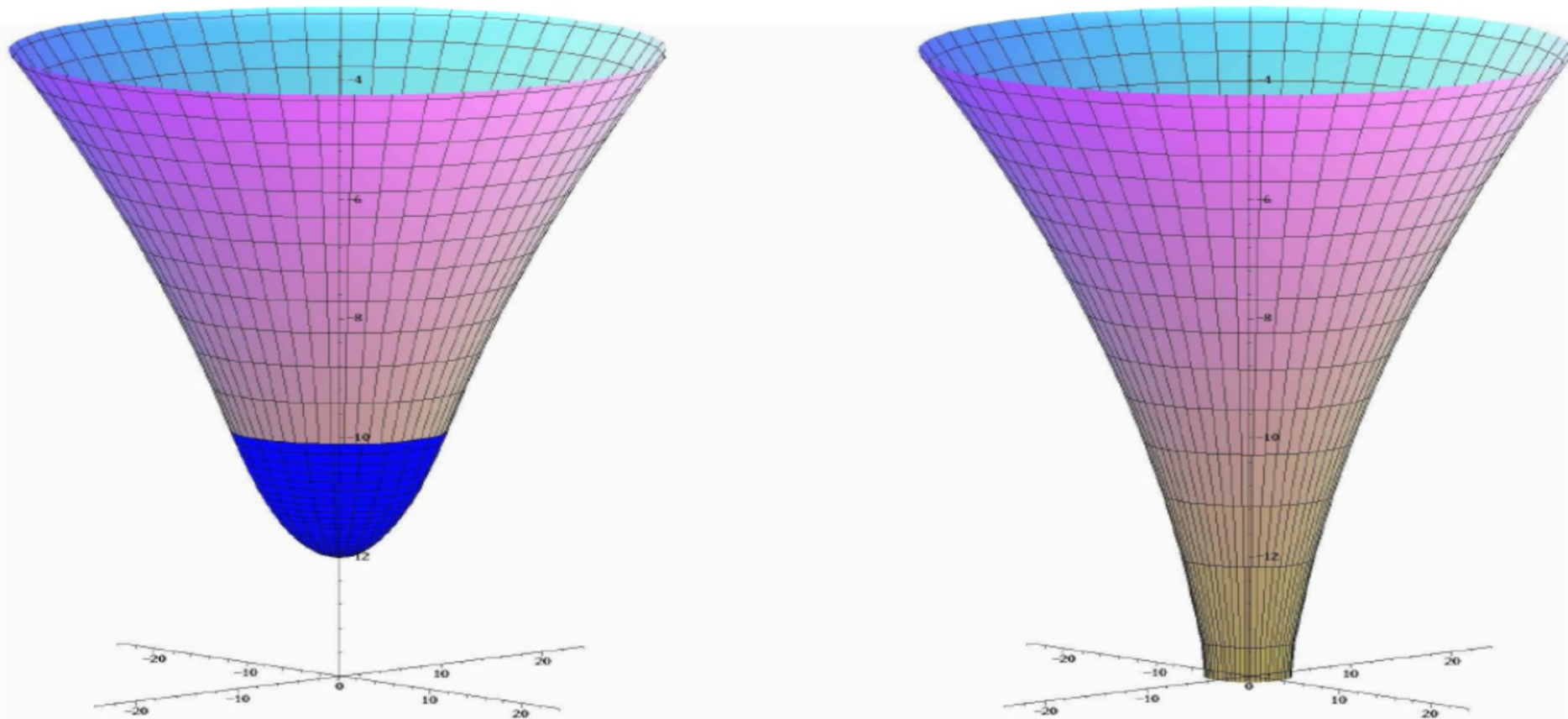
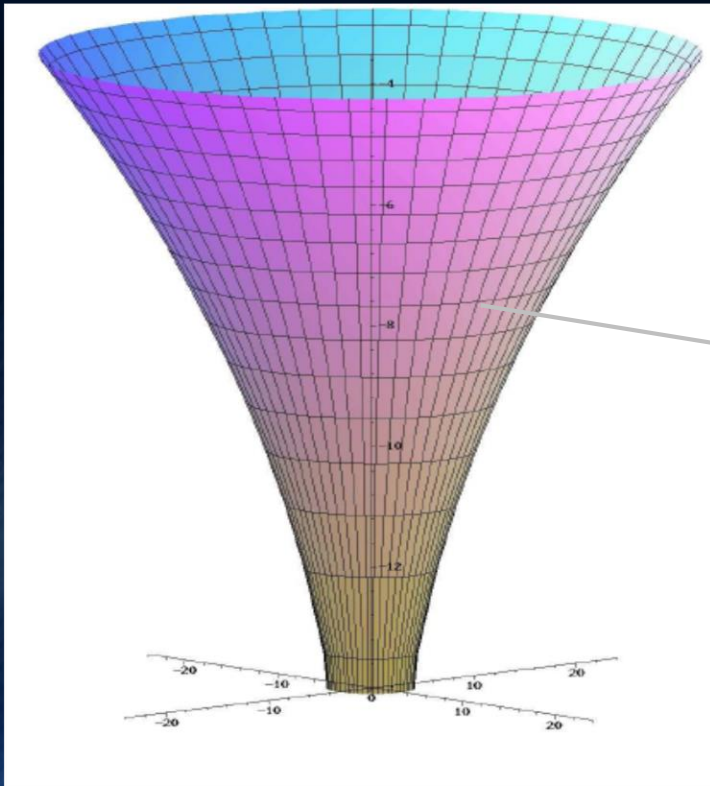


Abbildung 2.5: Eingebettetes Raumzeitdiagramm eines Neutronensterns (links) und eines schwarzen Loches (rechts) wobei $M = 1.4 M_{\odot}$ und die x- und y-Achse in Einheiten km dargestellt sind.

A good Illustration of the Properties of a Black Hole

The funnel looks exactly like the diagrams used to illustrate the curvature of a black hole



Black Holes and the German Reichstag



Event
Horizon

Ereignishorizont

Echte Singularität

Black Holes and the German Reichstag

